HISTONE METHYLTRANSFERASES REGULATE RESPONSES TO BIOTIC AND ABIOTIC FACTORS IN TOMATO

by

Carol Nunurai Bvindi

A Dissertation

Submitted to the Faculty of Purdue University

In Partial Fulfillment of the Requirements for the degree of

Doctor of Philosophy

Department of Botany and Plant Pathology

West Lafayette, Indiana

May 2020

THE PURDUE UNIVERSITY GRADUATE SCHOOL
STATEMENT OF COMMITTEE APPROVAL

Dr Tesfaye Mengiste, Chair
Department of Botany and Plant pathology

Dr Gurmukh Johal
Department of Botany and Plant Pathology

Dr Jing-rong Xu
Department of Botany and Plant pathology

Dr Steve Scofield
Agronomy Department

Dr Ying Li
Department of Horticulture and Landscape

Approved by:
Dr. Chris Staiger

To my family; Adonis, Uyeza, Luvuyo, and Mwaita.

ACKNOWLEDGMENTS

My sincere gratitude goes to Professor Tesfaye Mengiste for the guidance and patient in training me. I would not be where I am today without you, I really appreciate it. Many thanks go to Dr Ying Li for all your advice, guidance and inspiration to pursue my career. I would also want to acknowledge my committee members, Professor Jin-rong Xu, Professor Guri Johal, Professor Steve Scofield for all the guidance. I am grateful for my husband for all the prayers, encouragements, and patient during the time I pursued this degree. Without you I would have given up as early as I started. To my children Uyeza and Luvuyo I say thank you for your patience and loving and kind word when things were difficult. Forever grateful to Dr Sanghun Lee for mentoring me in this field of scientific discovery. Thankful for all Mengiste lab members, both past and present for your ideas, critique and help made it possible to get this far. To all who are not mentioned here who contributed to my knowledge, social and mental well-being during this time, I say thank you.

TABLE OF CONTENTS

LIST OF TABLES 9
LIST OF FIGURES 10
ABSTRACT 15
CHAPTER 1. LITERATURE REVIEW 18
1.1 Introduction 18
1.2 The histone code 19
1.3 Histone lysine methylation (HLM) 19
1.4 Plant responses to water stress 21
1.4.1 Physiological mechanism of drought response 22
1.4.1.1 Leaf traits 22
1.4.1.2 Photosynthesis 23
1.4.1.3 Modulation of root architecture 24
1.4.2.4 Osmotic adjustment 25
1.4.2.5 Antioxidant defense system 25
1.4.2.6 Phytohormones 26
1.5 Molecular mechanism of drought response. 27
1.6 Epigenetic regulation of plant responses to drought stress 29
1.6.1 DNA methylation 29
1.6.2 Histone post translational modification 30
Histone acetylation 30
Histone lysine methylation 31
Regulation of pathogen responses by histone lysine methylation 32
1.7 Rationale and objectives 34
CHAPTER 2. TOMATO HISTONE 3 LYSINE METHYLTRANSFERASES SDG33 AND SDG34 REGULATE PLANT RESPONSES TO STRESS AND PATHOGENS 36
2.1 Abstract 36
2.2 Introduction 37
2.3 Materials and methods 40
2.3.1 Plant materials and growth conditions 40

2.3.2 Generation of *sdg33* and *sdg34* mutants 40
2.3.3 Global methylation assay. 40
2.3.4 Stress tolerance assays....41
2.3.5 Determination of malondialdehyde (MDA) content 41
2.3.6 Lateral root and auxin response assays 42
2.3.7 RNA extraction and gene expression analyses....42
2.3.8 Statistical analysis 42
2.3.9 Complementation of *Arabidopsis sdg8* mutants. 43
2.3.10 Disease assays 43
2.4 Results 44
2.4.1 Characterization of tomato SDG33 and SDG34 encoding histone methyl transferases. 44
2.4.2 Characterization of *sdg33* and *sdg34* loss of function mutants.....48
2.4.3 SDG33 and SDG34 mutation affect global histone 3 lysine 4 and lysine 36 methylation. 51
2.4.4 Mutation in SDG33 and SDG34 improved drought stress tolerance 52
2.4.5 Expression of drought responsive gene in sdg33 and sdg34 mutant plants during water stress 56
2.4.6 Tomato *SDG33* and *SDG34* rescue the fungal susceptibility and early flowering phenotypes of *Arabidopsis sdg8* mutant 56
2.4.7 Mutations in SDG33 and SDG34 alter fruit morphology, lateral root development and auxin sensitivity....59
2.5 Discussion....61
CHAPTER 3. THE HISTONE METHYLTRANSFERASES SDG33 AND SDG34 MEDIATE NITRATE SIGNALING IN TOMATO 65
3.1 Abstract....65
3.2 Introduction 65
3.3 Materials and Methods 67
3.3.1 Transgenic plants....67
3.3.2 Plant growth conditions and treatments 67
3.3.3 RNA extraction....68

3.3.4 RNA sequencing and data analysis 68
3.3.5 Motif analysis 69
3.3.6 Phenotyping 69
Chlorophyll content 69
Root architecture measurements 70
Statistical analysis 70
3.4 Results 70
3.4.1 SlSDG33 and SlSDG34 regulate the expression of overlapping yet distinct downstream genes 70
3.4.2 Cis-regulatory motifs in the promoters of genes regulated by SDG33 or SDG34 75
3.4.3 SDG33 and SDG34 regulated genes overlap with *At*SDG8 targets in Arabidopsis 77
3.4.4 SDG33 and SDG34 mediate the transcriptional response to nitrogen in shoots and in roots. 78
3.4.5 Mutation in SDG33 and SDG34 alters nitrogen physiological response in tomato roots. 86
3.4.6 Chlorophyll a/b ratio is altered in *sdg33* and *sdg34 in* response to nitrogen 88
3.5 Discussion 89
CHAPTER 4. TOMATO HISTONE LYSINE METHYL TRANSFERASE SDG20 REGULATES PLANT IMMUNITY AND IS REQUIRED FOR PLANT VIABILITY 94
4.1 Abstract 94
4.2 Introduction 94
4.3 Materials and methods 98
4.3.1 Plant materials and growth conditions 98
4.3.2 Generation of *sdg20* mutants 98
4.3.3 Global methylation assay 99
4.3.4 Fungal culture and disease assays 99
4.3.5 Bacterial disease assays 99
4.3.6 RNA extraction 100
4.4 Results 100
4.4.1 Characterization of tomato SDG20, a putative histone methyltransferase. 100
4.4.2 Characterization of *sdg20* loss of function mutants. 102

4.4.3 Global histone lysine methylation is mediated by SDG20.....104
4.4.4 SDG20 is required for vegetative growth and proper leaf development.....104
4.4.5 SDG20 is required for disease resistance in tomato.....105
4.5 Discussion.....107
CHAPTER 5. IDENTIFICATION OF TOMATO RECEPTOR LIKE CYTOPLASMIC KINASES REQUIRED FOR RESISTANCE TO FUNGAL PATHOGENES. 110
5.1 Abstract.....110
5.2 Introduction 111
5.3 Materials and methods.....113
5.3.1 Plant materials and growth conditions 113
5.3.2 Generation of tpk07, tpk09, tpk011 and trk04 mutants.....113
5.3.3 Fungal culture and disease assays 114
5.3.4 Bacterial disease assays.....114
5.3.5 RNA extraction.....114
5.3.6 Virus Induced Gene Silencing.....115
5.3.7 Co-immunoprecipitation and immunoblot assays.....115
5.4 Results 115
5.4.1 Characterisation of Tomato Receptor Like Cytoplasmic Kinases (RLCKs) 115
5.4.2 Phylogenetic analysis of TPK07, TPK09, TPK011 and TRK04. 119
5.4.3 Characterization of *tpk07, tpk09, tpk011 and trk04* loss of function mutants.....121
5.4.4 TRK04 is required for resistance to *Botrytis cinerea* in tomato.....121
5.4.5 trk04 mutants are impaired in seedling growth response to jasmonic acid.....123
5.5 Discussion.....124
References 127

LIST OF TABLES

Table 3.1 . Summary of differential expressed genes (DEGs) from pairwise comparison of each genotype and WT. 71

Table 3.2.Motifs enriched in the promoters of DEGs upregulated and downregulated in the shoots and roots sdg33 and sdg34 identified from a de novo search using MEME software. Letter size indicates nucleotide frequency 76

Table 3.3. *P value* and number of genes the target genes shared between the targets of SDG33 and SDG34 with the target genes of its Arabidopsis homolog, *At*SDG8.....78

Table 3.4. Summary of differential expressed genes (DEGs) regulated by SDG33 and sSDG34 in a nitrogen dependent manner. Threshold for differential expression is log2 fold change > |1|, false discovery rate < 0.05. 79

Table 3.5. Analysis of variance of Chlorophyll A (chlA), Chlorophyll B (chlB) Chlorophyll a/b ratio (chla.b ratio), total chlorophyll, bushiness and root dry weight in response to nitrogen supply. 86

Table 5.1. Tomato Receptor Like Cytoplasmic Kinases (RLCKs) similar to *At*BIK1 and *Sl*TRK1 116

LIST OF FIGURES

Figure 2.1 Gene, protein structures and phylogenetic analysis of SDG33 and SDG34**.** Schematic diagram showing gene and protein structure of A) SDG33, B) SDG34. Black shaded boxes represent exons, the grey shaded boxes represent the UTRs boxes represent exon, and introns are shown as horizontal lines. For the protein structure the main domains are shown. C) Maximum Likelihood phylogenetic analysis of class 11 SDG protein from *Arabidopsis thaliana (*At*)*, *Solanum lycopersicum* (Sl), *Zea mays* (Zm) and *Oryza sativa* (Os). Phylogenetic analysis was performed using Mega7 package. The tree is drawn to scale with branch length measured in the number of substitutions per site. Bootstrap values higher than 50% are shown. 45

Figure 2.2 Expression of SDG33 and SDG34 in WT tomato in response to drought, fungal infection and plant hormones. A) Tissue specific expression of SDG33 and SDG34 in WT tomato plants. Induced expression of SDG33 and SDG34 with B) Drought, C) IAA, D) ABA, E) Methyl jasmonate (MeJa), F) Salicylic acid (SA), G) *B. Cinerea* and H) *P. syringae.* Bars represent the means; the error bars represent the standard deviations of three technical replicates of each treatment. The tomato β-actin gene was used as an internal control in the qRT-PCR. The experiment was repeated at least 2 times with similar results.....47

Figure 2.3. Molecular characterization of sdg33 and sdg34 loss of function mutants. A) and D) Diagrams showing the position of the deletions in sdg33 and sdg34 mutants. Black shaded boxes represent exons, the grey shaded boxes represent the UTRs boxes represent exon, and introns are shown as horizontal lines. B and E) PCR genotyping of *sdg33* and *sdg34* mutant alleles. C and F) Alignment of mutated alleles sequences identified from cloned PCR genotyping fragments and the WT sequences. The mutated alleles include deletions (shown by dashed lines) and insertions (shown by blue letters). Only aligned sequences and the mutations are shown. The targets are shown by letters in red and the protospacer adjacent motif (PAM) is shown by the bold-faced letters after the targets. SDG33 (G) and SDG34 (H) expression in the mutants. Bars represent the means; the error bars represent the standard deviations of three technical replicates of each treatment. The β-actin gene was used as an internal control in the qRT-PCR. The experiment was repeated at least 2 times with similar results. 49

Figure 2.4 Global histone lysine methylation levels in tomato sdg33 and sdg34 mutants. Western blot analysis of A) H3K4 B) H3K36 in WT, *sdg33* and *sdg34* alleles. Core histones were extracted from 4-week old plants and blotted with specific H3K4 and H3K36 antibodies.....51

Figure 2.5. Seedling growth of WT, *sdg33* and *sdg34* in response to osmotic stress**.** A) Phenotypes, B) Hypocotyl length and C) seedling weight of WT, *sdg33* and *sdg34* after treatment with 300mMmannitol. The data shown are the mean ± SE (n = 10), the experiment was repeated 2 times with similar results. The data shown are the mean ± SE (n = 36). *$p < 0.05$, **$p < 0.01$. 53

Figure 2.6. Mutation in SDG33 and SDG34 enhances drought tolerance in tomato. A) Phenotypes of WT, *sdg33* and *sdg34* during and after water stress treatment. WS-water stress, RW- re-watered. B) Relative Water Content of WT, *sdg33* and *sdg34* at day 6 of water stress. The data shown are the mean ± SE (n = 6). C) Survival rates after re-watering of WT, *sdg33* and *sdg34* after drought stress. The data shown are the mean ± SE (n = 42). Data shown is a representation of experiments

repeated at least 3 times. D) Shoot water content of WT, *sdg33* and *sdg34* measured at 3 days after re-watering. The data shown are the mean ± SE (n = 36). *p < 0.05, **p < 0.001. 55

Figure 2.7. Expression of drought-responsive genes under water stress in WT, *sdg33* and *sdg34*. A) dehydration-responsive element binding (DREB), B) Peroxidase (POD) and C) Superoxide dismutase 6 (SOD6) genes. qRT-PCR analysis of stress-responsive genes in WT and transgenic plants at day 6 after drought stress. 56

Figure 2.8. Tomato *sdg33* or *sdg34* mutants exhibit wild type levels of resistance to *B. cinerea* and *P. syringae*. Disease phenotypes of the single mutants in SDG33 or SDG34 genes in response to A) *B. cinerea*, B) *P. syringae*. The data shown are the mean ± SE (n >30). Different letters represent significant differences among genotype. C) The expression of CCR2 in *sdg33* and *sdg34* mutants. D-F) Leaf and flower phenotypes of the double mutant *sdg33sdg34* generated through Crispr/cas9. 57

Figure 2.9. Tomato SDG33 and SDG34 complement Arabidopsis *sdg8* mutation. A) Disease symptoms, B) Disease lesion size in Arabidopsis WT, *sdg8*, *sdg8:SDG33* and *sdg8:SDG34* lines 3 days after *B. cinerea* inoculation. C) Disease symptoms, D) Disease lesion size in WT, *sdg8*, *sdg8:SDG33* and *sdg8:SDG34* 5 days after inoculation with *Alternaria brassicicola*. E) and F) The growth and early flowering phenotypes of Arabidopsis *sdg8;*SDG33 and *sdg8*;SDG34. G) Expression of CCR2 in Arabidopsis WT, sdg8, *sdg8:SDG33* and *sdg8:SDG34* lines. The data shown are the mean ± SE (n >30). Different letters represent significant differences among genotype. 58

Figure 2.10 Mutation in tomato SDG33 and SDG34 alter responsiveness to IAA. A) Fruits from WT, *sdg33* and *sdg34* plants. B) Root growth of 10-day old seedlings of WT, *sdg33* and *sdg34* tomato plants. Only one allele of each mutant is shown. C) Number of lateral roots in WT, *sdg33* and *sdg34* at 10 days after germination on MS medium. D) Root growth of 10-day old seedlings of *sdg33*, *sdg34* and WT grown on medium supplemented with different IAA concentrations E) Lateral root numbers of *sdg33*, *sdg34* and WT seedlings shown in (D). The seedlings were germinated on filter paper for 3 days and transferred to MS medium supplemented with different IAA concentrations. The data shown are the mean ± SE (n ≥ 10). Asterisks indicate significant differences using Student's t-test. (*P < 0.05, **P < 0.01, ***P<0.001). The experiment was repeated at least 2 times with similar results, representative data is shown. 60

Figure 3.1. Genotypic effect of SDG33 and SDG34 mutation on tomato transcriptome. Hierarchal clustering of relative expression of DEGs based on the pairwise comparison of sdg33 or sdg34 and the WT in A) sdg33 roots, B) sdg34 roots, C) sdg33 shoot and D) sdg34 shoots. FDR < 0.05; $|\log_2$ fold change$| > 2$; Yellow and blue indicate higher and lower expression values, respectively. 72

Figure 3.2. Summary of DEGs in the roots. A) Venn diagram of up-regulated DEGs in *sdg33* and *sdg34* showing overlapping and exclusive DEGs. B) Heat maps showing common up-regulated DEGs between *sdg33* and *sdg34* and exclusive DEGs in *sdg33* and *sdg34*. C) Venn diagram of down-regulated DEGs in *sdg33* and *sdg34* showing overlapping and exclusive DEGs. D) Heat maps showing common down regulated DEGs between *sdg33* and *sdg34* and exclusive DEGs in

sdg33 and *sdg34*. FDR < 0.05; |$\log_2$ fold change| > 1; Orange and Yellow b indicate lower and higher expression values, respectively.....73

Figure 3.3. Summary of DEGs in the shoots. A) Venn diagram of up-regulated DEGs in *sdg33* and *sdg34* showing overlapping and exclusive DEGs. B) Heat maps showing common up-regulated DEGs between *sdg33* and *sdg34* and exclusive DEGs in *sdg33* and *sdg34*. C) Venn diagram of down-regulated DEGs in *sdg33* and *sdg34* showing overlapping and exclusive DEGs. D) Heat maps showing common down regulated DEGs between *sdg33* and *sdg34* and exclusive DEGs in *sdg33* and *sdg34*. FDR < 0.05; |$\log_2$ fold change| > 1; Orange and Yellow b indicate lower and higher expression values, respectively.....74

Figure 3.4 SDG33 and SDG34 mediate gene expression in a nitrogen dependent manner in the roots. A) Venn diagram of overlapping and exclusive sdg33 x nitrogen and sdg34 x nitrogen (Interaction) DEGs B) Hierarchal clustering of relative expression of DEGs regulated by sdg33 or sdg34 and nitrogen treatment. GO terms significant for the clusters are shown on the left C) Gene network and D) Go terms of gene network of DEGs regulated by sdg33 or sdg34 and nitrogen treatment. 80

Figure 3.5. SDG33 and SDG34 mediate gene expression in a nitrogen dependent manner in the roots. Expression of a representative set of genes whose expression is mediated by sdg33 or sdg34 and nitrogen treatment. A) Nitrogen assimilation genes, B) Transcription factors and C) Auxin responsive genes.....82

Figure 3.6.SDG33 and SDG34 mediate gene expression in a nitrogen dependent manner in the shoots. A) Venn diagram of overlapping and exclusive sdg33 x nitrogen and sdg34 x nitrogen (Interaction) DEGs B) Hierarchal clustering of relative expression of DEGs regulated by sdg33 or sdg34 and nitrogen treatment. GO terms significant for the clusters are shown on the left C) Gene network and D) Go terms of gene network of DEGs regulated by sdg33 or sdg34 and nitrogen treatment. 83

Figure 3.7.SDG33 and SDG34 mediate gene expression in a nitrogen dependent manner in the shoots. Expression of a representative set of genes whose expression is mediated by sdg33 or sdg34 and nitrogen treatment. A) Nitrogen assimilation genes, B) Transcription factors and D) Auxin responsive genes. 85

Figure 3.8. SDG33 and SDG34 mediates nitrogen response in tomato roots. Root phenotypic traits of *sdg33* and *sdg34* mutants and the wild type; a) Bushiness, b) Root biomass. c) Pictures of root phenotypes of the data presented in a. Data represent means ± SE (n = 10). Error bars indicate standard error (SE). Asterisk represent level of statistical significance based on student t test; * $P \leq$ 0.05, ** $P \leq$ 0.01, and *** $P \leq$ 0.001. The experiment was repeated two times with similar results and representative data from one of the experiments is shown. 87

Figure 3.9. SDG33 and SDG34 mutation does not alters chlorophyll content in response to nitrogen. a) Chlorophyll a, b) chlorophyll b and c) total chlorophyll content of sdg*33* and *sdg34* mutants and the wild type in response to nitrogen. Data represent means ± SE (n = 10). Bars labelled with different letters indicate significant difference between the treatments. Asterisk represent level of statistical significance based on student t test; * $P \leq$ 0.05, ** $P \leq$ 0.01, and *** $P \leq$ 0.001. The experiment was repeated two times with similar results and representative data from one of the experiments is shown. 88

Figure 4.1. Genomic structure and proteins domain in tomato SDG20. A) SDG20 genomic organization, protein structure and domain architecture of SDG20 showing the exons and intron. Exons- dark shaded bars and introns-horizontal lines between the exons. B) Maximum Likelihood phylogenetic analysis of class III SDG proteins from *Arabidopsis thaliana (*At*)*, *Solanum lycopersicum* (Sl), and *Oryza sativa* (Os). Phylogenetic analysis was performed using Mega7 package. The tree is drawn to scale with branch length measured in the number of substitutions per site. Bootstrap values higher than 50% are shown. 101

Figure 4.2. The expression profiles of SDG20 in WT and under different elicitors. A) Tissue specific expression of SDG20 in WT tomato plants. B) *B.cinerea* induced expression of SDG20 in 4 weeks old WT plants treated with 2.5 x10^5 spore/mL *B. cinerea* spore. C) Expression of SDG20 in the mock treated and MeJA and D) Expression of SDG20 in the mock treated and Acc treated WT plants. Bars represent the means; the error bars represent the standard deviations of three technical replicates of each treatment. The β-actin gene was used as an internal control in the qRT-PCR. The experiment was repeated at least 2 times with similar results.....102

Figure 4.3. Molecular characterisation of *sdg20* loss of function mutants. A) Schematic diagrams showing the position of the deletions in *sdg20* mutant. Black shaded boxes represent exons, the grey shaded boxes represent the UTRs boxes represent exon, and introns are shown as horizontal lines. B). SDG20 expression in the mutants. C) Alignment of mutated alleles sequences identified from cloned PCR genotyping fragments and the WT sequences. The mutated alleles include deletions (shown by dashed lines) and insertions (shown by blue letters). Only aligned sequences and the mutations are shown. The targets are shown by letters in red and the protospacer adjacent motif (PAM) is shown by the bold-faced letters after the targets. 103

Figure 4.4. Global histone lysine methylation levels in *sdg20*. Western blot analysis of A) H3K4 B) H3K36 in Wt and, *sdg20* mutants. Core histones were extracted from 4-week old plants and the blot probed with specific H3K4 and H3K36 antibodies. 104

Figure 4.5. Phenotypic Characterisation of in *sdg20* mutant. A) *sdg20* plants are shorter than the WT plants, B) Internode number in the *sdg20* mutant and WT plants. The data shown are the mean ± SE ($n \geq 10$). Asterisks indicate significant differences using Student's t-test (*$P < 0.05$, **$P < 0.01$, ***$P<0.001$). C) Leaf and, D) Flowers and fruits phenotypes of *sdg20* mutant and WT plants, D) Flowers and fruits. 106

Figure 4.6. SDG20 is required for defense against fungal and bacterial pathogens. A) Disease phenotypes of *sdg20* mutants and WT plants inoculated with *B. cinerea*, B) Lesion diameter of *sdg20* mutants and WT plants inoculated with *B. Cinerea.* Bacterial growth in *sdg20* mutants and WT plants inoculated with C) *Pst* DC3000 *hrcC*. The data shown are the mean ± SE ($n \geq 10$) for *B. cinerea*, (n=6) for Pseudomonas assays. Asterisks indicate significant differences using Student's t-test (*$P < 0.05$, **$P < 0.01$, ***$P<0.001$). The experiments were repeated at least 2 times with similar results, representative data is shown.....107

Figure 5.1. Tomato Receptor Like Cytoplasmic Kinases (RLCKs) interacts with tomato RIN4. RIN4- HA was transiently co-expressed with RLCK-MYC by agroinfiltration in *N. benthamiana* leaves. The empty vector expressing MYC was used as a negative control. Anti-HA

(α-HA) and anti-MYC (α-MYC) antibodies were used to detect protein accumulation in input or immunoprecipitated (IP) samples. 117

Figure 5.2. Tomato Receptor Like Cytoplasmic Kinases (RLCKs) interacts with FLS2. FLS2-HA was transiently co-expressed with RLCK -MYC by agroinfiltration in *N. benthamiana* leaves. The empty vector expressing MYC was used as a negative control. Anti-HA (α-HA) and anti-MYC (α-MYC) antibodies were used to detect protein accumulation in input or immunoprecipitated (IP) samples. 118

Figure 5.3. TRKO4, TPKO7, TPKO9 and TPKO9 are required for *B. cinerea* disease resistance. A) Lesion diameter 3 days after drop inoculation with *B.cinerea* spores on TPKO2, TPKO7, TPKO9, TPKO11 and TRKO4 Virus Induced Gene Silenced (VIGS) plants. B) Bacterial growth *(P. syringae) in* VIGs silenced plants. 119

Figure 5.4. Phylogenetic analysis, genomic structures and CRIPR/Cas9 deletions of TRKO4, TPKO7, TPKO9 and TPKO11. A) Maximum Likelihood phylogenetic analysis of RLCKs proteins from *Arabidopsis thaliana (*At*)*, and *Solanum lycopersicum* (Sl). Phylogenetic analysis was performed using Mega7 package. The tree is drawn to scale with branch length measured in the number of substitutions per site. Bootstrap values higher than 50% are shown. Schematic diagram showing gene and CRIPSR/Cas9 deletions of B) TPK07, C) TPK09, D) TPK011 and E) TRK04. Blue shaded boxes represent exons, the black shaded boxes represent the UTRs boxes represent exon, and introns are shown as horizontal lines. F) Relative expression of TRK04 in trk04 mutant alleles. 120

Figure 5.5. Basal and induced expression of TRKO4. A) Tissue specific expression of TRK04 in WT tomato plants. Induced expression of TRK04 in response to B) *B. Cinerea*, C) Methyljasmonate (MeJA), D) 1-aminocyclopropane-1-carboxylic acid ACC, and E) Salicylic acid (SA). Bars represent the means; the error bars represent the standard deviations of three technical replicates of each treatment. The β-actin gene was used as an internal control in the qRT-PCR. The experiment was repeated at least 2 times with similar results 122

Figure 5.6. TRKO4 mediates resistance to *B. Cinerea*. A) *B. Cinerea* disease lesion size and B) disease symptoms of *trk04* mutants. Bars represent the means; the error bars represent the standard deviations of three technical replicates of each treatment. Samples with different letters are statistically significant different (Student's *t* test, $P < 0.001$) 123

Figure 5.7. TRK04 mediates seedling growth responses to Jasmonic acid in tomato. A) Hypocotyl length, B) Overall seedling stature and C) Root length of trk04 mutants and WT seedlings grown in MS medium supplemented with or without Methyljasmonate (MeJA). Bars represent the means; the error bars represent the standard deviations of three technical replicates of each treatment. Asterisk represents statistically significant differences (Student's *t* test, $*p < 0.05$, $**p < 0.01$. $*p < 0.05$, $**p < 0.01$). 124

ABSTRACT

Plants are constantly exposed to biotic and abiotic factors throughout their developmental stages which threaten their growth and productivity. Environmental stresses limit crop productivity and are likely to increase in severity due to the drastic and rapid changes in global climate. In this project, we studied the genetic factors that contribute to plant adaption to pathogens and other environmental factors in tomato. The results of these are presented in chapters 2-4 of this thesis. Chapter 1 covers background information and the review of the current literature in plant responses to biotic and abiotic stress. Chapter 2 deals with functional analysis of tomato histone methyltransferases SDG33 and SDG34 and their role in plant defense and stress tolerance. Chapter 3 focuses on the role of SDG33 and SDG34 on plant responses to Nitrogen. Finally, Chapter 4 summarizes the results from a reverse genetic screen using CRISPR cas9 genome editing to identify Receptor Like Cytoplasmic Kinases (RLCKs) required for plant resistance to fungal pathogens.

Plant responses to environmental cues are underpinned by rapid and extensive transcriptional reprogramming. Post translational modification of histones orchestrate these reprogramming and cellular responses by altering chromatin structure and establishing permissive or repressive states. Histone lysine methylation (HLM) is a principal modification of chromatin that affects various cellular processes. HLM is mediated by histone methyltransferases (HMTs) that deposit methyl groups to specific lysine residues on n-terminal histones tails. Although it is known that chromatin modifications occur in response to environmental cues, the mechanisms by which this is achieved, and the biological functions of HMTs are poorly understood. The function of tomato histone methyltransferases Set Domain Group (SDG)33 and SDG34 in biotic and abiotic stress responses were studied using tomato mutants generated through CRISPR/cas9 genome editing.

SDG33 and SDG34 genes were induced by pathogens, drought stress, the plant hormones methyl jasmonate, salicylate and abscisic acid. The *sdg33* and *sdg34* mutants display altered global HLMs. SDG34 is required for global H3K36 and H3K4 mono, di- and tri-methylation while SDG33 is primarily responsible for di- and tri- H3K36 and H3K4 methylation. Tomato SDG33 and SDG34 are orthologues of the Arabidopsis SDG8, an H3K4 and H3K36 methyl transferase previously implicated in plant immunity and plant growth through epigenetic control of Carotenoid

Isomerase (CCR2) and other target genes. However, the tomato *sdg33* or *sdg34* single mutants showed no altered responses to fungal and bacterial pathogens likely due to functional redundancy of the tomato SDG33 and SDG34 genes consistent with their overlapping biochemical activities. Interestingly, tomato *SDG33* or *SDG34* genes rescued the disease susceptibility and early flowering phenotypes of Arabidopsis *sdg8* mutant. Expression of *CCR2* gene is completely inhibited in Arabidopsis *sdg8* mutant attributed to loss of H3K36 di- and tri methylation at CCR2 chromatin. CCR2 gene expression was partially restored by transgenic expression of tomato *SDG33* or *SDG34* genes in Arabidopsis *sdg8*. In tomato, the single *CCR2* gene is expressed independent of SDG33 or SDG33 genes suggesting that the genomic targets of the tomato HMTs are different. Unexpectedly, *sdg33* and *sdg34* plants were more tolerant to osmotic stress, maintain a higher water status during drought which translated to better survival after drought. Tolerance of *sdg33* and *sdg34* to drought stress is accompanied by higher expression of drought responsive genes. Collectively, our data demonstrate the critical role of tomato HLM in pathogen and stress tolerance likely through the regulation of gene expression.

In parallel, we characterized the role of SDGs in mediating nitrogen responses in tomato. The results are described in Chapter 2. Few studies have focused on the role of histone lysine methylation in regulating changes to nutrient availability. Transcriptome analysis in the shoot and roots showed that SDG33 and SDG34 have both overlapping and distinct regulated targets in tomato. In response to nitrogen, 509 and 245 genes are regulated by both SDG33 and SDG34 in response to nitrogen states in the roots and shoot respectively. In the roots these genes were enriched with GO terms such as 'regulation of gene expression', regulation of N metabolism' and 'regulation of hormone stimuli'. 'Response to stimulus', 'photosynthesis' and 'N assimilation' were the biological processes significantly enriched in the shoots. Overall, we show that SDG33 and SDG34 are involved in regulating nitrogen responsive gene expression and hence physiological nitrogen responses in the roots and shoots.

We also studied the Set Domain Group 20 (*Sl*SDG20) an orthologue of Arabidopsis SDG25 in tomato. The details of our observations are presented in Chapter 3. SlSDG20 belongs to class III HMTs, it has the SET, Post-SET domain and GYF domain important for proline-rich sequence recognition. *SlSDG20* is highly induced by *B. cinerea*, Methyl Jasmonate and Ethylene. To further understand the functions of SlSDG20 in tomato physiological development and plant immunity we generated *slsdg20* knockout mutants through CRSIPR/Cas9. We identified one homozygous

slsdg20 mutant with 151bp deletion in an exon immediately before the SET domain. Global methylation assay on the *slsdg20* mutant confirmed that *SlSDG20* is an H3K4 methyltransferase. The *slsdg20* mutant is shorter than the wild type, produce more adventitious shoots causing prolific branching, and produce narrow leaves. Further, the mutant produces abnormal fruit and few seeds that hardly germinate. The *slsdg20* mutant is highly susceptible to *B. cinerea* compared to the wild type. In response to *Pst* DC3000, *slsdg20* mutant plants are comparable of the wild type. Resistance to *hrcC* strain of *Pst* DC3000 was impaired in the *slsdg20* mutant, suggesting a possible role of *SlSDG20* in PTI. In sum, tomato SDG20 is regulates plant immunity and plant growth including fertility.

The final chapter focuses on tomato Receptor like cytoplasmic kinases (RLCKs). Plants perceive the presence of pathogens through Pattern Recognition Receptors (PRR) which are predominantly RLKs, and subsequently recruit RLCKs to signal to downstream regulators of defense responses. Many RLCKs were characterized from Arabidopsis for their role in signalling of responses to bacterial infection. An example of RLCKs is Arabidopsis BIK1 which is implicated in signal transmission of pathogen recognition event at the cell surface. The tomato genome encodes 647 RLK/RLCKs comprising about 2% of its predicted genes. The functions of most of these predicted tomato RLCKs and RLKs have not been determined. Previously, our lab characterized the Arabidopsis BIK1 and tomato TPK1b RLCKs for fungal resistance. Here, we conducted a reverse genetic screen focused on BIK1 and TPK1b related tomato RLCKs to identify a subset with defense functions. Virus induced gene silencing and pathogen assays conducted on 15 RLCKs identified four RLCK genes with potential role in plant immunity. Then, tomato knock out mutants were generated for four RLCK genes through CRISPR/cas9 genome editing to validate the VIGS data. Subsequently, we demonstrated that TPK07, TPK09, TPK011 and TRK04 are required for resistance to *B. cinerea*. The data are supported by the pathogen induced expression of these genes. Furthermore, *trk04* seedlings are impaired in seedling growth responses to Jasmonic acid. Our study establishes that tomato TPK07, TPK09, TPK011 and TRK04 contribute to defense against *B. cinerea* but their mechanism of function needs to be elucidated in future studies

CHAPTER 1. LITERATURE REVIEW

1.1 Introduction

Plants are not able to move in nature, hence are constantly exposed to environmental pertubations throughout their developmental stages. Adverse environmental conditions are detrimental to plant growth, development and reproduction. Environmental stresses can be classified as biotic and abiotic stresses. Biotic stress in plant is caused by living organisms such as insects, fungus, bacteria, viruses and weeds. In contrast, abiotic stresses are caused by non-living factors such as drought, heat, cold, flooding, salinity, and nutrient deficiencies (1). Plants have evolved several adaptive mechanisms to minimise damage while conserving resources for growth and reproduction under environmental stresses. Mechanisms involve physiological and biochemical changes activated and sustained by changes in the expression of genes required for stress response. Changes in gene expression in response to stress involve a complex regulatory network at the transcriptional and post transcriptional levels (2-4). Numerous studies have highlighted and improved our understanding of the complex regulatory networks involved in these mechanisms. Among these, epigenetic mechanisms which modulates chromatin structure or regulate the accumulation of RNA at post transcriptional level have often been associated with changes in gene expression during exposure to stress. Epigenetics is defined as heritable changes in gene expression resulting from the changes in DNA and it associated chromatin proteins without a change in the underlying nucleotide sequences (2, 5). Thus, epigenetic changes are reversible, and are associated with both activation and repression of genes.

Eukaryotic DNA is packed into chromatin, to tightly fit into the nucleus. The basic structure of chromatin is the nucleosome composed of 147bp of DNA wound around an octameric core of histone proteins H2A, H2B, H3 and H4. Chromatin forms a compact architecture which is a barrier to DNA templated processes. Alteration of chromatin structure modulates the ability of the transcriptional machinery to access DNA and control gene expression. Alteration in chromatin structure is achieved by different mechanisms including DNA methylation, histone post translational modifications, histone variants and small RNA related pathways (6-9). Many studies have provided wealth of information on how these mechanisms regulates responses to environmental stimuli mainly in model plants. However only a few studies have focused on histone

lysine methylation (HLM) as a regulatory mechanism of drought and changes to nutrient availability. Hence in this chapter, we will discuss histone lysine methylation changes in drought and nutrient stress. We will highlight the mechanisms of histone lysine methylation in regulating drought and nutrient stress responses.

1.2 The histone code

Genomic DNA in eukaryotes does not appear as free linear strands, it is condensed into nucleoprotein complex called chromatin. The basic structural unit of chromatin is the nucleosome which is made up of approximately 147 base pairs of DNA wound around a histone octameric core with two cores of each histone proteins H2A, H2B, H3, and H4. The histone linker protein H1 locks DNA into place by binding at the entry and exit sites of DNA thus creating a compact hierarchical architecture (Olins and Olins 2003, Lugerand Hansen 2005). Based on compactness chromatin is classified as heterochromatin and euchromatin. Heterochromatin represents condensed states and is aligned to the repressed transcriptional state whereas euchromatin represents an open state and is aligned to an active transcriptional state. Condensed chromatin state poses a barrier to all DNA templated processes such as transcription and DNA repair. Histones have N-terminal tails rich in basic amino acids which protrude from the nucleosomes, and these can be modified by acetylation, methylation, ubiquitylation, sumoylation, ADP-ribosylation, deamination, Proline isomeration, and phosphorylation (6, 10). Current models suggest that these modifications form the so called 'histone code' which influence chromatin structure, affecting accessibility of the transcriptional machinery to the corresponding DNA thus modulating gene expression and/or repression. In plants, changes in chromatin structure have been shown to affect different biological processes such as flowering, root growth, embryogenesis, organogenesis and responses to stresses (11).

1.3 Histone lysine methylation (HLM)

HLM is the transfer of methyl groups from the cofactor S-adenoslymethionine (AdoMet) to the ε-nitrogen of specific lysine and Arginine residues of on the N-terminal tails of histone H3 and H4. Lysine residues can be mono-, di- or tri methylated while Arginine residues can be monomethylated and asymmetrically or symmetrically di-methylated (6). Histone methyl

transferases (HMTs) have a conserved SU- (VAR) 3-9, Enhance of zeste E (Z) and Trithorax (TRX) (SET) domain originally identified in *Drosophila*. Notably, the SET domain is responsible for the enzymatic activity and is highly conserved in Bacteria, Archaea, and Eukaryota. To date, four lysine residues within histone H3 (K4, K9, K27 and K36) have been identified as being methylated by SET domain histone-lysine-methyltransferases (SDG proteins) in plants. Humans however have an additional lysine within histone H4 (K20) which is methylated by SDG proteins and one lysine within H3 (K79) which is being methylated by a non-SET-domain containing protein HKMT7 (6).

HLM has emerged as an important epigenetic mark that play differential roles in transcriptional regulation depending on the methylated residue and degree of methylation (mono-, di-, or tri-) (6, 10). Most actively transcribed genes are associated with H3K4 me1, H3K4me2, H3K4me3, H3K36me1, H3K36me2 and H3K36me3 (12). However, distribution of these methylation marks is not uniform across actively transcribed genes, each modification is enriched at a specific region. In plants, H3K4me2/3 are enriched at the 5' end of the transcribed regions, downstream of the transcription start site (TSS). The reminder of the transcribed region has H3K4me1 methylation marks. H3K36me3 is typically associated with H3K4me2 at the 5' end of the gene body while H3K36me2 is found near the 3' prime end of transcribed genes. H3K36me1 covers the 3' prime end as well as few base pairs downstream of the polyadenylation site (13, 14). H3K4me3 is important for many developmental processes and together with H3K4me2 they are linked to memory of environmental stresses such as diseases, drought and heat (15-17). Consistent with the fact that H3K4 and H3K36 are important for active transcription, several genes are downregulated in H3K4 and H3K36 loss of function mutants. Further, these mutants have several developmental defects (18-23). While several genes are downregulated in many H3K4 and H3K36 loss of function mutants, many other genes remain unchanged. For example, in Arabidopsis *sdg2* and *sdg8,* there is a decrease in global H3K4me3 and H3K36me3 respectively, yet transcriptional expression of several other genes remains unchanged. This suggest that H3K4 and H3K36 methylation act at a specific time or in response to environmental stimuli on specific genes to regulate the expression of genes (13).

In Arabidopsis, H3K27me1 is associated with heterochromatin, H3K27me2 is associated with gene rich euchromatin regions and repeat rich heterochromatin regions and H3K27me3 is enriched transcribed in regions of repressed genes (24, 25). H3K27me3 in plants is important for

developmental stage transition during seed germination, flowering, gametogenesis and fertilisation. SDG proteins MEDEA (MEA), CURLY LEAF (CLF) and SWINGER (SWN) are required for H3K27me3 mediated silencing of important developmental regulatory genes. CLF and SWN are required for repression of floral homeotic gene AGAMOUS and the homeobox SHOOTMERISTEMLESS (STM) in seedlings and the MADS-box gene PHERES (PHE1) in vegetative tissues. MEA is required for the repression of the maternal allele of PHE1 in endosperm and the developing embryo (26, 27). Epigenetic reprograming between generations also require H3K27me3, the flowering repressor *FLC* is silenced after prolonged cold by H3K27me3 HKMTase *PRC2*. Accumulation of H3K27me3 on *FLC* keeps the memory of cold in *cis* and can be inherited through cell division (28). H3K9me2 is enriched on heterochromatin and silenced transposons while H3K27 is distributed on genic regions. In *Arabidopsis*, H3K9 methylation is maintained by SUVH proteins. SUVH2, SUVH4 (KYPTONITE), SUVH5 and SUVH6 are required for the maintenance of H3K9me1 and H3K9me2 mediating transposon repression and DNA methylation (29-31). Also, mutation in the rice SDG714 which is required for H3K9 methylation causes activation and transpositioning of TOS17, a rice transposable element (32).

1.4 Plant responses to water stress

Drought can be defined as absence of adequate water necessary for plant to grow normally and complete its life cycle (33). Drought disrupts many cellular processes and whole-plant functions negatively affecting plant growth and reproduction. However, plants are remarkably plastic, they have evolved mechanisms to cope with drought stress to benefit their growth and development. Mechanisms are complex, they involve an array of molecular, cellular, morphological, physiological and biochemical adaptions (7, 34, 35). Plant responses to drought stress can be grouped into drought avoidance, drought escape, drought tolerance and drought recovery (36). Drought avoidance is the ability of a plant to maintain higher tissues water content in the presence of water stress. Here a plant is able to maintain fundamental physiological processes by adjusting morphological structures and certain growth parameters under drought stress (34, 36). Plants avoid drought by 1) enhancing soil water uptake by enhanced root system, increased hydraulic conductance and enhancing water storage abilities in specialised organs such as tubers, 2) limiting water loss by reducing transpiration through stomatal closure, leaf rolling, increased accumulation wax on leaf surfaces and reducing net radiation and 3) using water

efficiently through reducing plant size, leaf size, leaf area index etc (34, 36, 37). Drought escape is when rapid plant development enables a plant to complete its life cycle before the onset of seasonal or climate drought. Mechanisms for drought escape include rapid phenological development and developmental plasticity. Rapid phenological development is a result of very high metabolic rates, resulting in progressive cell expansion and division. This, together with high gas exchange rates facilitates effective photosynthesis and photorespiration with low water use efficiency resulting in very rapid plant development. Plants with developmental plasticity assumes alteration of phenological development in response to drought. Phenological development may be accelerated or slowed down to cope with the stress (38, 39). Drought tolerance is the capacity to sustain plant function under drought stress. Plant function is maintained through adaptive traits such as osmotic adjustments, cellular elasticity, increasing protoplasm adjustments and alleviation of drought damage (36, 37). Drought recovery encompasses the plant's ability to resume growth and development after an exposure to severe drought stress which causes complete loss of turgor pressure and leaf hydration (36). These responses are not mutually exclusive, in nature plants can combine a range of response types. Further, these responses are controlled by molecular mechanisms that regulate the expression of genes. In the following sections we discuss the widely known physiological processes important for drought stress response, and the molecular mechanisms that regulate them.

1.4.1 Physiological mechanism of drought response

1.4.1.1 Leaf traits

Leaf morphological and physiological traits importantly encompass the early responses in drought stress. Leaf responses to drought stress are important to reduce water loss through transpiration and promote higher water use efficiency. Leaf elongation is a function of cell turgor pressure, cell wall extensibility and cell wall threshold. However, under drought stress cell turgor is less than cell wall threshold, therefore, there is a reduction in leaf elongation, size and in the long run plant growth. Farooq and others reported that applied drought reduced leaf number, leaf specific area and total area (40). In another study, increase in drought intensity reduced leaf area index, leaf area duration and shoot dry matter of legumes (41). Further drought condition decreased leaf are index in soybean plants compared to well-watered conditions (42). Another

response to drought stress is leaf senescence mediated by the enhanced synthesis of the hormone ethylene under drought stress. Shedding of older leaves contributes to water saving through reduction in transpiration (34). In sunflower, drought caused early senescence, resulting in reduced leaf area, tiller formation and leaf expansion (43). Plant also respond to water stress by developing xeromorphic traits such as smaller and thicker leaves, more epidermal trichomes, thicker cuticle epidermis, smaller and denser stomata. These traits reduce water loss and increase water retaining abilities of plants to cope with drought stress (34, 36).

Stomatal closure, reduction in stomatal size and number under drought exposure is another early response to drought stress. Stomatal closure reduces excessive water loss through transpiration and leaf dehydration. Reduction in stomata size and number is associated with survival under drought conditions. Stomata density has been shown to increase under moderate water deficit while it declines under severe drought (44). Opening and closing of the stomata is controlled by the growth retardant hormone abscisic acid ABA. ABA synthesis is triggered by decrease in soil water content and leaf turgor. In addition to ABA, cytokinin also regulate stomata closure. In Arabidopsis and tomato increased ABA content results in reduced stomata aperture and concomitantly drought stress resistance (45, 46). Stomata closure is also controlled by the hydraulic architecture of the leaves and stems, carbon dioxide concentration, light intensity and leaf temperature. Hence at a given time stomata closure may not necessarily be in response to drought stress but may be responding from a complex set of factors (34, 35).

1.4.1.2 Photosynthesis

Drought stress causes metabolic changes that causes functional and structural rearrangement of the photosynthetic apparatus resulting in lower photosynthetic rates. Lower photosynthetic rates are directly caused by stomatal limitations and metabolic impairments and indirectly by damage caused by oxidative stress and photoinhibition (47, 48). Stomatal limitations are a consequence of decline in leaf turgor which concomitantly results in stomata closure, affecting intercellular carbon dioxide (CO_2) concentration and CO_2 assimilation rate (48, 49). In a study in soybean, stomatal conductance was responsible for reduced photosynthetic rates under drought stress (50). In early period of water stress, stomatal limitations play a major role in reducing photosynthesis in alfalfa (51), ash and oak trees (52). Mesophyll conductance is the diffusion of CO_2 from the sub stomata cavities to the carboxylation sites in the chloroplast. Under

drought stress mesophyll conductance is reduced due to resistance in CO_2 diffusion through the liquid phase or by alteration of the intercellular spaces structure due to leaf shrinkage (48, 53). Photosynthesis limitation under drought stress is determined by CO2 limitation at the carboxylation sites which is determined by stomata conductance and mesophyll conductance (53). Reduced supply of CO_2 during prolonged water stress causes inhibition of photosynthetic enzymes, decarboxylation of RuBiSco the key enzyme for carbon metabolism in the leaves and reduction in ATP synthesis. Riboluse 1.5 Biphosphate (RuBP) carboxylase regeneration was reduced due to drought stress and affects CO_2 saturation rate of photosynthesis (54-56). Furthermore, decrease in RuBP regeneration was linked to drought induced impairment of ATPase in the chloroplast (57). As relative water content (RWC) falls, ATP synthesis decreases causing a limitation in photosynthesis due to decreased ATP supply (58, 59). Continuous photosynthetic light reactions during drought stress causes damage to the photosynthetic apparatus and oxidative stress through the production of reactive oxygen species (ROS). Oxidative stress is measured by malondialdehyde (MDA) content and the presence of hydrogen peroxide. In tomato, drought sensitive cultivars had higher accumulation of hydrogen peroxide and MDA levels while drought tolerant transgenic lines had less (46). Studies have reported that stomatal limitations may be recognised as a major factor for reduction in photosynthesis in mild or early stages of drought stress while non-stomatal limiting factors are a major factor at high drought stress intensity and persistence duration (34).

1.4.1.3 Modulation of root architecture

The plant root system is the primary site that perceive drought stress signal and its growth is affected by drought stress. Depth and elongation of the primary root as well as lateral root number is adjusted to sustain the plant during drought stress. This adjustment is mediated by the phytohormone ABA in antagonism with auxin through unknown mechanisms (60). Primary root growth is not affected by drought stress but number and growth of lateral roots is significantly reduced (61). Upon mild drought stress, there are increases in expression of genes encoding enzymes important in root morphology like xyloglucan endotransglucosylase. The expression of these enzymes is positively corelated to root growth (62). In Arabidopsis, activation of *HDG11* causes extensive root system with deeper and more lateral roots and reduced stomata density enhancing drought tolerance (63). However, in another study also in Arabidopsis the R2R3-type

MYB transcription factor MYB96 overexpressing mutant shows enhanced drought tolerance with reduced lateral root formation (45). In addition to lateral root growth, other different anatomical root traits such as suberisation and compaction of sclerenchyma cells have been reported in response to drought stress. Suberisation and compaction of sclerenchyma cells decreased whereas suberisation of the endodermis increased under drought stress in rice plants (64).

1.4.2.4 Osmotic adjustment

Osmotic adjustment is when plants accumulate osmotically active molecules/ions in the cytochylema to increase water relations. Accumulation of solutes lowers the osmotic potential, causing water to move into the cell and increases turgor maintenance. In addition, these solutes stabilise enzymes and proteins, protect the cell membranes and the metabolic machinery against oxidation under drought stress (34, 36, 48). Studies have shown that drought resistant wheat varieties have a greater capacity of osmoregulation than less resistant varieties (65). Organic compounds such as mannitol, proline, glycine, betaine, trehalose, fructan, inositol and inorganic ions are the known predominant solutes that accumulate in response to water stress. Proline accumulation is widespread response under water stress in higher plants. Proline accumulation increased in pea cultivars under water stress (66) and drought tolerant Petunia varieties accumulated free proline which acted as an osmoprotectant under water stress (67). Overexpression of Arabidopsis Enhanced Drought Tolerant 1 (*AtEDT1*) in cotton and poplar increased drought tolerance through accumulation of solutes such as proline and soluble sugars (68). Inorganic ions such as K^+, Ca^{2+}, Na^+ and Cl^- contribute to osmotic adjustments by maintaining ion transport processes under drought stress (4, 48, 69). In soybean, drought stress treatment increased accumulation of phosphorus (P), potassium (K), calcium (Ca), molybdenum (Mo), manganese (Mn), copper (Cu), and zinc (Zn) compared to well-watered treatments (70). It should be pointed out that osmotic adjustment mechanisms are not in effect until severe dehydration occurs, suggesting that the mechanism is for survival under drought stress (71).

1.4.2.5 Antioxidant defense system

Oxidative stress describes damage caused by reactive oxidative species (ROS) such as hydrogen peroxide (H_2O_2), the superoxide ($O_2^{\bullet-}$) and hydroxyl ($OH^{\bullet}$) radicals and the singlet ($^1O_2$).

Under normal circumstances, plants have an antioxidant system that scavenges for ROS making the system operate in a dynamic equilibrium between generation and removal of ROS. Drought stress accelerates the production of ROS breaking this equilibrium and causing excessive accumulation of ROS. Production of ROS is linear with the severity of drought stress (72). ROS may react with carbohydrates, proteins and DNA causing oxidative damage and impairing normal functioning of the cell (36, 72, 73). Furthermore, the membrane phospholipids and fatty acids are sensitive to over accumulation of ROS, resulting in lipid peroxidation of membranes (36). Plant antioxidant systems consist of non-enzymatic antioxidants (ascorbic acid (ASH); glutathione (GSH); phenolic compounds, alkaloids, nonprotein amino acids, and a-tocopherols) and enzymatic systems (ROS detoxification and scavenging; superoxide dismutase (SOD); catalase (CAT); ascorbate peroxidase (APX); glutathione reductase (GR); monodehydroascorbate reductase (MDHAR); dehydroascorbate reductase (DHAR); glutathione peroxidase (GPX); guaicol peroxidase (GOPX); glutathione-S- transferase (GST); and lipoxygenase (LOX1) (74). Overexpression of *Solanum penilli Annsp2* gene in cultivated tomato increased drought tolerance by elimination of ROS. The transgenic plants had lower lipid peroxidation, increased peroxidase activity including CAT, APX and SOD and higher proline content under drought stress (46). In wheat, a drought tolerant cultivars showed higher membrane stability index, lower H_2O_2 accumulation, higher activity of antioxidant enzymes CAT, APX, GPX and SOD under water stress compared to the sensitive genotype (75).

1.4.2.6 Phytohormones

Phytohormones play an important role in plants' response to drought stress by mediating a wide range of adaptive processes. Under drought stress, the endogenous abscisic acid and ethylene increases while that of auxin, gibberellins and cytokinin decrease (72). Decreasing water availability in soil is perceived by the roots resulting in increase of ABA release from the stellar tissues of the root to the xylem for transport to the shoot (76). ABA is also produced in the leaf veins and specialised guard cells (77). Guard cells respond rapidly to the increasing ABA levels by closing the stomata reducing transpirational water loss (76). Inhibited leaf production, growth and development is another response by the shoot to increase in ABA concentrations. In addition, ABA acts as a signal that initiates varieties of responses involved in adaptation to water stress. ABA dependent processes are crucial to plant response to water stress, ABA deficient mutants are

susceptible to water stress (78, 79). Overexpression of ABA responsive binding elements in Arabidopsis resulted in hypersensitivity to ABA, reduced transpiration and enhanced drought tolerance (80). In tomato, *Annsp2* overexpressing transgenic plants have enhanced ABA production under drought stress, which resulted in stomata closure and reduced water loss (46). Cytokinins is antagonistic to ABA, and drought stress results in decreased levels of cytokinin. However, both up and down regulation of cytokinins were reported to enhance drought tolerance (81-83). Cytokinins regulate plant growth and stabilise the photosynthetic machinery during drought stress. Ethylene mediates drought stress response by negatively affecting plant growth and development, inducing foliar abscission and leaf senescence. Ethylene positively regulates drought response, ethylene mutants or mutants that repress ethylene emission are susceptible to drought stress (84-86). Auxins play a key role in drought stress response by inducing new root formation, and a prolific root system is important for drought stress response. Drought stressed plants limit the production of auxin when ABA and ethylene contents increase. However, several studies have shown that elevated auxin levels in transgenic plants expressing auxin biosynthesis genes *YUCCA7* and *YUCCA6* in Arabidopsis and potato respectively enhanced drought tolerance (87, 88). These studies suggest that auxin contributes to drought tolerance through regulation of root architecture, ROS metabolism and ABA responsive gene expression. On the other hand, Park and others showed that overexpression of *GH3* lowered IAA levels, reduced growth and enhanced drought tolerance (89). Thus, the role of auxin and drought response is complex and the specific role of auxins in drought stress remain elusive.

1.5 Molecular mechanism of drought response.

Plants perceive drought stimuli through direct perception of osmotic imbalance across the membrane or indirectly by perceiving the indirect effects of osmotic imbalance on the membrane, cell wall or membrane-cell wall system (90). The signal perceived is transmitted through multiple signal transduction pathways resulting in the expression of drought responsive gene expression and specific drought response. Secondary messengers such as Ca2+, ROS, phosphogycerol, diglycerol, ABA and transcriptional regulators play significant roles in signal transmitting pathways (36). Several Calcium dependent protein kinases (CDPK) and mitogen activated protein kinases (MAPKs) have been identified in plants subjected to water stress and have been shown to transduce the dehydration signal form the membrane to the nucleus (91). After signal perception

and transduction events, cell to organ response diverge into two pathways; ABA dependent and ABA independent pathways.

ABA dependent pathway like the name suggest is dependent on the accumulation of ABA activating various stress responsive genes whose products are either regulatory such as protein kinases or functional such as aquaporins or enzymes for osmoprotectant synthesis. The ABA signal is perceived by three different type of cellular receptors; nucleocytoplasmic, plasma membrane, and chloroplast receptors (92-94). Binding of ABA to PYR/PYL/RCARs nucleocytoplasmic receptors results in inactivation of type 2C protein phosphatases (PP2Cs). This inactivation activates accumulation of sucrose non-fermenting 1-related protein kinase 1 (SnRK2) which in turn regulates ABA responsive two basic leucine zipper (bZIP) transcription factors ABA-responsive element binding protein/ABRE-binding factor (AREB/ABF). These transcription factors bind to ABA-responsive cis element (ABRE) on the ABA-regulated genes and activating their expression and thus physiological response (48, 95). ABRE motifs are important *cis*-acting elements controlling the expression of ABA responsive expression of response to dehydration 29B *RB (29B)* and 9-cis-epoxycarotenoid dioxygenase (*NCED*) in Arabidopsis (96, 97). MYC, MYB, NAC, and RD26 are other transcription factors that induce the expression of drought responsive genes in an ABA dependent manner. The Arabidopsis *MYC2* and *MYB2* transcription factors bind to *cis*- acting elements on response to dehydration 22 (*RD22*) promoter and cooperatively activate *RD22* in response to drought (98). The ABA dependent pathway regulates the expression of genes that results in cellular osmotic adaptation, ROS scavenging and detoxification, membrane stability and maintenance of cellular energy and supply (3, 99).

The ABA independent pathway relies on the osmotic stress signal to regulate the expression of drought responsive genes. Transcription factors C repeat binding factor (*CBF*) 1 and DRE-binding protein (*DREB1 & 2*) bind to *cis*-acting element DRE/CRT (dehydration-responsive element/ C-Repeat) of drought responsive genes inducing their expression (48). Another transcription factor NAC binds to the cis-acting element of early response to dehydration 1 (*ERD1*) (100). ABA independent pathway results in expression of genes involved in Late embryogenesis abundant (LEA) and, dehydrins protein synthesis as well as proteins involved in membrane stability (99). Some drought responsive genes share the ABA dependent and ABA independent pathway for their induction. A gene may have both ABRE and DRE elements in its promoter or may be induced downstream of the first stress recognition and signalling event.

Arabidopsis *RD29A* contains both a DRE and ABRE and is independent of ABA in the early hours of dehydration but dependent on ABA in the later stages of expression (101). Furthermore, studies have shown that ABA-dependent proteins *AREB1/AFB2*, *AREB2/ABF4* and AFB3 interact with ABA independent *DREB2A*, *DREB1A* and *DREB2C* in regulating drought response (102, 103). A NAC transcription factor *ANACO96* in the ABA independent signalling pathway physically interact with ABA-dependent transcription factors ABF2 and ABF4 to regulate gene expression in response to drought stress (104). These studies show that there is a complex relationship between the ABA dependent and ABA independent signalling pathways in response to drought.

1.6 Epigenetic regulation of plant responses to drought stress

Epigenetics is the study of heritable phenotype changes that do not involve alteration of DNA sequence. Epigenetic mechanisms include DNA methylation, histone modifications, chromatin remodelling, and regulation mediated by non-coding RNA like micro RNAs (miRNA) and long non-coding RNAs (lncRNA). Here we review the role of DNA methylation, the histone modification histone lysine methylation, and small RNA mediated DNA methylation in regulating drought response.

1.6.1 DNA methylation

DNA methylation involves the addition of methyl groups to the fifth carbon atom of cytosine or the sixth nitrogen atom of adenine nucleotides. Cytosine methylation occurs in three sequence contexts CG, CHG and CHH (were H can either be A, C or T but can never be a G). In plants, DNA methyltransferase 1 (DMT1) and chromomethylatransferase 3 (CMT3) maintain symmetric (on both DNA strands) CG and CHG methylation. Asymmetric methylation on the CHH sites is maintained by domain rearranged methyltransferase 2 (DRM2) via the RNA-directed DNA methylation (RdDM) pathway (105-107). Owing to its heritability DNA methylation is a powerful means of supressing the expression of unwanted or excess genes. Drought stress induces genome wide DNA methylation changes leading to altered gene expression level. Both DNA hypermethylation and hypomethylation have been reported in response to drought stress. DNA hypermethylation at CG and not CHG sites at two heterochromatic loci have reported in tobacco cell suspension culture under osmotic stress (108). DNA hypermethylation has been reported on

pea root tips under water deficit and has associated with playing a direct role in reducing metabolic activity. In tomato, brief exposure to simulated drought causes removal of methylation marks on the CHH sites regulatory body of *Asr2 (109)*. Further, in rice, drought stress reduced DNA methylation levels in roots and leaves of the two lines analysed at the tillering stage. The two lines 'DK151' and its recurrent parent 'IR64' showed differential DNA methylation pattern, which accounted for drought tolerance in 'DK151' and susceptibility in 'IR64' and these drought induced methylation patterns were reversed upon recovery (110). Also in rice, DNA hypermethylation and hypomethylation was reported in drought tolerant and drought susceptible cultivars respectively (109).

Small RNA (siRNA) mediate sequence specific de *novo* DNA methylation through the RdDM pathway. Recently siRNAs have emerged as important modulators of drought response via the control of drought responsive genes. The rice miR820 and its target OsDRM2 are downregulated by drought stress. miR280 is processed by DCL1/3 to produce miR820.1 and miR820.2. miR820.1 is involved in cleaved of DMR2 by AGO1 and miR820.2 mediates DNA methylation of its loci and of its target OsDRM2 (111). Drought induced miRNA downregulate their target mRNAs which may be proteins involved in negative drought stress responses. On the other hand, the downregulation of other miRNAs leads to the accumulation of their target mRNAs that contribute to the positive drought stress response. In soybean, 8 miRNAs are upregulated in the drought sensitive cultivar (Br16) while the same set had higher basal level and downregulated under drought stress in the drought tolerant cultivar (Embrapa) (112). Conversely, miR166f had the same basal level in both cultivars, but upregulated in the sensitive cultivar and downregulated in the tolerant cultivar (112). Similarly, in rice, miR408-3p decrease upon drought stress in sensitive cultivars (PB1and IR64) but up-regulated in drought tolerant cultivars (Vandana and N22) (113).

1.6.2 Histone post translational modification

Histone acetylation

Histone acetylation plays important roles in regulating gene expression and thus many different biological processes. Histone acetylation occurs on specific lysine residues of histone proteins H3 and H4 and is catalysed by histone acetyltransferases (HATs). Deacetylation reverses

acetylation and is catalysed by histone deacetylases (HDACs). Histone acetylation reduces charge interaction between histone protein and DNA resulting in activation of gene expression whereas histone deacetylation increases the charge interaction between histone proteins and DNA resulting in transcriptional repression (2, 6). Eukaryotic euchromatin is marked by H3K9ac, thus, H3K9ac has been consistently associated with gene activation. Under drought stress conditions, H3K9ac is enriched on drought responsive genes *RD2A*, *RD29B*, RD*20* and *At2g20880* in Arabidopsis. Upon rehydration, H3K9ac is removed on these genes (114, 115). In rice, drought stress induced the expression of four HAT genes *OsHAC703*, *OsHAG703*, *OsHAF701*, and *OsHAM701*; and was corelated to the enhanced global acetylation of H3K9, H3K18, H3K27, and H4K5 (116). Recently Li and others (117) have shown that in *Populus. trichocarpa*, ABA responsive element (ABRE) binding protein PtrAREB1-2 binds to ABRE motifs associated with drought responsive genes *PtrNAC006*, *PtrNAC007*, and *PtrNAC120* and recruits the histone acetyltransferase unit ADA2b-GCN5. This recruitment enables GNC5-mediated H3K9 acetylation at *PtrNAC006*, *PtrNAC007*, and *PtrNAC120* genes and thus their activation under drought stress. Overexpression of *PtrNAC006*, *PtrNAC007*, and *PtrNAC120* enhances drought tolerance in *P. trichocarpa* (117).

Recent studies also indicated the role of HDACs in drought stress tolerance. In Arabidopsis, *HDA9* act as a negative regulator of drought stress response. In *hda9* drought stress related genes are upregulated and hyper-deacetylated. The mutant shows enhanced tolerance to drought stress (118-120). Overexpression of plant specific HD2 type HDACs; *HD2C* and *HD2C* in Arabidopsis enhance drought tolerance (121, 122). Further, *HD2C* functionally associates with *HDA6* to regulate ABA responsive genes through histone deacetylation (123). In rice, overexpression *HDT701* also a HD2 type HDAC result in drought stress tolerance (124). *HDA6* regulates the drought responsive gene network in which plants trigger acetate synthesis to stimulate the jasmonate (JA) signalling pathway to confer drought tolerance (125).

Histone lysine methylation

HLMs regulate transcription of drought stress responsive genes whose products function in drought tolerance and response. In a study to establish the whole genome pattern of H3K4me1, H3K4me2 and H3K4me3 under dehydration stress conditions, van Dijk and others (126) observed a correlation between H3K4me3 enrichment and the transcript levels of drought responsive genes in Arabidopsis. Similar findings were reported in moss (127) and rice (128). Consistent with these

findings, H3K4me3 was found to gradually increase in response to dehydration stress on four drought inducible genes *RD2A*, *RD29B*, RD*20* and *RAP2.4* and was corelated to their upregulation in Arabidopsis (114). Further, Arabidopsis ATX1 a H3K4me3 methyltransferase, regulates the transcriptional induction of *RD2A* and *RD29B* in an ABA-dependent manner during dehydration stress. ATX1 plays a role in drought stress signalling both in the ABA dependent and ABA independent pathway and *atx1* mutant show decreased tolerance to dehydration. Sensitivity to drought stress of *atx1* is in part by reduced ABA synthesis resulting from low transcript levels of NCED3, a key enzyme in stress induced ABA synthesis. ATX1 is required for the increased levels of *NCED3* transcripts and nucleosome H3K4me3 enrichment during drought stress (16, 129). ATX1 also regulates the expression of ABA-independent pathway genes under drought stress like *RD29A* (114).

Heritability of chromatin modification through mitosis and meiosis offers potential mechanism of storage of information on environmental stress events in the lifespan of an individual (somatic memory) and across generations (transgenerational memory). Studies have reported histone lysine methylation changes under drought stress are maintained upon rehydration as a mechanism of stress memory (115). In a study on drought-inducible genes *RD20, RD29A* and *AtGOLS2* and a rehydration-inducible gene *ProHD*, H3K9ac and H3K4me3 were enriched on these genes during drought stress. Upon rehydration, H3K9ac was rapidly removed from these genes, but H3K4me3 was gradually removed and was maintained at a low level after rehydration on these genes suggesting that H3K4me3 may function as a mark for stress memory (115). During recurring dehydration stresses Arabidopsis plants showed increased rates of transcription and transcript level of a set of drought inducible genes (trainable genes) as a sign of transcriptional memory of the stress. The transcriptional memory was associated with high H3K4me3 marks on the trainable genes and lasts as long as transcriptional memory response last (17). These studies suggest the role of histone methylation in inheritance of stress memory, however it's still debatable whether these changes are inherited across generations or that they can be translated into adaptable traits.

Regulation of pathogen responses by histone lysine methylation

Plant pathogenic fungi can be classified as biotrophs, hemi-biotrophs and necrotrophs. Biotrophic pathogens live in their host obtaining nutrients from them, while necrotrophic

pathogens kill their host before or during colonization and acquire nutrients from the dead cells. Hemi-biotrophs have a characteristic biotrophic phase during early infection stages and later kill their host to complete their life cycle on dead cells. Despite of the differences in pathogen's mode of infection plants respond by distinct yet overlapping mechanisms that impede the establishment of pathogens. Plants recognize conserved pathogen molecular structures called pathogen associated molecular patterns (PAMPs) and plant generated molecules that signals damage called damage associated molecular patterns (DAMPs) to perceive danger and induce defense responses called pattern triggered immunity (PTI). PTI is a basal form of defense response and is independent of the lifestyle of the pathogens. Salicylic acid (SA) pathway, hypersensitive response (HR) and programmed cell death mediate resistance to biotrophic pathogens. While resistance to necrotrophic pathogens is mediated by perception of chitin, polygalacturonase, oligogalacturonides fragments, among others, triggering a typical PTI response (130, 131). Defense responses such as camalexin, cell wall composition and plant hormones such as ethylene (ET) and jasmonic acid (JA) are activated in response to perception of pathogens which then mediate plant immunity to necrotrophs (132-136).

Recently, HLM has emerged as one of the mechanisms that modulate plant immunity to biotrophic and necrotrophic pathogens (137). In *Arabidopsis thaliana*, 49 SET domain group (SDG) proteins have been identified and 31 have or are thought to have histone methyltransferase activity (137, 138). *Arabidopsis* SDG proteins play an important role in many plant developmental processes (139). More importantly *SDG8* and *SDG25* are required for the expression of genes involved in plant defense making them important players in the regulation of plant immunity to bacterial and necrotrophic pathogens. SDG8 is an H3K36 and/ or H3K4 methyl transferase required for H3K36me3 of *LAZARUS 5 (LAZ5),* a TIR-class NB-LRR R-protein, regulating its transcription and to maintain its transcriptionally active state. In the same study, *SDG8* mutation resulted in low H3K36me3 on chromatin of *RPM1* and *RPS5* regulatory regions and thus their low transcripts which corroborated to susceptibility to *Pseudomonas syringae* DC3000 expressing *AvrRpm1* and *AvrPphB,* respectively (140). *SDG25/ATRX7* an H3K4 methyltransferase, was shown to interacts with MODIFIER OF SNC1 9 (MOS9) and this interaction is required for the full expression of *suppressor of npr1-1, constitutive 1* (*SNC1*) and *RECOGNITION OF PERONOSPORA PASITICA 4 (RPP4*) which are Toll Interleukin1 Receptor (TIR) like Nucleotide Binding Leucine Rich Repeat (NB-LRR) containing R-proteins (TIR-NLR) involved in plant

immunity. Furthermore, loss of *SDG25* results in reduced H3K4me3 marks on the promoter region of *RPP4* and *SNC1* which correlates to their reduced expression and thus increased susceptibility to *Hyaloperenospora arabidopsidis* (141).

SDG8 is required for the expression of *PLANT DEFENSIN1.2 (PDF1.2), VEGETATIVE STORAGE PROTEIN2 (VSP2)* and *Mitogen-Activated Protein Kinase (MAPK) Kinase 5 (MKK5)* genes involved in the JA/ET mediated defense pathway in response to *B. cinerea* and *Alternaria brassicicola* thus playing an important role in plant immunity to necrotrophic pathogens. We identified orthologues of *AtSDG8* and *AtSDG25* tomato. Arabidopsis *SDG8* is orthologous to tomato *SlSDG33* and *SlSDG34* and *AtSDG25* is orthologous to *SlSDG20*. The results described in chapter 2 of this thesis demonstrate that expression of *SlSDG33* or *SlSDG34* rescues the disease susceptibility of the Arabidopsis *sdg8* mutant to *B. cinerea.* In addition, tomato mutants in the *SlSDG20 gene displayed* susceptibility to *B. cinerea*. *SlSDG33, SlSDG34* and *SlSDG20* are induced by *B. cinerea* and Methyl Jasmonate.

1.7 Rationale and objectives

Despite the overwhelming evidence for the important role histone methyltransferases play in plant environment stress response the underlying mechanism of their action is not known (142). Specifically, evidence of how histone methyltransferases are activated, mechanisms of targeting specific stress response genes, upstream regulators, the downstream targets and how the methylation marks are translated to a plant defense outcome is lacking in crop plants. Hence, we proposed to decipher the molecular mechanism underlying the function of *SlSDG33, SlSDG34* and *SlSDG20* histone methyltransferases in tomato environmental stress response. Cultivated tomato (*Solanum Lycopercicum*) serves as an important source of nutrients to the human diet and as a model species for studies in dicotyledonous plant species and fruit development (143, 144). Tomato has unique features such as fleshy fruit, sympodial shoots, compound leaves and pedicel abscission zone development that other model species like rice and Arabidopsis do not have. Moreover tomato is closely related to other economically important *Solanaceae* crops such as potato, tobacco, pepper, eggplant and petunia (145). Understanding the molecular mechanism underlying the function *SlSDG33, SlSDG34* and *SlSDG20* should make it possible to predict how tomato respond to various environmental pertubations and this has implications in the development of resilient tomato cultivars.

The goal of this research is to decipher the molecular mechanism through which tomato histone methyltransferases *SlSDG33, SlSDG34* and *SlSDG20* regulate tomato response to environmental stress. We hypothesise that tomato *SlSDG33, SlSDG34* and *SlSDG20* regulate responses to pathogens, water stress and nitrogen though histone lysine methylation at stress responsive genes. To test these, we took genetic approaches involving CRISPR-cas9 mediated gene knockout, *in vitro* histone methyltransferase activity assays, genome wide transcriptome profiling to decipher the molecular and biochemical mechanisms employed by histone methyltransferases in regulating tomato environmental stress responses. In parallel, we conducted a reverse genetic screen to identify new components of tomato response signalling. The specific objectives are:

- Determine the function of tomato histone methyltransferases *SlSDG33, SlSDG34* and *SlSDG20* in global histone lysine methylation
- Characterise the function of *SlSDG33* and *SlSDG34* in disease resistance, water stress and nitrogen responses.
- Characterise the functions of *SlSDG20* in plant defense to bacterial and fungal pathogens.
- Identify tomato receptor like cytoplasmic kinases which contribute to fungal resistance.

CHAPTER 2. TOMATO HISTONE 3 LYSINE METHYLTRANSFERASES SDG33 AND SDG34 REGULATE PLANT RESPONSES TO BIOTIC AND ABIOTIC STRESS.

2.1 Abstract

Histone lysine methylation (HLM) is known to regulate gene expression underlying various biological processes in different eukaryotes. The biological functions of HLMs and the enzymes effecting the modifications are poorly understood in plants. Here we studied the function of tomato Set Domain Group (SDG)33 and SDG34 genes in biotic and abiotic stress responses. *SDG33* and *SDG34* genes were induced by pathogen infection, drought stress, the plant hormones methyl jasmonate, salicylate and abscisic acid. The *sdg33* and *sdg34* mutants generated through Crispr/cas9 display altered global HLM. SDG34 is required for global H3K36 and H3K4 mono, di- and tri-methylation while SDG33 is primarily responsible for di- and tri- H3K36 and H3K4 methylation. Tomato SDG33 and SDG34 are orthologues of the Arabidopsis SDG8, an H3K4 and H3K36 methyl transferase, previously implicated in plant immunity and plant growth through control of the expression of *CAROTENOID ISOMERASE* (CCR2) and other target genes. However, the tomato *sdg33* or *sdg34* single mutants showed no altered responses to fungal and bacterial pathogens likely due to functional redundancy of the tomato *SDG33* and *SDG34* genes consistent with their overlapping biochemical activities. Interestingly, tomato *SDG33* or *SDG34* genes rescued the disease susceptibility and early flowering phenotypes of Arabidopsis *sdg8* mutant. Expression of *CCR2* gene is completely inhibited in Arabidopsis *sdg8* mutant attributed to loss of H3K36 di- and tri methylation at CCR2 chromatin. CCR2 gene expression was partially restored by transgenic expression of tomato *SDG33* or *SDG34* genes in Arabidopsis *sdg8*. In tomato, the single *CCR2* gene is expressed independent of SDG33 or SDG33 genes suggesting that the genomic targets of the tomato HMTs are different. Unexpectedly, *sdg33* and *sdg34* plants were more tolerant to osmotic stress, maintain a higher water status during drought which translated to better survival rates after drought stress. Tolerance of *sdg33* and *sdg34* to drought stress is accompanied by higher expression of drought responsive genes. Collectively, our data demonstrate the critical role of tomato HLM in pathogen and water stress tolerance likely through the regulation of adaptive gene expression.

2.2 Introduction

In eukaryotes, DNA is wrapped in nucleoprotein complex known as chromatin. Chromatin is made up of nucleosomes which consist of ~ 147bp of DNA wound around an octameric core of histone proteins H2A, H2B, H3 and H4 (6). This packaging of DNA into chromatin is a barrier to DNA templated processes. Chromatin remodelling machines, histone-modifying complexes, and DNA methylation can overcome or enhance these barriers. The amino acids on the histone N-terminus tails are subject to post-translational modifications such as methylation, acetylation, ubiquitination and phosphorylation. These modifications influence chromatin structure, affecting accessibility of the transcriptional machinery to the corresponding DNA thus modulating gene expression and/or repression (146). Histone lysine methylation is the addition of methyl residues on the lysine residues of H3 and H4 proteins catalysed by histone methyltransferases (HKMTs). Plant histone lysine methyl transferases have a conserved SU- (VAR) 3-9, Enhance of zeste E (Z) and Trithorax (TRX) (SET) domain originally identified in *Drosophila*. Notably, the SET domain is responsible for the enzymatic activity and is highly conserved in Bacteria, Archaea, and Eukaryota. Histone lysine residues can be mono-, di-, or tri-methylated depending on the specific function of the associated methyltransferase with varying effects on gene expression (147). Chromatin changes mediated by histone lysine methylation play an important role in plant response to environmental stress (6). Hence loss of function mutants of histone methyltransferases, enzymes that mediates histone lysine methylation, display sensitivity to different environmental stresses (4, 18, 21, 22, 107). In plants many studies have correlated changes in histone lysine methylation with transcriptional status of genes in response to pathogens (18, 148, 149), cold (150, 151), heat (152, 153) and salt stress (153, 154). While most changes in histone lysine methylation reset to basal level after stress, some have been reported to be inherited through meiosis or mitosis and are suggested to carry 'stress memory' (155, 156).

Genome wide and locus specific reprograming of gene expression patterns are highly dependent on the chromatin structure which determine the accessibility of the transcriptional machinery to the underlying DNA. In turn, such transcriptional reprogramming of gene expression is likely to precede plant responses to biotic or abiotic stress and ultimately adaption to stress. Drought is absence of water for a period enough to deplete soil moisture and injure plants. When plant water loss exceeds the ability of the roots to absorb water from the ground, plant water content is reduced interfering with normal plant processes. This phenomenon is referred to as

drought stress (72). Drought stress is a critical limitation to global crop productivity and is likely to increase in severity due to the drastic and rapid changes in global climate. Plants have evolved different mechanisms to escape, avoid, tolerate and recover from drought and minimize its the detrimental effect. These mechanisms require rapid changes in gene expression patterns at the onset and persistence of drought stress. Upon drought stress, plants activate signalling pathways that rapidly change the gene expression patterns and cellular physiology that provide survival mechanisms (7, 109). Regardless of the environmental cue, there is massive reprograming of gene expression as an active mechanism of plant biotic and abiotic stress tolerance.

Responses to drought stress in plants is highly dependent on timely transcription of drought responsive genes. Various drought responsive genes have been identified and characterised in plants. These drought responsive genes encode proteins with metabolic or regulatory functions (157). Conserved and specie-specific proteins that have metabolic function such as membrane stabilising proteins, late embryogenesis proteins (LEA) which increases cell's water binding capacity, heat shock proteins (HSPs) which prevent protein denaturing under drought stress, and those involved in osmolyte biosynthesis, detoxification, ion transport, and proteolysis of cellular substrates have been identified and studied (72, 158, 159). These components mainly play a role in protecting plants against the adverse effects of drought. On the other hand, the regulatory proteins described control signal transduction pathways and gene expression during drought stress leading to activation of mechanisms for drought tolerance (160). Proteins which play regulatory roles during drought stress have been identified in plants and these include transcription factors (myeloblasts (MYB), dehydration responsive element binding (DREB), C-repeat binding factor (CBF), abscisic acid responsive elements binding factor (ABF), ABRE binding (AREB), and NAM, $ATAF_{1/2}$, and CUC_2 containing proteins) (NAC). Transcription factors regulate gene expression by binding to the *cis* elements on the promoter of their target genes. Alteration in the expression of these transcription factors has an impact on drought tolerance (98, 161, 162). In addition, mitogen activated protein kinases (MAPK), calcium-dependent protein kinases (CDPK), receptor protein kinases, ribosomal protein kinases, and transcription regulation protein kinases, and protein phosphatases (phosphoserines and phospholipase) have been implicated as important regulators of signal transduction and gene expression during drought stress (48, 160).

Transcriptional responsiveness of drought responsive genes is associated with changes in histone modifications patterns. Accumulation of histone marks on the core histones of drought

responsive genes are associated with active transcription during drought stress (7, 163). In *Arabidopsis,* tri-methylated histone 3 Lysine 4 (H3K4me3) enrichment was positively correlated to transcript levels of drought responsive genes under dehydration stress (126). Similar findings were reported in *moss* (*Physcometrella patens)* (127) and rice (128). Consistent with these findings, H3K4me3 was found to gradually increase in response to dehydration stress on four drought inducible genes *RD2A*, *RD29B*, *RD20* and *RAP2.4* and was correlated to their upregulation in *Arabidopsis* (114). In addition, *Arabidopsis* ATX1 a major H3K4me3 methyltransferase, plays a role in drought stress signalling both in the ABA-dependent and ABA-independent pathway and *atx1* mutant is sensitive to dehydration (16, 32, 129). Under drought stress, the *atx1* mutant accumulates low levels of *NCED3* transcripts, a rate-limiting enzyme in ABA synthesis. Low levels of *NCED3* correlate with low H3K3me3 levels on its nucleosomes. Further, ATX1 also regulates the transcriptional induction of two drought responsive genes *RD2A* and *RD29B* in an ABA-dependent manner during dehydration stress (129). This study on *Arabidopsis* ATX1, has provided insights on the regulatory role of histone methyltransferase in drought stress response.

Apart from *Arabidopsis,* nothing is known about the function of histone methyltransferases in regulating biotic and abiotic stress responses in other plant species. Cultivated tomato (*Solanum lycopercicum*), an important source of nutrients to the human diet, is moderately sensitive to drought stress and is highly susceptible to pathogens (143, 144, 164). The tomato genome is predicted to encode 52 putative methyl transferases but the biological function of any of these has not been studied. Here, we report the function of two tomato histone lysine methyltransferases Set Domain Group protein 33 (SDG33) and SDG34 in regulating drought stress and pathogen responses. Loss of function mutants of SDG33 and SDG34 generated through gene editing survive prolonged drought better than wild type plants suggesting that SDG33 and SD34 are negative regulators of drought stress tolerance. The mutant plants *sdg33* and *sdg34* osmotically adjust to maintain turgor and a water potential gradient favourable for water influx during drought stress. Our results show that SDG33 and SDG34 negatively regulate drought stress tolerance, but the mechanistic details require further studies.

2.3 Materials and methods

2.3.1 Plant materials and growth conditions

Tomato (*Solanum lycopersicum)* cultivar Casstlemart II were grown in plastic pots containing compost soil (Sun Grow Metro mix 510) in a growth chamber under extended 12-hour photoperiod at 24 ^{0}C. Castlemart11 is referred to as the wild throughout this paper and all the mutants were generated in the Castlemart11 background. For seedling assays, seeds were surface sterilised with 20% Sodium Hypochlorite, washed several times in distilled water and germinated on full Murashige and Skoog (MS) medium with 2% (w/v), sucrose 0.8% (w/v), 1.5% bacto agar, and supplemented with Gamborg's vitamins under 16hour light, 8-hour dark at 24 ^{0}C.

2.3.2 Generation of *sdg33* and *sdg34* mutants

To generate *sdg33* and *sdg34* mutants, two specific guide RNA (gRNA) of SDG33 and SDG34 were designed using the CRISPR Plant gRNA design software https://www.genome.arizona.edu/crispr/CRISPRsearch.html . The two gRNA were cloned into the CRISPR/Cas9 vector pKSE401 according to (165). Tomato cultivar Casstlemart11 cut cotyledons explants were suspended in *Agrobacterium* carrying the constructs for 30 minutes and the explants blot dried on sterile blot paper to remove excess *Agrobacterium*. *Agrobacterium* infected explants were co-cultivated on MS medium with 0.8% gelrite + acetosyringone + and incubated in the dark at 21 °C 48 hours. After co-cultivation, the explants were then transferred to regeneration MS medium supplemented with 75mgL^{-1} Kanamycin to induce callus formation. Green callus was transferred to shoot induction medium MS medium. Regenerated plantlets were transferred to rooting MS medium supplemented with 75mgL^{-1} Kanamycin and the rooting hormone Indole butyric acid. Full rooted plants were transferred into the soil and genotyped by PCR with primers covering the expected deletion. The deletions were confirmed by sequencing.

2.3.3 Global methylation assay.

Core histone proteins were extracted form 4 weeks old *sdg33,sdg34* and WT plants as described by (166). Proteins were separated on 15%SDS-PAGE gel and transferred to PVDF membranes. The membranes were immunoblotted with primary antibodies anti-H3K4me1 (07-436; EMD Millipore), anti-H3K4me2 (07-030; EMD Millipore), anti-H3K4me3 (07-473; EMD

Millipore), anti-H3K36me1 (ab9048; Abcam), anti-H3K36me2 (07-369-I; EMD Millipore), anti-H3K36me3 (ab9050; Abcam), and anti-H3 (ab1791; Abcam) as a loading control. Anti-rabbit was used as the secondary antibody. Visualisation of the bound primary antibody was done with the enhanced chemiluminescence (Thermo Scientific) detection system according to the manufacturer's protocol.

2.3.4 Stress tolerance assays

For osmotic stress tolerance, *sdg33*, *sdg34* and WT seeds were surface sterilised germinated on MS medium for three days. When the radicle emerged, they were transferred to MS medium supplemented with 300mM Mannitol. Seedling length and weight were measured after 10 days. For drought assays, 6 plants per genotype were grown in square pot and ten pots per genotype with enough water for 4 weeks, drought stress was induced by withholding water for a period of 10 days. Plants were re-watered and survival rate was calculated daily for three days. To measure Relative Water Content (RWC), leaves were collected at day 6 after drought was induced, weighed to get fresh weight (LFW), incubated in water petiole down in a 50ml conical tube overnight. Leaves were blotted dry and weighed to get saturated weight (LTW). Leaves were then dried at 60°C for three day and weighed to get dry weight (LDW). RWC was calculated as (LFW-LDW)/(LTW-LDW). Shoot water content was determined for the whole shoot (leaves and stems) according to the formula (FW − DW)/DW, where FW is the fresh weight and DW the dry weight obtained oven dried for 3 days at 60 °C.

2.3.5 Determination of malondialdehyde (MDA) content

Lipid peroxidation was measured in terms of malondialdehyde (MDA) content according to (167). Briefly, fresh tissue (0.2 g) was ground in liquid nitrogen and homogenised in 4 mL of 0.1% trichloroacetic acid (TCA). The homogenate was centrifuged at 15,000 g for 5 min. 4.0 mL of 20% TCA containing 0.5% thiobarbituric acid (TBA) was added to 1.0 mL aliquot of the supernatant. The reaction mixture was incubated at 95°C in a hot water bath for 30 min and terminated in an ice bath. After centrifugation at 10,000 g for 10 min, the absorbance was measured at 532 and 600 nm from 200µl of the supernatant. The MDA equivalent was calculated as MDA (nmol/mL FW) = ((A532-A600)/155, 000) Å~106.

2.3.6 Lateral root and auxin response assays

In all the experiments we used full strength Murashige and Skoog (MS) medium with 2% (w/v), sucrose 0.8% (w/v), bacto agar, and supplemented with Gamborg's vitamins. For the lateral root assay, seeds were surface sterilised, germinated on filter paper for three days in the dark. When the radicles had emerged, they were transferred into MS medium, square plates were placed vertically at 25°C under 12h light cycle. Lateral root number and root length were counted and measured respectively 10 days after germination under a dissection microscope. For the auxin response assays, seeds were germinated on filter paper in the dark and transferred after 3 days to MS medium with designated auxin concentrations. Lateral root number and root length was analysed ten days later. The auxin dose response assay was done according to (168).

2.3.7 RNA extraction and gene expression analyses.

Total RNA was extracted from the shoot and root using the Trizol (Invitrogen) according to the manufacturer's instructions. After extraction, RNA was treated with DNASE (New England Biolabs) according to the manufacturer's instruction. RNA was precipitated with 3M Sodium acetate and three-times volume of 100% ethanol. Integrity of RNA was accessed by the Agilent Bioanalyzer (Agilent technologies). 2µg of RNA was used for first strand cDNA synthesis using MLV reverse transcriptase (Promega). Quantitative PCR (qPCR) analyses with SYBR Green master mix (Biomake) using the CFX96 qPCR machine (Biorad). Three technical replicates were used for each sample and each experiment was replicated at least twice. Expression levels were calculated by the comparative threshold Ct method. Primers used for qRT-PCR are listed in supplemental table 1.

2.3.8 Statistical analysis

Analysis of Variance (ANOVA) was performed to test the impact of genotype, nitrogen treatment and their interaction on each phenotypic trait. ANOVA was performed in the R software, version 3.3.1 (R Core Team, 2016) using the Agricolae package. Statistical significance was determined at the level ($P \leq 0.05$). To further analyse which means are significantly different, means were compared using the LSD method in the JMP software package. Basis on significance was assessed by least significance differences ($p=0.05$).

2.3.9 Complementation of *Arabidopsis sdg8* mutants.

We cloned tomato SDG33 and SDG34 full length coding sequence (CDS) in the pCambia HA vector under their respective native promoter. The vectors were confirmed through sequencing. We used agrobacterium mediated transformation of *Arabidopsis sdg8-2* (SALK_026442) in the Col-0 ecotype background to generate transgenic line expression tomato SDG33 and SG34. Positive transformants were screened on half-strength Murashige and Skoog (1/2 MS) medium supplemented with the herbicide basta. Protein or mRNA levels of SDG33 and SDG34 were verified by immunoblotting analysis with anti-HA-specific antibody and qPCR assays. Plants were grown in a growth chamber at 24°C, 70% relative humidity, 110 to 130 μE m^{-2} s^{-1} light intensity by fluorescence tubes (model F32T8/TL741) with a 12-h-light/12-h-dark cycle.

2.3.10 Disease assays

Arabidopsis disease assays were done as previously described by (148). Briefly, *B. cinerea* was cultured on V8 media, and spores were suspended in 1% Sabouraund maltose broth buffer (BD Difco). 5-μL droplets of 2.5×10^5 spores/mL spore solution were drop inoculated on the detached leaves of 5-week-old plants. Inoculated pants were kept at high humidity for 3 days, and disease susceptibility was assessed by measuring the lesion diameter. For tomato disease assay 4-week-old plants were used.

2.4 Results

2.4.1 Characterization of tomato SDG33 and SDG34 encoding histone methyl transferases.

SDG33 and SDG34 were previously described in a genome wide sequence analyses of 52 putative in tomato histone methyltransferases (169). SDG33 contains 17 exons which encodes a 1397 amino acid protein with an estimated molecular weight of 154.037kD (Figure 1A). SDG34 is a 17-exon gene encoding a 1666 amino acid protein with an estimated molecular weight of 183.6kD (Figure 1b). SDG33 and SDG34 proteins belong to class 11 according to the classification of SET Domain Group (SDG) proteins by Springer and colleagues (170). Similar to other class 11 proteins, they contain the evolutionarily conserved SET domain (PF00856) (Figure 2.1A, B), a characteristic of histone methyltransferases and responsible for their catalytic activity (171). In addition to the SET domain, SDG33 and SDG34 proteins have an N-terminal Associated With SET (AWS) (SM00570) and Post SET (SM00508) conserved class 11 domains typical of class 11 type histone methyltransferases (Figure 2.1A, B) (169). Besides the canonical domain peculiar to class 11 SDG proteins, SDG33 and SDG34 have an additional zinc finger with cysteine and tryptophan conserved amino acids (zf-CW) (PFam 07496) (172). The zf-CW domain has been shown to be important for binding to DNA and specific histone methylation states (173). Structural analysis of SDG33 and SDG34 suggest that they are histone methyltransferases which function by recognizing and modifying histone methylation patterns. Sequence and phylogenetic analyses revealed the relationship between SDG33/SDG34 and other class 11 SDG proteins from other species with an identity ranging from 32 to 72%. SDG33 and SDG34 share a 60% identity at the amino acid level with 100% identity shared on the SET domain. Arabidopsis SDG8 and rice SDG725 are the two class 11 SDG proteins closely related to SDG33 and SDG34 sharing a 53% and 60% identity, respectively.

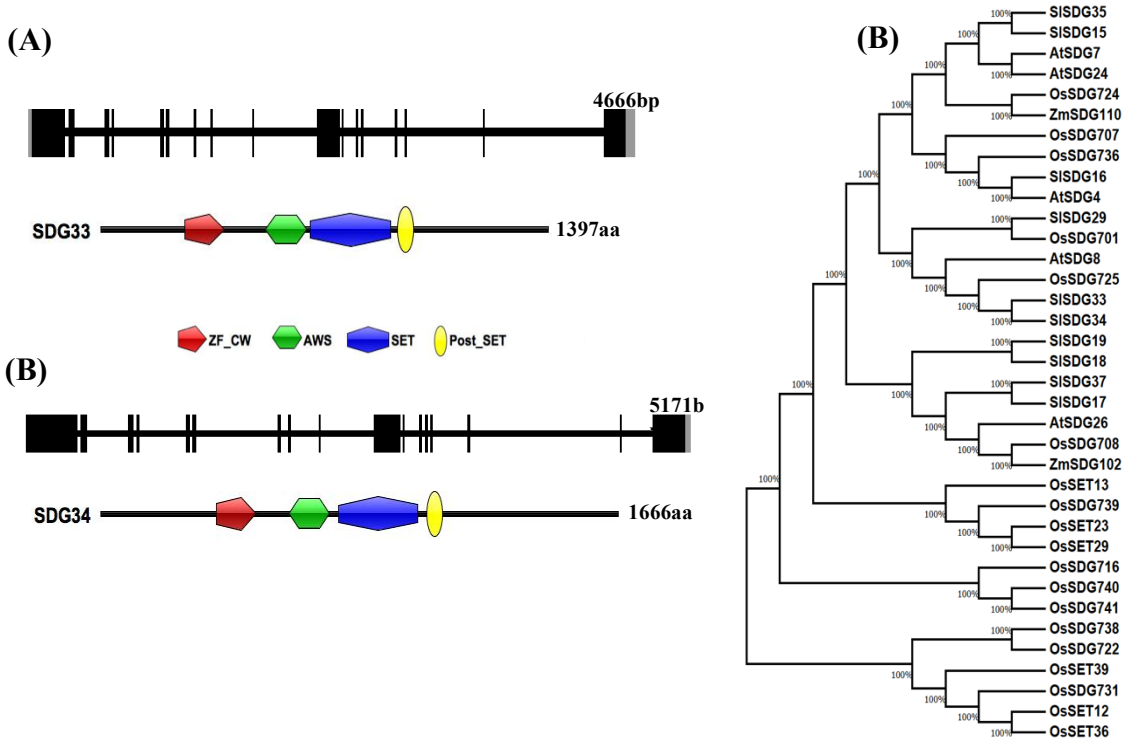

Figure 2.1 Gene, protein structures and phylogenetic analysis of SDG33 and SDG34**.** Schematic diagram showing gene and protein structure of A) SDG33, B) SDG34. Black shaded boxes represent exons, the grey shaded boxes represent the UTRs boxes represent exon, and introns are shown as horizontal lines. For the protein structure the main domains are shown. C) Maximum Likelihood phylogenetic analysis of class 11 SDG protein from *Arabidopsis thaliana (*At*)*, *Solanum lycopersicum* (Sl), *Zea mays* (Zm) and *Oryza sativa* (Os). Phylogenetic analysis was performed using Mega7 package. The tree is drawn to scale with branch length measured in the number of substitutions per site. Bootstrap values higher than 50% are shown.

To gain better insight into the biological functions of SDG33 and SDG34, we examined their expression patterns in leaves, roots, flower structures, green fruits, and red fruits using RT-qPCR (Figure 2.2A). Both SDG33 and SDG34 are expressed in all tissues with the highest expression in the roots and petals respectively. SDG33 expression is notably higher in the roots followed by the petals which showed twenty-four-fold lower expression compared to the roots but about fifty-fold higher expression compared to leaves. The expression of SDG33 in stamens and stigma is relatively higher compared to the leaves and the fruits at all stages of ripening. Leaves display the least SDG33 expression, while green and red fruit ripening stages show about two folds higher expression than in leaves. SDG34 expression is notably higher in the petals, about five hundred-fold higher compared to expression in leaves which has the lowest expression of SDG34. Following the petals, the roots also have a notably high expression of SDG34. The stigmas and the

stamens exhibit four-fold higher expression of SDG34 than leaves, while expression in red and green fruits is not significantly different form the expression in the leaf tissue.

To determine the functional relevance of SDG33 and SDG34 genes, we first examined their expression profiles under drought stress, two pathogens *B. Cinerea* and *P. syringae* and plant hormones, Indole acetic acid (IAA), abscisic acid (ABA), Methyljasmonate and Salicylic acid using RT-qPCR. In response to drought stress SDG33 and SDG34 transcripts showed about threefold induction after 8 days of water stress suggesting a function in water stress response (Figure 2.2B). SDG33 and SDG34 were highly induced by IAA as early as 4 hours after treatment indicating a role of SDG33 and SDG34 in mediating auxin responses (Figure 2.2C). In response to the stress hormone ABA, SDG33 is induced at 4 and 8 hours after treatment while SDG34 is not (Figure 2.2D). SDG33 and SDG34 were highly induced by MeJA a precursor in Jasmonic acid synthesis, and Salicylic acid a defense response hormone indicating a probable role in tomato defense responses. (Figure 2.2E-F). Furthermore, B. *cinerea* and *P. syringae* induce SDG33 and SDG34 as early as 24 hours after treatment consistence with a possible function in defense response (Figure 2.2G-H).

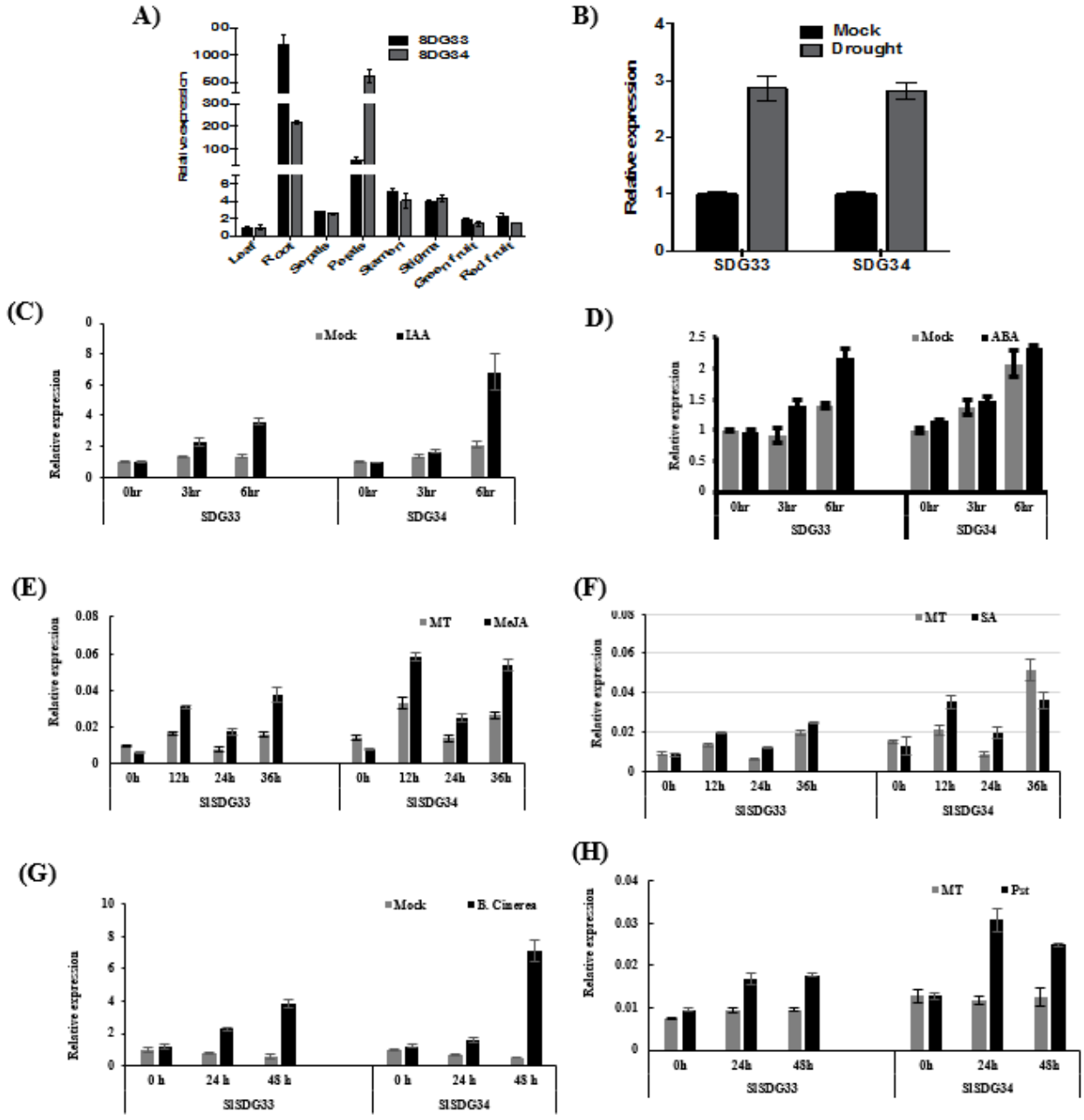

Figure 2.2 Expression of SDG33 and SDG34 in WT tomato in response to drought, fungal infection and plant hormones. A) Tissue specific expression of SDG33 and SDG34 in WT tomato plants. Induced expression of SDG33 and SDG34 with B) Drought, C) IAA, D) ABA, E) Methyl jasmonate (MeJa), F) Salicylic acid (SA), G) *B. Cinerea* and H) *P. syringae.* Bars represent the means; the error bars represent the standard deviations of three technical replicates of each treatment. The tomato β-actin gene was used as an internal control in the qRT-PCR. The experiment was repeated at least 2 times with similar results.

2.4.2 Characterization of *sdg33* and *sdg34* loss of function mutants.

To study the function of SDG33 and SDG34 we generated gene edited lines through CRISPR/Cas9-induced mutation. Two guide RNAs (gRNAs) were designed to generate mutations in each of SDG33 and SDG34 genes (Supplementary table S1). To ensure that the sgRNAs were specific and to avoid off target mutagenesis we used the gRNA design software www.genome.arizona.edu/crispr. The gRNAs were expressed under the control of Arabidopsis U6 promoter. Two independent mutations for SDG33 and several mutations for SDG34 were recovered in T0 generation. Two homozygous lines for each gene were studied in detail (Figure 2.3). The *sdg33b* mutant allele carried a deletion of 58bp, and a *sdg33s* displayed a deletion of 6bp and a single nucleotide insertion within exon 10 (Figure 2.3A-C). Further analysis indicated that the deletions in *sdg33b* and *sdg33s* introduced premature stop codons suggest that a truncated protein is made. For SDG34, one homozygous mutant allele *sdg34.76* had a deletion of 119bp and another allele *sdg34.27* had a 150bp deletion and a 3bp insertion (Figure 2.3D-F). All the deletion in *sdg34* mutants were in the last exons and introduced premature stop codons Furthermore, quantitative Reverse Transcription Polymerase Chain Reaction qRT-PCR showed that SDG33 and SDG34 transcripts were severely reduced in the *sdg33* and *sdg34* mutants compared to the WT (Figure 2.3G-H). Although there were still small amounts of SDG33 and SDG34 transcripts in the *sdg33* and *sdg34* mutants, the transcripts are frame shifted, the corresponding proteins truncated and probably non-functional.

Figure 2.3. Molecular characterization of sdg33 and sdg34 loss of function mutants. A) and D) Diagrams showing the position of the deletions in sdg33 and sdg34 mutants. Black shaded boxes represent exons, the grey shaded boxes represent the UTRs boxes represent exon, and introns are shown as horizontal lines. B and E) PCR genotyping of *sdg33* and *sdg34* mutant alleles. C and F) Alignment of mutated alleles sequences identified from cloned PCR genotyping fragments and the WT sequences. The mutated alleles include deletions (shown by dashed lines) and insertions (shown by blue letters). Only aligned sequences and the mutations are shown. The targets are shown by letters in red and the protospacer adjacent motif (PAM) is shown by the bold-faced letters after the targets. SDG33 (G) and SDG34 (H) expression in the mutants. Bars represent the means; the error bars represent the standard deviations of three technical replicates of each treatment. The β-actin gene was used as an internal control in the qRT-PCR. The experiment was repeated at least 2 times with similar results.

(A)

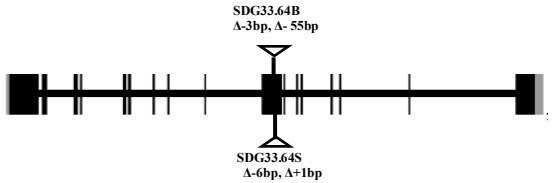

(B)

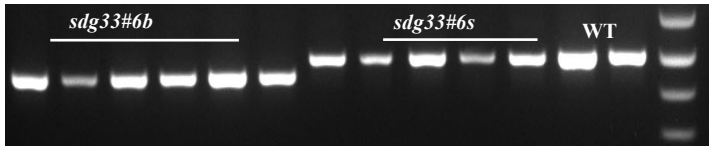

(C)

```
>SDG33 WT GTGTCTGTGGCTCGCCTCGCTGTCTGGGCTATATAGGTGGAG//CTCCAGGGGAAACACCTAAAAACAAATATAAACTGGATGAACCTTTTACTGGAAACCTGGAGACTACCACCC
>33.64B   GTGTCTGTGGCTCGCCTC---GTCTCGGCTATATAGGTGGAG//CTCCAGGGGAAA----------CACCC -3bp, -55bp
>33.64S   GTGTCTGTGGCTCGCC------TCTGGGCTATATAGGTGGAG//CTCCAGGGGAAACACCTAAAAACAAATATAAACTGGATGAACCTTTTTACTGGAAACCGGAGACTACCACCC -6bp +1bp
```

(D)

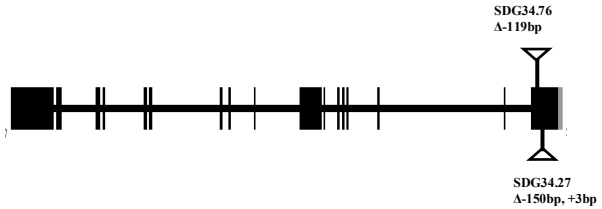

(E)

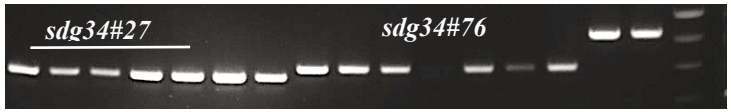

(F)

```
>SDG34WT AGGTGCAGCAAT//CCTTTACCTCCATATCCCTGTGATAGAAGAGGTTTTGTGCCTACTGCTAGTGAGCTGCCTCAAAATGCTGGAGAAG---ATT//TCTGGAGCAGACCAGCCTCAGGATGGCAA
>34.27    AGGTGCAG----//----------TACCGAAGAAGGTAATT//TCTGGAGCAGAC---------AATGGCAA -141bp -9bp +3bp
>SDG34WT
ACCTCCATATCCCTGTGATAGAAGAGGTTTTGTGCCTACTGCTAGTGAGCTGCCTCAAAATGCTGGAGAAGATTGGGGTGCTTGTTCACCTAGTCACTTGGCTCAAAATCCTCCAAGCGTATCTGGAGCAGACCAGCCTCAGGATGGCAA
>34.76    ACCTCCATATCCCTGTGATAG----------AGGATGGCAA -119bp
```

(G)

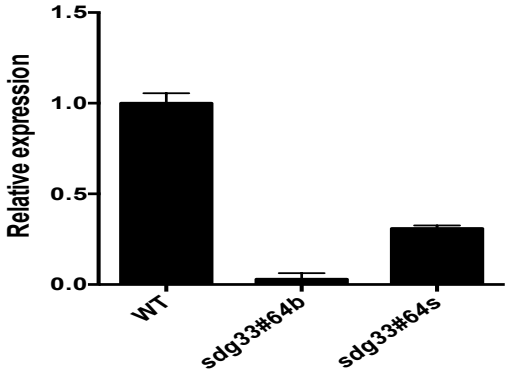

(H)

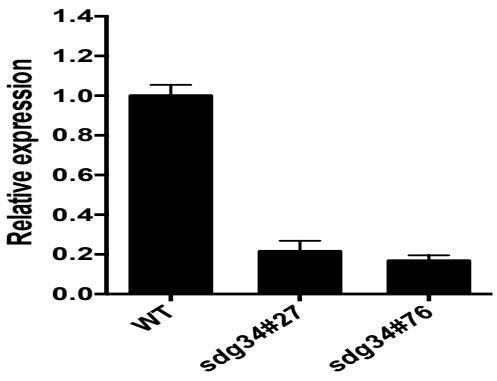

2.4.3 SDG33 and SDG34 mutation affect global histone 3 lysine 4 and lysine 36 methylation.

Based on the structure and phylogenetic relationships, SDG33 and SDG34 are putative histone methyltransferases. To gain insights to whether loss of SDG33 and SDG34 affect any histone methylations globally, we employed western blot analysis and antibodies specific to the different histone modifications, to analyse global histone methylation patterns in *sdg33* and *sdg34* mutant plants (Figure 2.4). Loss of SDG33 caused a decrease in the level H3K36me2, H3K36me3, H3K4me1 and H3K4me3 (Figure 2.4). H3K36me1 and H3K4me2 levels in *sdg33* mutants were higher than the WT (Figure 2.4A). Loss of SDG34 resulted in global decrease of mono-, di- and tri-H3K36 and H3K4 methylation levels. Taken together, the data indicate SDG34 plays a major role in global H3K36 and H3K4 while SDG33 is primarily responsible for di- and tri-methylation of H3K36 and H3K4 in tomato.

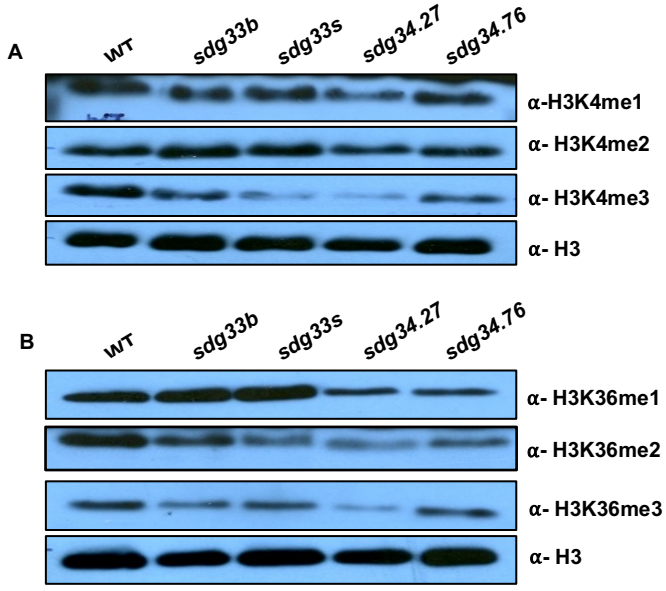

Figure 2.4 Global histone lysine methylation levels in tomato sdg33 and sdg34 mutants. Western blot analysis of A) H3K4 B) H3K36 in WT, *sdg33* and *sdg34* alleles. Core histones were extracted from 4-week old plants and blotted with specific H3K4 and H3K36 antibodies

2.4.4 Mutation in SDG33 and SDG34 improved drought stress tolerance

SDG33 and SDG34 were highly induced by water stress (Figure 2.2C) suggesting their important role in mediating responses to water deficit. To further analyse the function of SDG33 and SDG34 in water stress, we first tested the seedling performance of the mutant lines under 300mM mannitol (Figure 2.5). Mannitol is an osmoticum which lowers water potential of a medium. We measured seedling length and weight of the *sdg33* and *sdg34* mutants and the wild type genetic background Castlermart II in the presence of mannitol induced osmotic stress. In the MS medium, there were no significant differences between the WT and *sdg33* in seedling length. However, there were slight differences between WT and *sdg34* with the mutants showing 10-12% longer hypocotyl than the WT (Figure 2.5A). Upon mannitol treatment, hypocotyl length decreased by 66% for the WT, 50-52% for the *sdg33* mutants and 56% to 63% for the *sdg34* mutants (Figure. 2.5A, B). The *sdg33* and *sdg34* weighed significantly more than the WT in the MS medium. Seedling weight decreased in mannitol treatment for all the genotypes but the *sdg33* weighed significantly higher than the WT. In contrast, *sdg34* biomass was not significantly different from the WT (Figure 2.5C). Overall, the growth of *sdg33* and *sdg34* in mannitol was less affected than the WT suggesting that SDG33 and SDG34 mediates tolerance to osmotic stress.

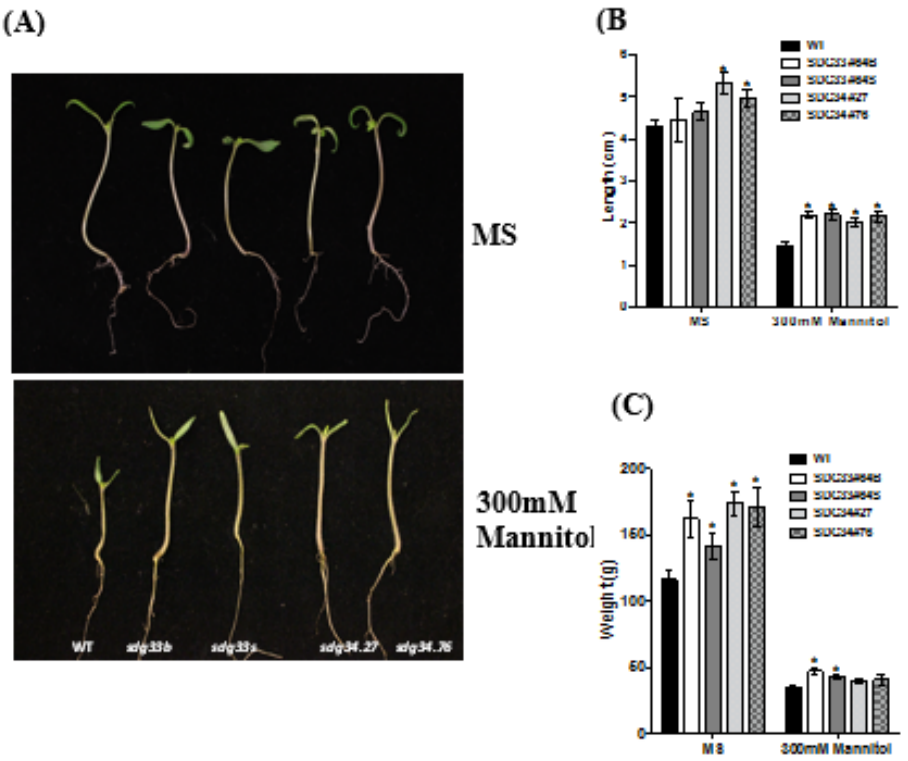

Figure 2.5. Seedling growth of WT, *sdg33* and *sdg34* in response to osmotic stress**.** A) Phenotypes, B) Hypocotyl length and C) seedling weight of WT, *sdg33* and *sdg34* after treatment with 300mMmannitol. The data shown are the mean ± SE (n = 10), the experiment was repeated 2 times with similar results. The data shown are the mean ± SE (n = 36). *p < 0.05, **p < 0.01.

To confirm the role of SDG33 and SDG34 in drought stress tolerance, we investigated the response of WT, *sdg33* and *sdg34* plants to water stress by withholding water. Four-week-old soil grown *sdg33* and *sdg34* mutants and WT plants were exposed to water stress by withholding water for 10 days. After 6 days the WT showed severe wilting symptoms while the *sdg33* and *sdg34* mutants showed slight wilting symptoms with most of the leaves maintaining their turgor (Figure 2.6A). Slight differences in wilting were observed at day 10, all the genotypes showed severe wilting symptoms. Drought response can also be evaluated by the ability to survive and regenerate new green parts after a prolonged drought period (34). After 10 days of water stress, plants were re-watered and survival rate was measured for three days. After 3 days of re-watering, 24% of the WT survived while about 64% of *sdg33* and *sdg34* plant survived (Figure 2.6B).

Wilting reflects the turgor pressure in a cell which is highly dependent on the water content of the cells. To monitor plant water status, we measured relative water content (RWC) 6 days after water stress. The values for RWC was slightly lower in *sdg33* but similar between *sdg34* and WT

in the control plants. However, in water stressed plants both *sdg33* and *sdg34* showed significantly higher (P<0.05) RWC than the WT (Figure 2.6C). The higher water status of *sdg33* and *sdg34* mutants at day 6 is also visually evident as shown by slight wilting symptoms (Figure 2.6A). One possible explanation of higher water status of a plant could be that stomata closure was greater in *sdg33* and *sdg34* mutants during water stress thereby restricting water loss through transpiration. However, stomata conductance was similar in WT, *sdg33* and *sdg34* mutants throughout the water stress regime (data not shown). Further, transpiration rate did not differ between the mutants and the WT during stress. The differences in wilting symptoms of the WT, *sdg33* and *sdg34* mutants is further reflected in the shoot water content at the end of the water stress cycle. The WT had lower shoot water content compared to *sdg33* and *sdg34* (Figure. 2.6D). Although high shoot water content reflects lower transpired water in the shoot (175), we did not detect any significant differences in transpiration rate, leaf water loss and plant water loss during the water stress experiments (176).

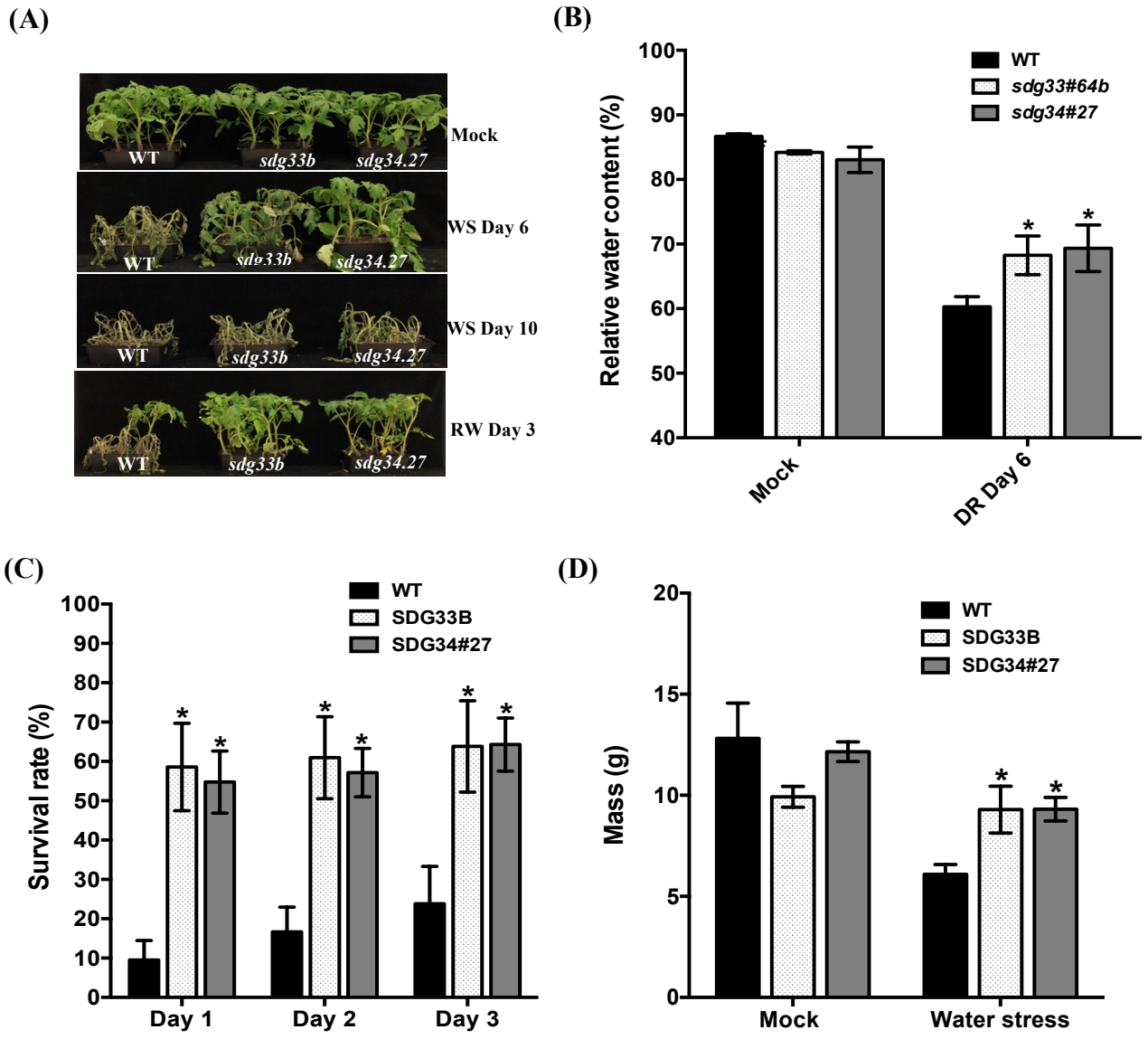

Figure 2.6. Mutation in SDG33 and SDG34 enhances drought tolerance in tomato. A) Phenotypes of WT, *sdg33* and *sdg34* during and after water stress treatment. WS-water stress, RW- re-watered. B) Relative Water Content of WT, *sdg33* and *sdg34* at day 6 of water stress. The data shown are the mean ± SE (n = 6). C) Survival rates after re-watering of WT, *sdg33* and *sdg34* after drought stress. The data shown are the mean ± SE (n = 42). Data shown is a representation of experiments repeated at least 3 times. D) Shoot water content of WT, *sdg33* and *sdg34* measured at 3 days after re-watering. The data shown are the mean ± SE (n = 36). *$p < 0.05$, **$p < 0.001$.

2.4.5 Expression of drought responsive gene in *sdg33* and *sdg34* plants during water stress

We performed RT-qPCR to determine the expression of drought responsive genes during our drought experiments. We examined the expression of dehydration-responsive element binding (DREB), Peroxidase (POD), and Superoxide dismutase 6 (SOD6) genes (Figure 2.7). All the three genes were lower than the WT in the mutants in well-watered plants, however upon water stress their expression was induced higher than the WT. DREB expression was induced by water stress both in the mutants and the WT but the induction in both mutants is significantly higher than the WT. Overexpression of DREB genes has been associated with drought tolerance in tomato (46). POD and SOD6 expression are lowered in the WT under water stress but POD is highly induced in both *sdg33* and *sdg34* under water stress. SOD6 expression is significantly reduced in the *sdg33* mutants under water stress compared to control plants. However, in the *sdg34* mutants, it is significantly increased under water stress compared to the control plants. The expression of both POD and SOD6 in the mutants is however higher than the WT under water stress. Higher expression of POD and SOD is often associated with lower oxidative stress under water stress. Malondialdehyde (MDA) is a well-established marker for oxidative stress (46), thus we measured MDA content in the mutants and WT under water stress. MDA content was slightly lower in the mutants than the WT although not statistically significant. This shows that mutation in SDG33 and SDG34 alters the expression of drought responsive genes and suggest that overexpression of some of these genes in *sdg33* and *sdg34* may result in drought stress tolerance.

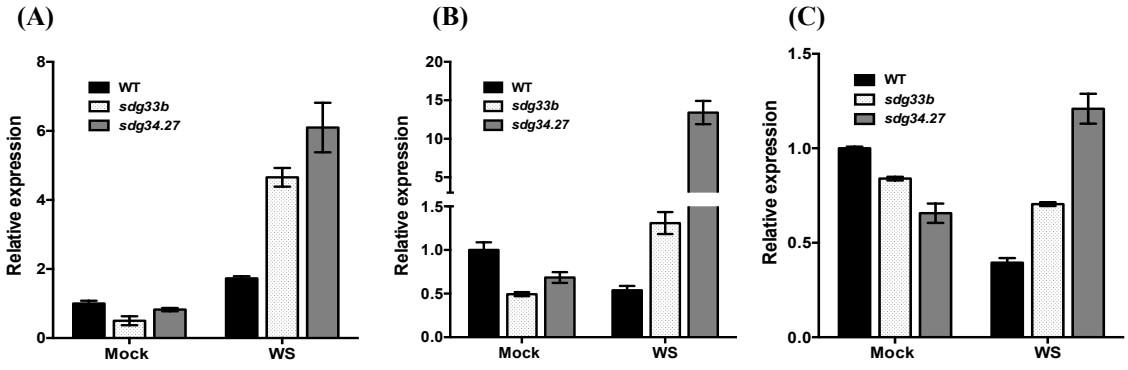

Figure 2.7. Expression of drought-responsive genes under water stress in WT, *sdg33* and *sdg34*. A) dehydration-responsive element binding (DREB), B) Peroxidase (POD) and C) Superoxide dismutase 6 (SOD6) genes. qRT-PCR analysis of stress-responsive genes in WT and transgenic plants at day 6 after drought stress.

2.4.6 Tomato SDG33 and SDG34 rescue the fungal susceptibility and early flowering phenotypes of Arabidopsis *sdg8* mutant

We studied the function of SDG33 and SDG34 in defense response. We tested *sdg33* and *sdg34*'s response to *B. cinerea* and *P. Syringae*. The mutants showed a WT response to both *B. cinerea* and *P. Syringae* (Figure 2.8A, B). Since SDG33 and SDG34 have overlapping global methylation patterns, it could be that a mutation in SDG33 is compensated for SDG34. Hence, we checked for transcript abundance of SDG34 in *sdg33* and vice versa. SDG34 transcripts in *sdg33* and SDG33 transcripts in *sdg34* were similar to the WT. Another possibility is that SDG33 and SDG34 have overlapping functions in disease response. We generated *sdg33/sdg34* double mutants, however we got chimeric mutations and the plants had malformed leaves, flowers and parthenocarpic fruits (Figure 2.8C-F). This data suggests that SDG33 and SDG34 may have overlapping functions in regulating disease response.

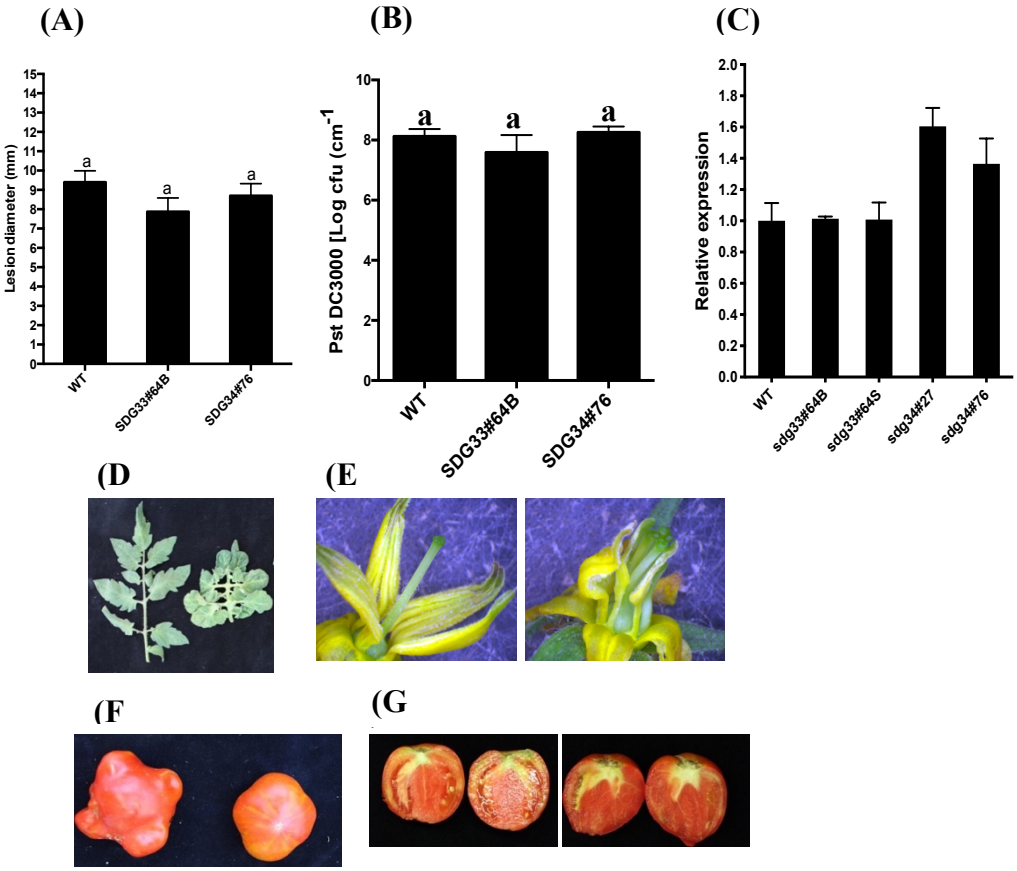

Figure 2.8. Tomato *sdg33* or *sdg34* mutants exhibit wild type levels of resistance to *B. cinerea* and *P. syringae*. Disease phenotypes of the single mutants in SDG33 or SDG34 genes in response to A) *B. cinerea*, B) *P. syringae*. The data shown are the mean ± SE (n >30). Different letters represent significant differences among genotype. C) The expression of CCR2 in *sdg33* and *sdg34* mutants. D-F) Leaf and flower phenotypes of the double mutant *sdg33sdg34* generated through Crispr/cas9.

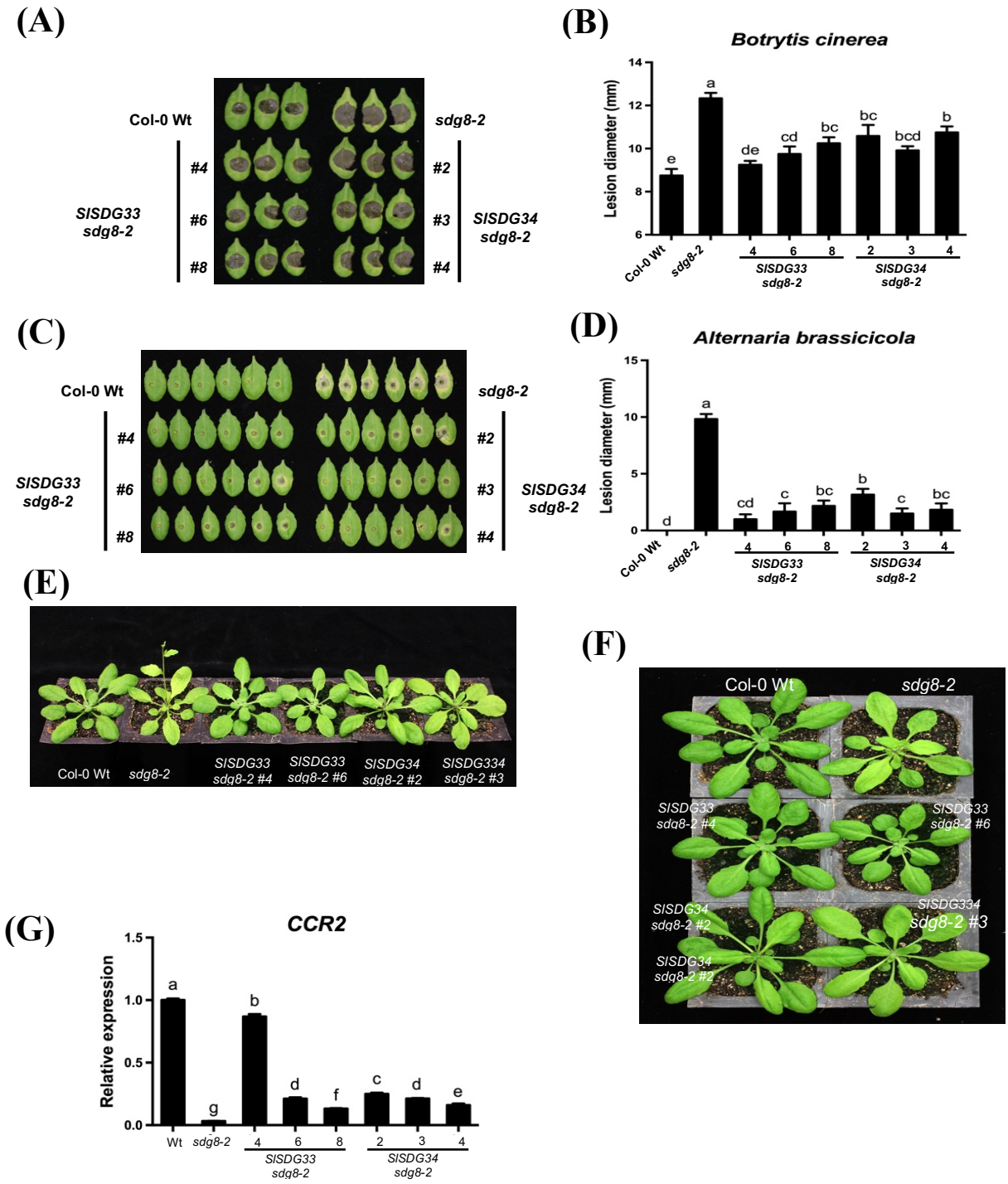

Figure 2.9. Tomato SDG33 and SDG34 complement Arabidopsis *sdg8* mutation. A) Disease symptoms, B) Disease lesion size in Arabidopsis WT, *sdg8*, *sdg8:SDG33* and *sdg8:SDG34* lines 3 days after *B. cinerea* inoculation. C) Disease symptoms, D) Disease lesion size in WT, *sdg8*, *sdg8:SDG33* and *sdg8:SDG34* 5 days after inoculation with *Alternaria brassicicola*. E) and F) The growth and early flowering phenotypes of Arabidopsis *sdg8;*SDG33 and *sdg8*;SDG34. G) Expression of CCR2 in Arabidopsis WT, sdg8, *sdg8:SDG33* and *sdg8:SDG34* lines. The data shown are the mean ± SE (n >30). Different letters represent significant differences among genotype.

Previously, we described the role of *Arabidopsis* SDG8 in plant immune response functions (148). Tomato SDG33 and 34 are also polygenically closely related to *Arabidopsis* SDG8. To determine whether SDG33 and SDG34 are functionally related, we generated *Arabidopsis sdg8* mutants plants expressing tomato SDG33 or SDG34 (*sdg8*:*SDG33*, *sdg8*:*SD34*). These transgenic plants rescued the *B. cinerea* and *A. brassiciola* susceptibility of the *Arabidopsis sdg8* mutants to wild type level (Figure 2.9A-D). In addition, the expression of the Arabidopsis *CCR2 (CAROTENOID ISOMERASE2 CHROMATIN* 2) gene is dependent on H3K4 methylation mediated by SDG8. The *sdg33* and *sdg34* mutant lines show no altered expression of the tomato CCR2 gene. However, expression of the CCR2 gene was partially rescued in most *sdg8:SDG33* and *sdg8:SDG34* lines with the highest expression of SDG33 almost restoring CCR2 gene expression to wild type levels (Figure 2.9E). Similarly, the *sdg8* mutants flower significantly earlier than the wild type, which was also rescued by expression of the tomato SDG33 and SDG34 (Figure 2.9F). Thus, *Arabidopsis* SDG8, and tomato SDG33 and SDG34 plants are functionally related.

2.4.7 Mutations in SDG33 and SDG34 alter fruit morphology, lateral root development and auxin sensitivity.

sdg33 and *sdg34* plants show normal vegetative growth comparable to the wild type background cultivar Castlemart II plants. However, fruits of *sdg33* had a pointy tip at the bottom giving them an oxy heart shape in contrast to the round bottom of the WT fruits (Figure 5A). In *sdg34* fruits, this phenotype was not consistent between the alleles and appears to be less penetrant (Figure 2.9A). Seed size, and seed morphology was not affected in *sdg33* and *sdg34* mutants. Fruit development is under the complex regulation of hormones auxins, gibberellins, ethylene and cytokinins (177, 178). Oxy-heart shaped fruits in tomato have been associated with increased auxin sensitivity (179, 180). In addition, the number of lateral roots were significantly reduced in the edited lines ($P<0.05$, Figure 2.9B-C). The *sdg33* mutants' alleles show a severely reduced lateral roots than both the wild type and *sdg34* plants. SDG33 and SDG34 are highly induced by auxin within hours of treatment (Figure 2.2C) and lateral root formation is under tight auxin regulation (181). Therefore, we speculated that these two gene may have functions in growth responses to auxin. To test this hypothesis, we determined the auxin sensitivity of *sdg33, sdg34* mutants and the wild type to different concentrations of the natural auxin Indole-3-Acetic Acid (IAA). Root

length was similarly inhibited in both the mutants and wild type when the media is supplemented with 0.5 and 1µM IAA. However, there were no significant differences between *sdg33*, *sdg34* and WT in root length at the different IAA concentrations tested. Lateral root number was significantly ($P \leq 0.05$) lower in *sdg33* and *sdg34* than the WT in the MS medium control. This difference was maintained in medium supplemented with 0.5 and 1µM IAA between *sdg33* and the WT (Figure 2.9D-E). The *sdg34* mutants had significantly lower lateral root number than the WT when the medium was supplemented with 1µM IAA (Figure 2.9E). These results indicate that *sdg33* and *sdg34* mutants are less responsive to auxin induced lateral root growth inhibition compared to the WT.

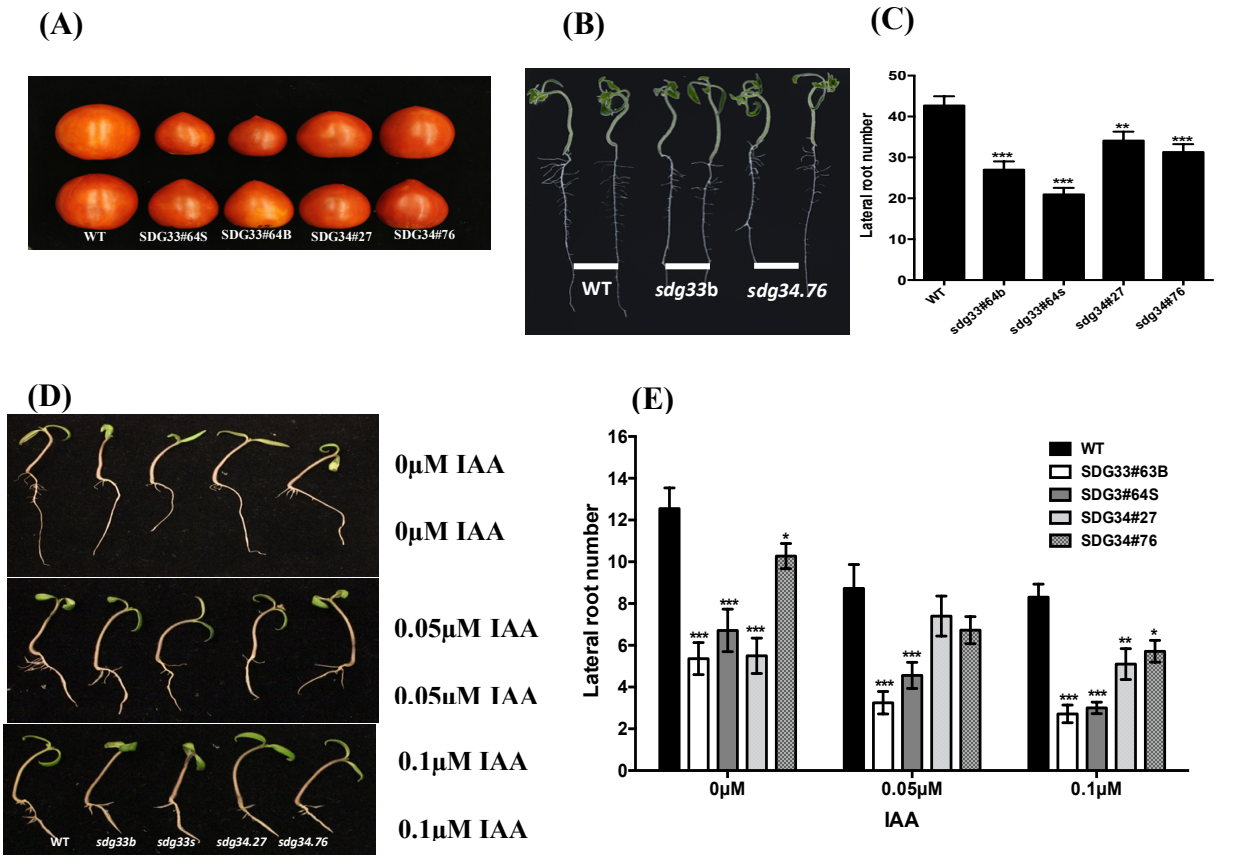

Figure 2.10 Mutation in tomato SDG33 and SDG34 alter responsiveness to IAA. A) Fruits from WT, *sdg33* and *sdg34* plants. B) Root growth of 10-day old seedlings of WT, *sdg33* and *sdg34* tomato plants. Only one allele of each mutant is shown. C) Number of lateral roots in WT, *sdg33* and *sdg34* at 10 days after germination on MS medium. D) Root growth of 10-day old seedlings of *sdg33*, *sdg34* and WT grown on medium supplemented with different IAA concentrations E) Lateral root numbers of *sdg33*, *sdg34* and WT seedlings shown in (D). The seedlings were germinated on filter paper for 3 days and transferred to MS medium supplemented with different IAA concentrations. The data shown are the mean ± SE ($n \geq 10$). Asterisks indicate significant differences using Student's t-test. (*P < 0.05, **P < 0.01, ***P<0.001). The experiment was repeated at least 2 times with similar results, representative data is shown.

2.5 Discussion

Histone lysine methylation play important roles in regulation of biotic and abiotic stress responses in plants. Hence plant histone methyltransferases have been widely reported as key regulators of biotic and abiotic stress response. We have previously reported that mutation in *Arabidopsis* histone methyltransferases SDG8 and SDG25 compromise PTI, ETI and Systemic Acquired Resistance (SAR) plant immunity pathways(148). Loss of H3K36 and H3K4 methylation in *sdg8* and *sdg25* compromise the expression of CCR2 and CER genes important regulators of carotenoid and cuticular wax biosynthesis, respectively, linking SDG8 and SDG25 regulated immune responses to carotenoid and lipid accumulation (148). In a genomic survey of tomato chromatin modifying enzymes, SDG8 orthologues were previous described in tomato as SDG33 and SDG34 (169). In this study, we describe the function of tomato histone methyltransferases SDG33 and SDG34, their role in drought responses, root and fruit development, as well as fungal resistance. We show that; 1) SDG33 and SDG34 rescues the disease and the early flowering phenotype of *Arabidopsis sdg8* mutation. 2) Although tomato SDG33 and SDG34 complement Arabidopsis SDG8 mutation, single mutants in SDG33 and SDG34 does not compromise tomato immunity to bacterial and fungal pathogens. 3) Mutations in SDG33 and SDG34 alters global H3K36 and H3K4 methylation profiles in tomato with SDG33 primarily affecting H3K4 tri-methylation and H3K36 di- and tri-methylation, and SDG34 affecting H3K4 and H3K36 at all the three levels. 4) SDG33 and SDG34 negatively regulate drought responses. *sdg33* and *sdg34* mutants survive better after water stress than the WT and drought responsive genes are upregulated in the mutants in response to drought. 5) SDG33 and SDG34 affect auxin mediated lateral root development and fruit shape.

The function of tomato histone methyltransferases has not been determined and a few have been characterised in *Arabidopsis*. SDG33 and SDG34 are closely related to *Arabidopsis* SDG8, sharing 100% similarity in the SET domain, responsible for the catalytic activity (169). Consistently, SDG33 and SDG34 complement the disease, early flowering and SDG8 dependent CCR2 expression in Arabidopsis *sdg8* indicating that SDG33, SDG34 and SDG8 have conserved functions in tomato and *Arabidopsis* (Figure 2.9A-F). This is further confirmed by the overlapping methylation activity of SDG8, SDG33 and SDG34. SDG8 is mainly a di- and tri- H3K4 and H3K36 methyltransferase (148, 182). Similarly, SDG33 and SG34 are primarily responsible for di- and tri- H3K4 and H3K36 methylations. Interestingly, although the methylation function

appears to be conserved between SDG8, SDG33 and SDG34, the disease resistance function is distinct. Mutation in SDG8 severely affects plant immune responses to bacterial and fungal pathogens (18, 21, 148) yet the single mutants of tomato *SDG33* and *SDG34* do not alter tomato immune responses to *B. cinerea* and *P. syringae* (Figure 2.8 A, B). Since SDG33 and SDG34 have overlapping methylation functions, it is plausible that there is functional redundancy in tomato which may account for the wild type responses of the sdg*33* and *sdg34* mutants for fungal or bacterial infection. Furthermore, Arabidopsis SDG8 mediates resistance to *B. cinerea* by regulating the expressions of CCR2 (148). In tomato *sdg33* and *sdg34*, the expression of CCR2 is not altered (Figure 2.8C) although SDG8, SDG33 and SDG34 share overlapping functions in histone lysine methylation patterns. These observations suggest that the tomato and Arabidopsis proteins regulate different targets. Indeed, rice SDG708 rescues the late flowering phenotype, SOC1 expression and H3K4 and H3K36 trimethylation, in the Arabidopsis *sdg26.1* mutant but the misexpression of other genes is not restored, and the expression of OsMADS50 the closest homologue of SOC1 in rice is not affected in SDG708 deficient mutant (183).

In this study, abiotic stress conditions such as water stress and ABA induced the expression of SDG33 and SDG34 (Figure 2.2B, D) indicating that they may function in abiotic stress tolerance. Loss of functions mutations *sdg33* and *sdg34* caused less growth inhibition of seedlings at high concentration of mannitol (Figure 2.4). In addition, *sdg33* and *sdg34* plants showed a less severe level of wilting than the WT (Figure 2.6A) which is further reflected in the higher RWC in *sdg33* and *sdg34* during water stress (Figure 2.6B). RWC reflects the balance between water supply to the leaf and transpiration rate and it influence the ability of the plant to recover from stress (184). Higher RWC in the mutants influenced higher survival rates in *sdg33* and *sdg34* mutants compared to the WT after water stress (Figure 2.6C). Other physiological indices like transpiration rate, stomata conductance, net carbon dioxide assimilation and chlorophyll fluorescence are the typical physiological parameters for evaluating abiotic stress tolerance in plants (185, 186). Interestingly, only RWC was significantly higher in the mutants than the WT while the other physiological indices tested were not affected. This shows that mutants employ other mechanisms other than stomata closure to maintain their higher water status which is critical for their physiological function and survival under water stress. Various transcription factors play critical role in water stress tolerance by activating downstream genes whose metabolic products are essential for water stress tolerance. The DREB (dehydration-responsive element-binding)

DREB proteins constitute a subfamily of the plant-specific AP2/ERF transcription factors and they bind to *cis*-acting element DRE/CRT (dehydration-responsive element/ C-Repeat) of drought responsive genes inducing their expression (48). High expression of DREB genes is associated with drought tolerance (46). For instance, transgenic lines overexpressing OsDREB1and ZmDREB1 resulted in drought tolerance in Arabidopsis (187, 188). In this study, we showed there is higher expression of tomato DREB in *sdg33* and *sdg34* mutants than the WT under water stress (Figure 2.8A) corroborating the role of high DREB expression in water stress tolerance. However, the mechanism of how this high expression of DREB results in water stress tolerance remains to be characterised. Accumulation of Reactive oxidative Species (ROS) is an inevitable consequence of water stress. In the absence of scavenging antioxidant organisms, ROS oxidises and damage cellular components resulting in oxidative stress. ROS defense mechanisms include the synthesis of antioxidant compound and enzymes. Studies have shown that induction of antioxidant enzymes such as POD and SOD contribute to enhanced water stress tolerance (46, 189). It is plausible to say that the enhanced water stress tolerance of *sdg33* and *sdg34* mutants can be partially attributed to high expression of the enzymes SOD and POD (Figure 2.8B, C) and thus a protection against ROS induced damages. In summary, our findings suggest that SDG33 and SDG34 negatively regulate water stress responses through misregulation of DREB, POD and SOD expression.

H3K4 and H3K36 methylation marks are associated with active gene transcription in plants (190). Here we show that loss of SDG33 and SDG34 results in loss of global H3K4 and H3K36 methylation marks (Figure 2.4). Interestingly, in response to water stress, loss of SDG33 and SDG34 results in upregulation of stress responsive genes DREB, POD and SOD. Even though H3K4 and H3K36 methylation are positive marks for gene expression, SDGs have been shown to also negatively regulate gene expression (148, 191, 192). In addition, histone lysine methylation is not necessarily correlated directly with transcriptional regulation but may generate a context for other factors to regulate gene expression at a specific environmental condition (193). Considering this, it is plausible that loss of SDG33 and SDG34 indirectly cause misregulation of DREB, POD and SOD expression. However, changes in H3K4 and H3K36 methylation patterns at these genes in response to water stress will shed light on the function of H3K4 and H3K36 methylation as well as SDG33 and SDG34 in regulating water stress responsive genes.

In conclusion, we present our observations on tomato SDG33 and SG34 genes and show that SDG33 and SDG34 negatively regulate water stress responses through misregulation of water

stress responsive genes. These finding provide new insights and generate new hypotheses in the regulation and function of water stress responsive genes.

CHAPTER 3. THE HISTONE METHYLTRANSFERASES SDG33 AND SDG34 MEDIATE NITRATE SIGNALING IN TOMATO

3.1 Abstract

Histone posttranslational modifications play an important role in regulating plant responses to environmental cues. Few studies have focused on the role of histone lysine methylation in regulating changes to nutrient availability. Here, we describe the functions of Set Domain Group 33 (SDG33) and SDG34, histone lysine methyltransferases in mediating nitrogen responses in tomato. Transcriptome analysis in the shoot and roots showed that SDG33 and SDG34 have both overlapping and distinctly regulated targets in tomato. In response to nitrogen, 509 and 245 genes are regulated by SDG33 and SDG34 in response to nitrogen states in the roots and shoot respectively. In the roots these genes were enriched with GO terms such as 'regulation of gene expression', regulation of N metabolism' and 'regulation of hormone stimuli'. 'Response to stimulus', 'photosynthesis' and 'N assimilation' were the biological processes significantly enriched in the shoots. Overall, we show that SDG33 and SDG34 are involved in regulating nitrogen responsive gene expression and hence physiological nitrogen responses in the roots and shoots.

3.2 Introduction

Nitrogen is an essential nutrient to plants. It limits growth, development and productivity of most crop plants (194). Inorganic fertilisers are the most common source to supplement nitrogen in the soil (195). Plants absorb nitrogen mainly from soil in the form of ammonium (NH_4^+) and nitrate (NO_3^-). Nitrate (NO_3^-) is easily leached from the soils to the waterways. Therefore, availability of nitrogen in soils is variable spatially and temporally. As a result, plant have to device mechanism to adapt to variable nitrogen availability in the soil. Plants respond to nitrogen levels in the soil morphologically and physiologically, which are controlled by complex gene networks. At the morphological level, plants alter their root architecture to effectively exploit the available nitrogen in the soil. Nitrogen-abundant conditions promote lateral root proliferation and increase nitrate or ammonium uptake capacity (196-199). Whereas nitrogen-deficient conditions promote primary/axial root elongation and the development of the aerenchyma (170, 200, 201). While

these morphological changes take days, physiological changes proceeds within minutes or hours. Physiological responses to nitrogen availability include modulation of nitrogen uptake under nitrogen deficiency conditions (202, 203), higher carbon assimilation rate in response to higher nitrogen leaf content (204, 205) and earlier transition from vegetative to reproductive stages under low nitrogen conditions (206). The observed morphological and physiological changes in response to different nitrogen supply are due to changes in gene expression at the molecular level. Multiple genes involved in nitrogen sensing, signalling, uptake and metabolism have been characterised and their expression is regulated by complex gene regulatory machinery (194, 206, 207). In addition, epigenetic mechanisms have emerged as an important player in regulation of gene expression under nutrient stress and have been associated with concomitant gene expression changes (5, 20).

Histone lysine methylation (HLM) is a post-translational modification of histone proteins H3 and H4. Methyl groups are added on lysine residues and this process is catalysed by enzymes called histone methyl transferases (HKMTs) using the cofactor adenosyl-methionine. Lysine residues can be mono-, di-, or tri-methylated depending on the specific function of the associated HKMTs. Histone lysine methylation influence chromatin structure and accessibility of the transcriptional machinery to the corresponding DNA, thus modulating gene expression and/or repression (6, 23, 208). The lysine residue methylated and the different levels of lysine methylation (mono-, di- or tri- methylation) can be associated with activation or repression of gene expression, thus adding to the complexity of gene expression regulation. (147).

Few studies have focused on the role of HLM in regulating changes to nutrient availability. Histone 3 Lysine 4 tri-methylation (H3K4me3) has been shown to mediate the expression of gene involved in responses to phosphate deficiency including root elongation (209). The repression of the nitrate transporter *NRT2.1* expression is associated with the induction of Histone 3 Lysine 27 tri-methylation (H3K27me3) accumulation and with the decrease of H3K4me3 and Histone 3 Lysine 36 tri-methylation (H3K36me3) levels on chromatin of *NRT2.1* in *Arabidopsis*. HNI9/AtWS1, an evolutionary conserved component of the RNA polymerase II complex is the key factor depositing H3K27me3 on *NRT2.1* chromatin, evidenced by that *hni9/atws1* is impaired in systemic feedback repression of *NRT*2.1 in high nitrogen supply (210). Despite the association of histone lysine methylation marks with the expression of genes involved in nutrient response, the specific role of HKMTs in regulating genes involved in nutrient responses have not been

studied, especially at a genome-wide scale. Such a study will further our understanding of the molecular regulation in response to nutrient supply changes, which is critical in improving nutrient use efficiency in crop plants.

In this study, we show that two tomato histone lysine methyltransferases *SDG33* and *SDG34* are important for nitrogen responses both in the roots and shoots. Mutation in SDG*33* and *SDG34* abolish the root growth in response to nitrogen. Further, chlorophyll a/b ratio is altered in *sdg33* and *sdg34* under low nitrogen condition. Global transcriptional profiling of *sdg33* and *sdg34* mutants in response to nitrogen supply show several nitrogen responsive genes misregulated and thus SDG33 and SDG34 are involved in regulating nitrogen responsive gene expression and hence physiological nitrogen responses in the roots and shoots.

3.3 Materials and Methods

3.3.1 Transgenic plants

To study the physiological role of SDG33 and SDG34, we generated the CRISPR mutants according to (165). gRNA specific to each gene were identified using CRISPR-PLANT software (198). Two guide RNA (gRNA) expression cassettes targeting adjacent sites of SDG33 or SDG34 were PCR generated using the vector pCBC-DT1DT2 (Addgene 50590) and cloned into the CRIPSR/Cas9 vector pKSE401 (Addgene 62202). Plasmids were sequenced to confirm the presence of the gRNA. We used agrobacterium mediated plant transformation and plant mutants were generated through tissue culture. Mutation were confirmed by PCR on genomic DNA using markers flanking the target gRNAs and sequencing of the PCR products.

3.3.2 Plant growth conditions and treatments

Tomato (*Solanum lycopersicum)* cultivar CastlemartII was used in this study. *sdg33* and *sdg34* CRISPR mutants were generated as described above. Seeds were surface sterilized with 20% sodium hypochlorite for 20 minutes and rinsed with distilled water. The seeds were germinated on filter paper in the dark until the radicle emerged and transferred into black sand for the seedlings to established for one week. Seedlings where then grown hydroponically in foil tapped plastic containers with one litre nutrient medium, which consisted of 1.2 mM KNO_3, 0.8mM $Ca(NO_3)_2$, 0.2mM $NH_4H_2PO_4$, 0.2mM $MgSO_4$, 50μM KCl, 12.5 μM H_3BO_3, 1 μM $MnSO_4$,

1 μM$ZnSO_4$, 0.5 μM$CuSO_4$, 0.1 μM H_2MoO_4, 0.1 μM $NiSO_4$ and 10 μM Fe-EDDHA (211). Plants where grown in the green house with photoperiod of 16-h light and 8-h dark at 24 °C. Two plants where grown in one container and aeration was provided for one hour daily to increase the oxygen content of the nutrient medium. Nutrient medium was refreshed every three days.

After two week of growth in nutrient medium, plants were transferred into starvation medium, which is identical to the nutrient medium except for that 1.2 mM KNO_3, 0.8mM $Ca(NO_3)_2$, 0.2mM $NH_4H_2PO_4$ were replaced by 0.6mM K_2SO_4, 0.8mM $CaSO_4$, 0.2mM KH_2PO_4 respectively. After two days in the starvation medium, plants were transferred into two treatment media: (1) with nitrogen (+N); and (2) with potassium chloride (KCl). The +N treatments medium was the same as the growth medium and the KCl treatment medium the same as starvation solution. Plants where growth in respective treatments for seven days and phenotyped on the eighth day.

3.3.3 RNA extraction

Plants were grown hydroponically as described above. Three independent plants were pooled to make one replication and three replications per treatment per genotype were used for RNA extraction. RNA for transcriptome profiling was extracted from root and shoot samples harvested at five hours after nitrogen and KCl treatments. Total RNA was extracted from the shoots and roots using Trizol (Invitrogen) according to the manufacturer's instructions. After extraction, total RNA was treated with DNase (New England Biolabs) according to the manufacturer's instruction. RNA was then precipitated with 3M sodium acetate and three-times volume of 100% ethanol and resuspended in DEPC treated water. RNA was then concentrated using ZYMO RNA clean and concentrator kit (ZYMO Research) according to the manufacturer's instructions. Integrity of RNA was accessed by the Agilent Bioanalyzer (Agilent technologies).

3.3.4 RNA sequencing and data analysis

RNA samples were submitted to the Purdue Genomics Core for RNA-Seq library preparation and sequencing on an Illumina Novaseq platform with paired-end 50bp format. On average, approximately 25 million read pairs were generated for each library. The raw sequencing reads were trimmed by the Purdue Genomics Core to remove adaptors and low-quality reads. Next, trimmed reads were mapped against tomato genome (build 3.0, assessed on June 5 2019) using

BBmap (212). Next, mapped reads were used to generate a count for each gene feature in the genome, using the tomato gene models ITAG3.2 and the annotated miRNA loci based on miRbase (213), using FeatureCounts (214)[. Finally, differentially expressed genes were detected using DESeq2 (215) with the design (~Genotype+Treatment+Genotype:Treatment), for *sdg33* and *sdg34*, separately.

3.3.5 Motif analysis

A promoter database was created by extracting1kb upstream sequence of every gene in the ITAG3.2 genome annotation using NCBI blast toolkit (216). Cis-regulatory motif analysis was then performed for gene sets of interest, by running MEME (217)on the 1kb promoters of the gene set using the following parameters: revcomp=yes, mod=anr, nmotifs=5, and w=10. The identified significant motifs (E value <0.001) were then annotated using TOMTOM(218) by comparing against known TF binding motifs (p-value <0.0001).

3.3.6 Phenotyping

Chlorophyll content

Chlorophyll (Chl) content was first analysed during the N treatments by measuring chlorophyll fluorescence with a SPAD-502(219). The Soil Plant Analysis (SPAD) units read by the equipment are correlated to plant chlorophyll content. Measurement were taken daily on three fully expanded leaves per plant at the same time. Averaged values were taken as the chlorophyll content.

For a more precise quantification of chlorophyll content, shoots were harvested at the end of the treatments and frozen in liquid nitrogen. The shoot tissue was ground to fine powder, weighed and chlorophyll was extracted with methanol by incubating at room temperature for 10 min with gentle rotation. The extract was centrifuged at 13000rpm for seven minutes and the supernatants were used for absorbance measurement. The absorbance was measured using supernatant at 750, 665 and 652nm by a Tecan microplate reader (Tecan Switzerland), using methanol as the blank. Chlorophyll a (Chla), Chlorophyll b (Chlb), ratio of Chla:b, and total chlorophyll were calculated according to (169, 220).

Root architecture measurements

Root systems grown in hydroponics solutions were laid in a single pane in a transparent tray on top of a light box and imaged by a fixed height digital camera. Images were uploaded in the root imaging software GiA roots (221) for processing and phenotyping. The GiA root pipeline consists of image preparation steps (scaling, rotating and cropping), creating a grey scale image, and applying double adaptive imaging thresholding with pre-set parameters to produce binary foreground (root) or background (non-root). The binary images were then processed for all the root architecture trait calculations. Pixels were scaled to the appropriate dimension; millimetres, square millimetres or cubic millimetres using a reference ruler in the image.

Statistical analysis

Two-way ANOVA was performed to test the impact of genotype, nitrogen treatment and their interaction on each phenotypic trait. ANOVA was performed in the R software, version 3.3.1 (R Core Team, 2016) using the Agricolae package. Statistical significance was determined at the level $P \leq 0.05$. To further analyse which means are significantly different, means were compared using the student 's T test. Nitrogen response was also determined by comparing the means in the nitrogen treatment (+N) to the control treatment using two sample *t*-test assuming unequal variance.

3.4 Results

3.4.1 SlSDG33 and SlSDG34 regulate the expression of overlapping yet distinct downstream genes

Arabidopsis SDG8 was previously shown to mediate H3K36me3 changes in genes that regulate nitrate assimilation, signalling and reduction (Li et al, 2019). Interestingly, two tomato genes SDG33 and SDG34 were previously identified as orthologues of AtSDG8 (169). The functions of SDG33 and SDG34 in nitrogen response is not known. We hypothesised that the function of AtSDG8 and tomato SDG33 and SDG34 in regulating nitrogen response is conserved and that SDG33 and SDG34 have similar function in regulating nitrogen response in tomato. To test these hypotheses, we generated transcriptome profiles of sdg33 or sdg34 mutants and WT treated with nitrogen and without nitrogen using RNA-seq. Specifically, *sdg33* and *sdg34* mutants

and wild type plants were grown in nitrogen rich media hydroponically for two weeks, starved for nitrogen for forty-eight hours and transferred either into media supplemented with nitrate and ammonium or into media with salt controls (see methods). Shoots and roots were harvested after 5-hour of treatment for RNA-Seq to elucidate the genome wide regulatory impact of SDG33 and SDG34 in response to nitrogen treatments.

We first identified differentially expressed genes (DEGs) that are affected by the main factor genotype (*i.e.* WT vs mutant) with log2 (fold change) > |2| at an FDR cut-off of 5% in the roots and shoots. In the roots, 416 genes were upregulated and 167 downregulated in *sdg33* (Table 1, Figure 3.1A, Supplemental table S1) and in *sdg34,* 350 genes were upregulated and 120 were downregulated *sdg33* (Table 1, Figure 3.1B, Supplemental table S2). In the shoots, 653 genes were upregulated in *sdg33* and 951 were downregulated (Table 1, Figure 3.1C, Supplemental table S3) and in *sdg34*, 634 genes were upregulated and 683 were downregulated (Table 1, Figure 3.1D, Supplemental table S4).

Table 3.1 . Summary of differential expressed genes (DEGs) from pairwise comparison of each genotype and WT.

		***sdg33* vs WT**	***sdg34* vs WT**	**Shared between *sdg33* and *sdg34***
Shoots	Up-regulated	653	634	479 (76%)
	Down-regulated	951	683	558 (82%)
Roots	Up-regulated	416	350	260 (74%)
	Down-regulated	167	120	83 (69%)

To investigated whether SDG33 and SDG34 have diverged function in regulating downstream genes, we compared these DEGs detected in *sdg33* and *sdg34*. In the roots, 260 genes were common between upregulated genes in *sdg33* and *sdg34* (Figure 3.2A, B) and 83 common between the down regulated genes (Figure 3.2C, D) The common up-regulated genes are enriched with GO terms such as “response to auxin” and “oxidation-reduction process” (Supplemental table S5), while the unique genes only up-regulated in either *sdg33* or *sdg34* have no significant GO terms (FDR cutoff 5%). The common and *sdg34* down-regulated genes did not have any significant

enriched GO term, while the unique genes down-regulated in the *sdg33* mutant had the GO term "oxidoreductase activity" overrepresented (Supplemental Table S6).

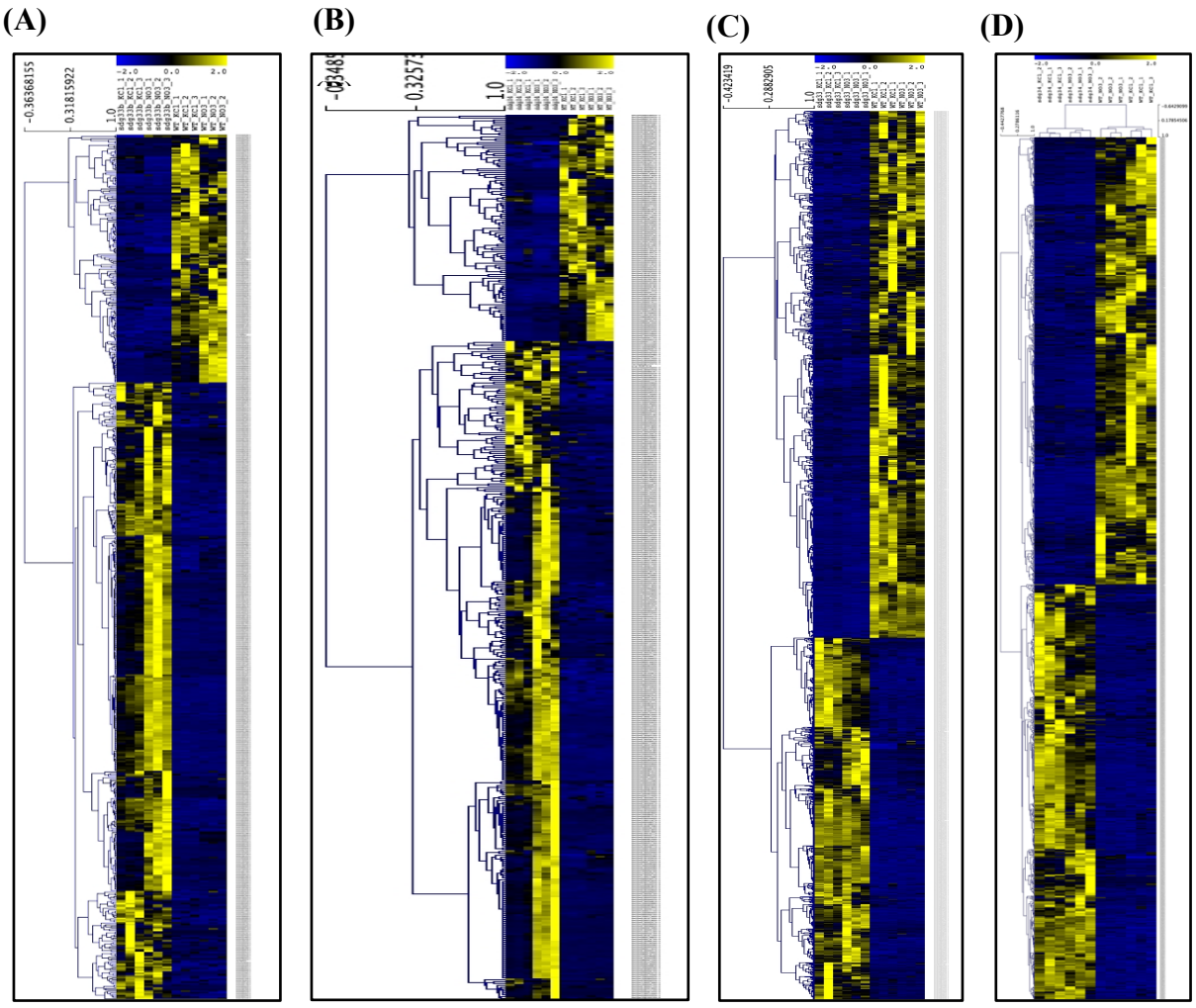

Figure 3.1. Genotypic effect of SDG33 and SDG34 mutation on tomato transcriptome. Hierarchal clustering of relative expression of DEGs based on the pairwise comparison of *sdg33* or *sdg34* and the WT in A) *sdg33* roots, B) *sdg34* roots, C) *sdg33* shoot and D) *sdg34* shoots. FDR < 0.05; $|\log_2$ fold change$| > 2$; Yellow and blue indicate higher and lower expression values, respectively.

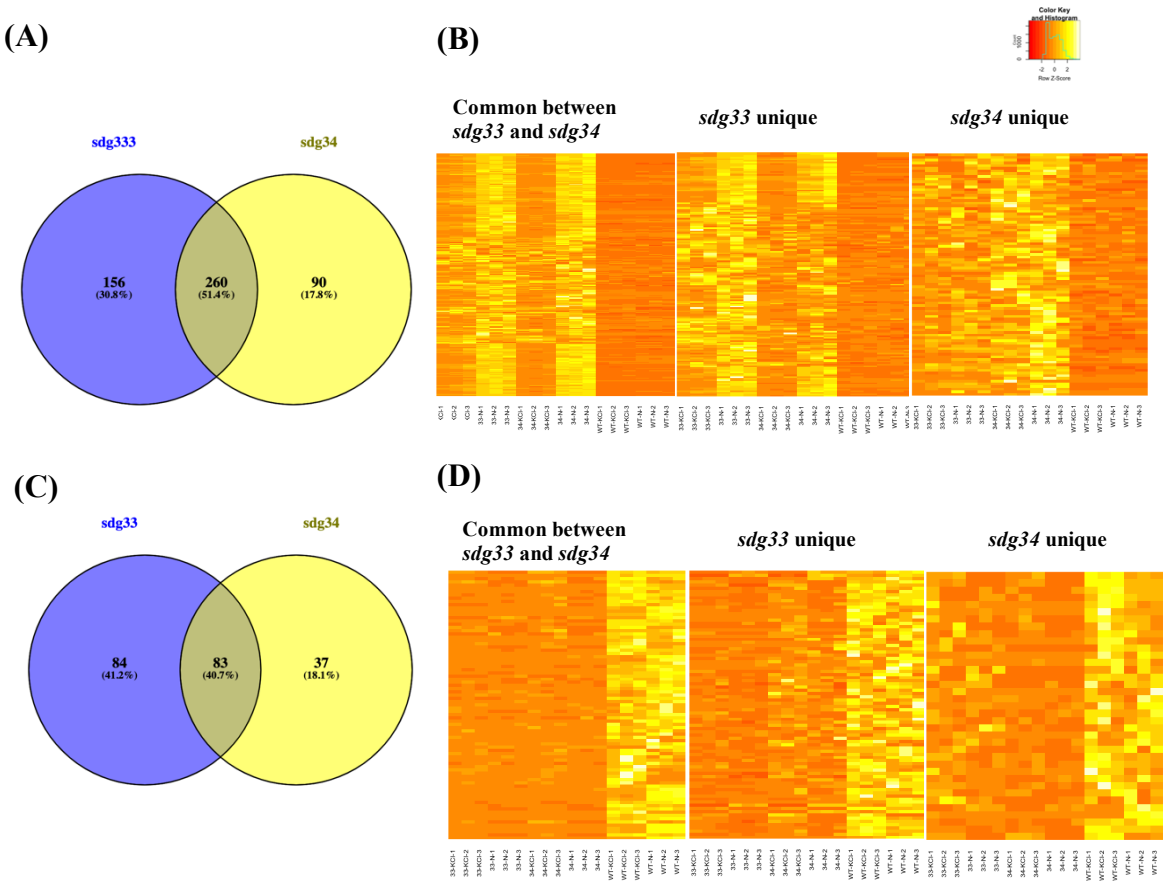

Figure 3.2. Summary of DEGs in the roots. A) Venn diagram of up-regulated DEGs in *sdg33* and *sdg34* showing overlapping and exclusive DEGs. B) Heat maps showing common up-regulated DEGs between *sdg33* and *sdg34* and exclusive DEGs in *sdg33* and *sdg34*. C) Venn diagram of down-regulated DEGs in *sdg33* and *sdg34* showing overlapping and exclusive DEGs. D) Heat maps showing common down regulated DEGs between *sdg33* and *sdg34* and exclusive DEGs in *sdg33* and *sdg34*. FDR < 0.05; $|\log_2$ fold change$| > 1$; Orange and Yellow b indicate lower and higher expression values, respectively.

In the shoots, 479 were common between *sdg33* and *sdg34* for the up-regulated genes *sdg34* (Figure 3.3A, B), and 558 are shared between *sdg33* and *sdg34* for the down regulated genes *sdg34* (Figure 3.3C, D). The common genes repressed by SDG33 and SDG34 (hence upregulated in *sdg33* and *sdg34*) are enriched with GO terms "response to auxin" and "oxidoreductase activity. (Supplemental Table S7). The genes that are uniquely repressed by SDG33 also have the significant GO term "response to auxin" and "oxidoreductase activity" (Supplemental Table S8). The genes that are uniquely repressed by SDG34 has only one significant GO term "extracellular region" (FDR<0.0062). The common genes activated by SDG33 and SDG34 (hence downregulated in *sdg33* and *sdg34*) are enriched with GO terms "transcription factors", "primary metabolism", and "nitrogen compound biosynthetic process" (Supplemental Table S9). The genes

that are only activated by SDG33 are enriched with GO terms "DNA binding" (FDR<0.019), and the genes that are only activated by SDG34 had no significant GO terms.

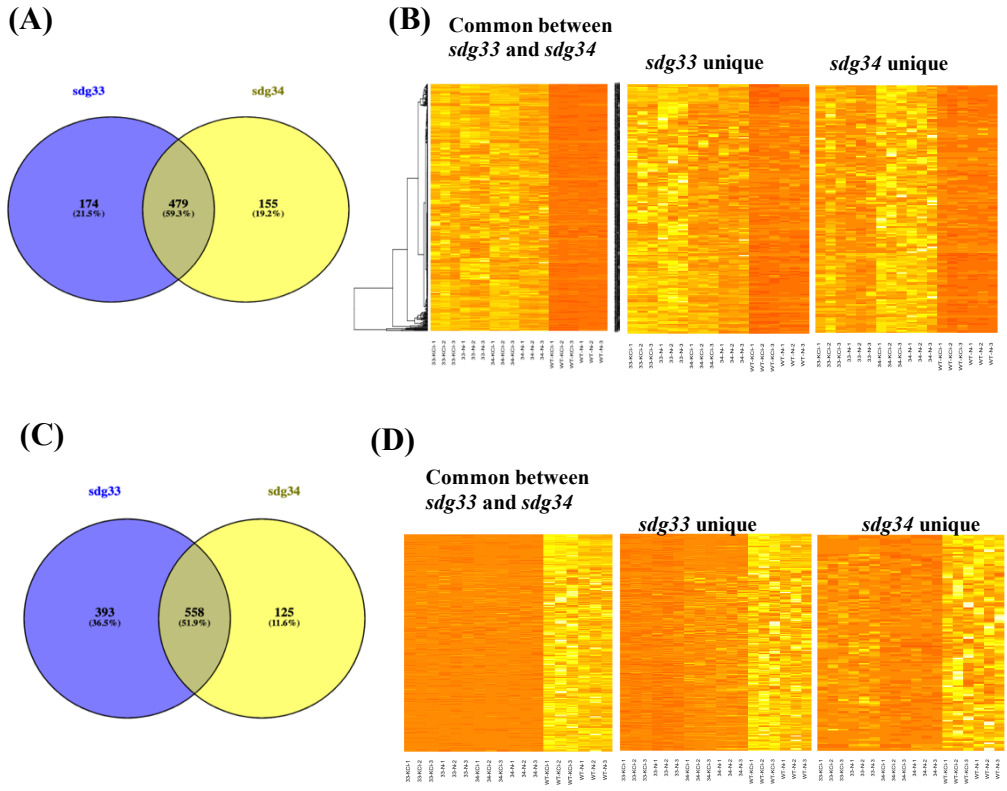

Figure 3.3. Summary of DEGs in the shoots. A) Venn diagram of up-regulated DEGs in *sdg33* and *sdg34* showing overlapping and exclusive DEGs. B) Heat maps showing common up-regulated DEGs between *sdg33* and *sdg34* and exclusive DEGs in *sdg33* and *sdg34*. C) Venn diagram of down-regulated DEGs in *sdg33* and *sdg34* showing overlapping and exclusive DEGs. D) Heat maps showing common down regulated DEGs between *sdg33* and *sdg34* and exclusive DEGs in *sdg33* and *sdg34*. FDR < 0.05; $|\log_2$ fold change$| > 1$; Orange and Yellow b indicate lower and higher expression values, respectively.

In summary, our data shows that many genes are commonly regulated by SDG33 and SDG34, indicating overlapping functions between SDG33 and SDG34. SDG33 and SDG34 seem to repress the expression of genes involved in auxin response and oxidation-reduction process in both shoots and roots. In the shoots, SDG33 and SDG34 activate genes involved in primary metabolism and encoding transcription factors. While SDG33 and SDG34 have overlapping functions, our data also shows that they also have distinct functions shown by the unique genes regulated by SDG33 or SDG34, often enriched with distinct GO terms. SDG33 seem to affect a bigger number of genes than SDG34 in both shoots and roots, and for either up-regulation or down-

regulation. GO term analysis also suggest that the genes that are uniquely regulated by SDG33 are functionally more similar to the genes that are commonly regulated by SDG33 and SDG34.

3.4.2 Cis-regulatory motifs in the promoters of genes regulated by SDG33 or SDG34

To investigate the mechanism by which the two homologs SDG33 and SDG34 regulate different downstream genes, we analysed the cis-regulatory motifs in the promoters of genes regulated by SDG33 and SDG34. We used MEME (222) motif analysis to analyse 1000bp upstream of the SDG33 and SDG34 commonly regulated genes. The significant motifs were matched to the Arabidopsis motif database using TomTom (218). Overall, genes regulated by SDG33 or SDG34 seem to share a common motif with the core sequence GGGGNGGGG. Additional motifs that are specific to tissue types (shoots vs roots), direction of regulation (up-regulation vs down-regulation), and homologs (SDG33 vs SDG34) were also identified (Table 3.2).

In the roots, the common upregulated genes had the cis-regulatory motifs AAGAAAAAGA (E-value= 5.0e-007) that is similar to a BPC5 binding site, TTTT$_{T/A}$TTTT$_{T/G}$ (E-value= 1.3e-019) that is similar to a REM19 binding site and GGGGGNGGGG. In addition, genes upregulated in *sdg34* had the TTG$_{T/A}$GGG$_{G/A}$CC motif (E-value= 2.0e-003) matched to the TCP family binding site (Table 3.2). The downregulated genes between *sdg33* and *sdg34* share a CCAAGGG$_{C/T}$G motif. Furthermore, genes downregulated in *sdg33* have additional significantly overrepresented motifs in the promoters: AAAA$_{A/T}$A$_{A/G}$AA (E-value= 1.2e-015) that is matched to the C2C2 DOF transcription factor family, and CCGTGTGTGC (E-value= 4.5e-010).

Table 3.2.Motifs enriched in the promoters of DEGs upregulated and downregulated in the shoots and roots *sdg33* and *sdg34* identified from a de novo search using MEME software. Letter size indicates nucleotide frequency

		Motif	Best transcription factor match
Root Upregulated	**Shared between *sdg33* and *sdg34***	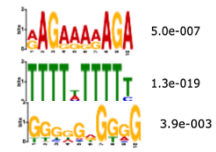	**BRBBPC (BPC5) (P= 4.31e-05)** **REM (REM19)(P= 1.69e-06)**
	sdg33		
	sdg34	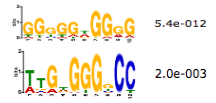	**TCP Binding site (P=4E-5)**
Root Downregulated	**Common (*sdg33* and *sdg34)***	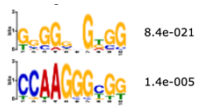	
	sdg33	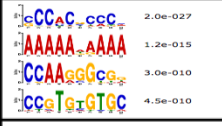	**C2C2 DOF (P=7E-7)**
	sdg34	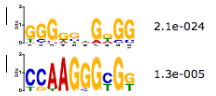	
Shoot Upregulated	**Common (*sdg33* and *sdg34)***		**C2H2 (P=6.40E-04)**
	sdg33	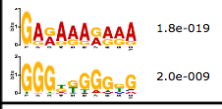	**C2C2 DOF (P=9E-5)**
	sdg34	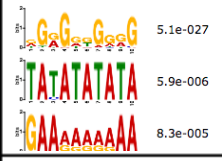	**TCP Binding site (P=7E-7)** **ABI3 VP1 (P=1.7E-5)**
Shoot Downregulated	**Common (*sdg33* and *sdg34)***	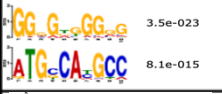	**TCP (P=7.05E-04)**
	sdg33		
	sdg34		**C2C2 GATA (P=1E-5)**

In the shoots, in addition to the GGGGNGGGG core motif that is shared by the promoters of genes upregulated in both *sdg33* and *sdg34,* the GA[G/A]AAA[G/A]AAA motif (E-value= 1.8e-019) of C2C2 DOF family transcription factors is enriched in the promoters of genes repressed by SDG33. In *sdg34* the upregulated genes had the cis-regulatory motifs TATATATATA (E-value= 5.9e-006) and GAAAAAAAAA (E-value= 8.3e-005) over-represented (Table 3.2). The genes downregulated in both *sdg33* and *sdg34* have the ATGNCANGCC (E-value= 8.1e-015) motif in addition to the GGGGNGGGG core sequence in the promoters. In addition, in *sdg34* the downregulated genes had the CA/CT/CCA/CC/TCG/ACC (E-value= 9.9e-003) that is similar to the C2C2 GATA transcription factors (Table 3.2).

Overall, our results suggest that SDG33 and SDG34 might interact with an unknown transcription factor that binds GGGGNGGGG to regulate downstream targets. In addition, SDG33 and SDG34 might interact with different transcription factors in different organs to up-regulate or down-regulate downstream genes.

3.4.3 SDG33 and SDG34 regulated genes overlap with *At*SDG8 targets in Arabidopsis

To test if the downstream targets of histone methyltransferase are conserved between species, we compared the target genes of SDG33 and SDG34 with the target genes of its Arabidopsis homolog, *At*SDG8. To do this, we first identified the best Arabidopsis homologs for each tomato genes regulated by SDG33 or SDG34 by BLASTP (Supplemental Table S3 &S4; best hit by BLASTP with E value cutoff 1e-6). Next, we compared these gene lists with the AtSDG8 targets (Li et al 2015). Interestingly, both the down-regulated and up-regulated genes in *slsdg33* and *slsdg34* mutants have significant overlap with the *bona fide* AtSDG8 targets ($p<0.001$; Table 3.3), which are largely down-regulated in Arabidopsis *sdg8* mutant (Li et al 2015). This result supports a certain level of conservation of targets between *At*SDG8 and the tomato homologs SDG33 and SDG34, as well as indicate possible functional divergence as the gene activated by AtSDG8 could be repressed by the tomato homolog.

Table 3.3. *P value* and number of genes the target genes shared between the targets of SDG33 and SDG34 with the target genes of its Arabidopsis homolog, *At*SDG8.

SlSDG33/34 regulatory targets in shoots		High Confidence Direct targets (728)	**AtSDG8 genomics targets**
Down-regulated genes	*Slsdg33* vs WT (638)	0.001(29)	
	Slsdg34 vs WT (460)	<0.001 (25)	
Up-regulated genes	*Slsdg33* vs WT (465)	<0.001 (30)	
	Slsdg34 vs WT (447)	<0.001 (27)	

3.4.4 SDG33 and SDG34 mediate the transcriptional response to nitrogen in shoots and in roots.

To understand the role of SDG33 and SDG34 in regulating nitrogen response, we analysed the DEGs whose response to nitrogen is dependent on SDG33 or SDG34 (i.e. *sdg33* x N and *sdg34* x N) in the roots and shoots, separately. In the roots, 708 gene were regulated by the interaction between SDG33 and nitrogen treatment and 1212 genes were regulated by SDG34 and nitrogen treatment. Of these genes 509 were common between those regulated by the interaction between nitrogen and SDG33 or SDG34 (Table 3.4, Figure 3.4A).

Table 3.4. Summary of differential expressed genes (DEGs) regulated by SDG33 and sSDG34 in a nitrogen dependent manner. Threshold for differential expression is log2 fold change > |1|, false discovery rate < 0.05.

Number of DEGs	*sdg33* X N	*sdg34* X N	Shared between sdg33 and sdg34
Shoots	471	711	245 (52%)
Roots	708	1211	509 (72%)

We visualised the expression pattern of the common genes and clustered them based on similarity of gene expression pattern. We further did a GO term enrichment on the specific clusters. The 509 genes that are commonly regulated by the interaction between nitrogen and SDG33 or SDG34 clustered into four major groups. Surprisingly, most of these genes are nitrogen responsive in the mutant, but not in WT, indicating a hypersensitivity to nitrogen in the mutant. The first and biggest cluster had genes that are induced by nitrogen treatment in the mutants but not in the WT (Figure 3.4B). Genes in this cluster are enriched with the GO terms such as 'regulation of RNA biosynthetic process', 'Regulation of transcription, DNA templated' and 'regulation of nitrogen metabolic process'. The second cluster had genes whose expression goes down in the mutants in response to nitrogen but do not change in the WT. Overrepresented genes in this cluster had GO terms such as 'transport', 'establishment of localisation'. The third and fourth cluster had gene that are induced by nitrogen in the WT but not in the mutants and those whose expression induced by nitrogen in the WT but goes down in the mutants respectively (Figure 3.4B).

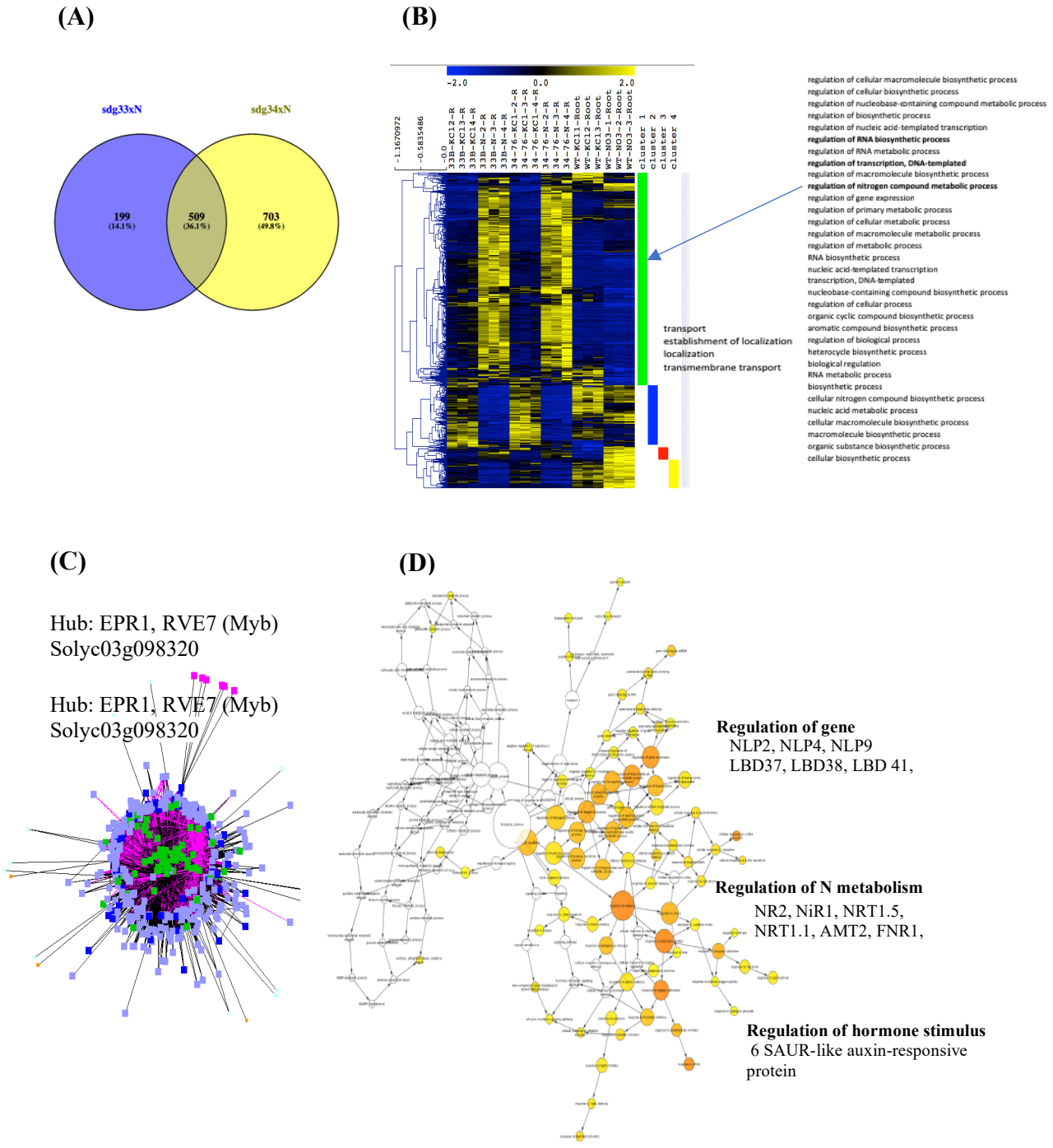

Figure 3.4 SDG33 and SDG34 mediate gene expression in a nitrogen dependent manner in the roots. A) Venn diagram of overlapping and exclusive *sdg33* x nitrogen and *sdg34* x nitrogen (Interaction) DEGs B) Hierarchal clustering of relative expression of DEGs regulated by sdg33 or sdg34 and nitrogen treatment. GO terms significant for the clusters are shown on the left C) Gene network and D) Go terms of gene network of DEGs regulated by *sdg33* or *sdg34* and nitrogen treatment.

To further investigate the function of gene network regulated by SDG33 and SDG34 in mediating nitrogen response in the roots, we studied the regulatory relationship between the genes regulated by SDG33 and SDG34 in a nitrogen dependent manner by exploiting the known gene-to-gene interactions in Arabidopsis homolog genes. To do this, we used network analysis in VirturalPlant (223) to construct a gene network from the 509 genes that are commonly regulated by the interaction between nitrogen and SDG33 or SDG34. The gene network analysis identified a MYB family transcription factor Solyc03g098320 (Arabidopsis homolog: AT1G18330) as the hub gene (Figure 3.4C). We also identified the enriched GO terms in this gene network using BINGO (224). The gene networks were significantly enriched with biological processes GO terms such as 'regulation to hormone stimulus', 'regulation of N metabolism' and 'regulation of gene expression' (Figure 3.4D). Therefore, we further investigated the genes related to these functions. A couple of SAUR auxin responsive proteins are responsive to N in the WT, but not in the mutant *sdg33* or *sdg34* (Figure 3.5). Relevant to 'regulation of N metabolism' and 'regulation of gene expression', structural and regulatory genes related to nitrogen uptake and assimilation, including transporters (NRT1.1, AMT2), assimilation enzymes (NR2, NiR, and FNR1), master regulators NLPs (NLP2, NLP4, NLP8) and LBDs (LBD38 and LBD37), are misregulated in mutant compared to WT (Figure 3.5A&B). The expression profiles of these genes are presented in figure (Figure 3.5).

(A)

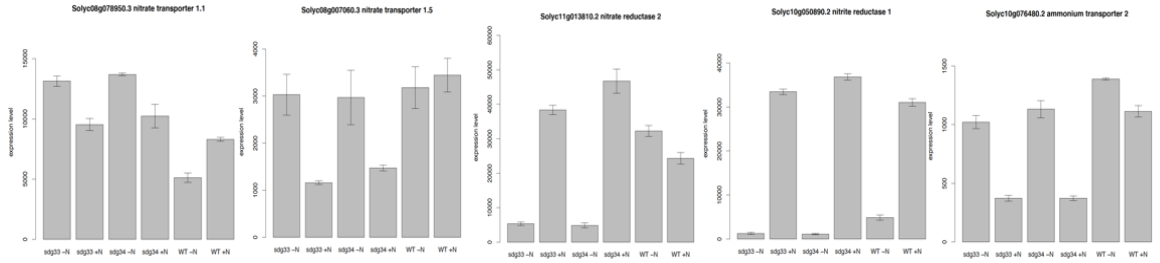

(B)

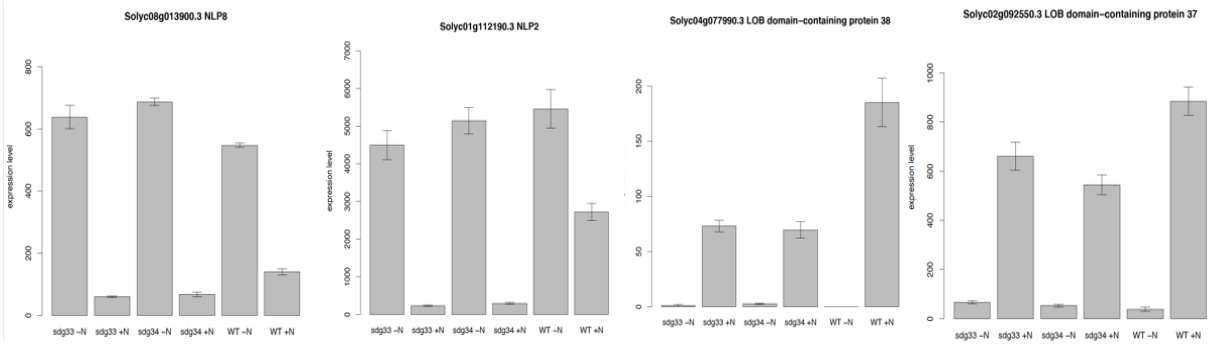

(C)

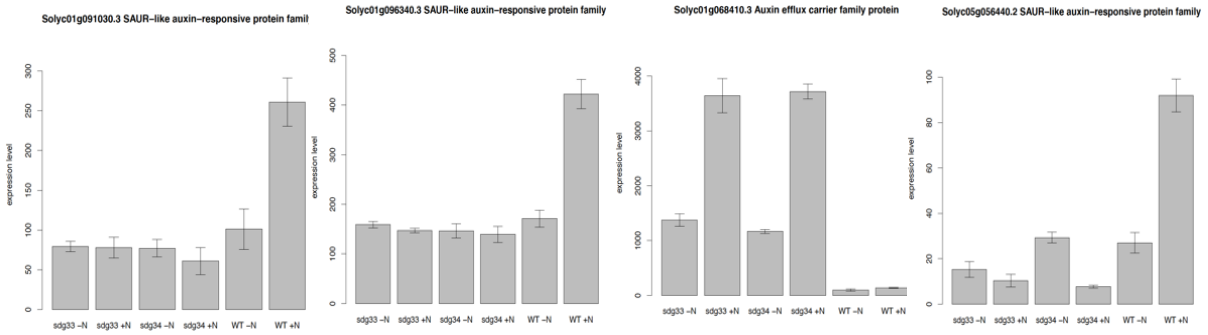

Figure 3.5. SDG33 and SDG34 mediate gene expression in a nitrogen dependent manner in the roots. Expression of a representative set of genes whose expression is mediated by *sdg33* or *sdg34* and nitrogen treatment. A) Nitrogen assimilation genes, B) Transcription factors and C) Auxin responsive genes

In the shoots, 472 genes were regulated by the interaction between SDG33 and nitrogen treatment and 712 genes were regulated by SDG34 and nitrogen treatment. Of these genes 245 were common between those regulated by the interaction between nitrogen and SDG33 or SDG34 (Figure 3.6A).

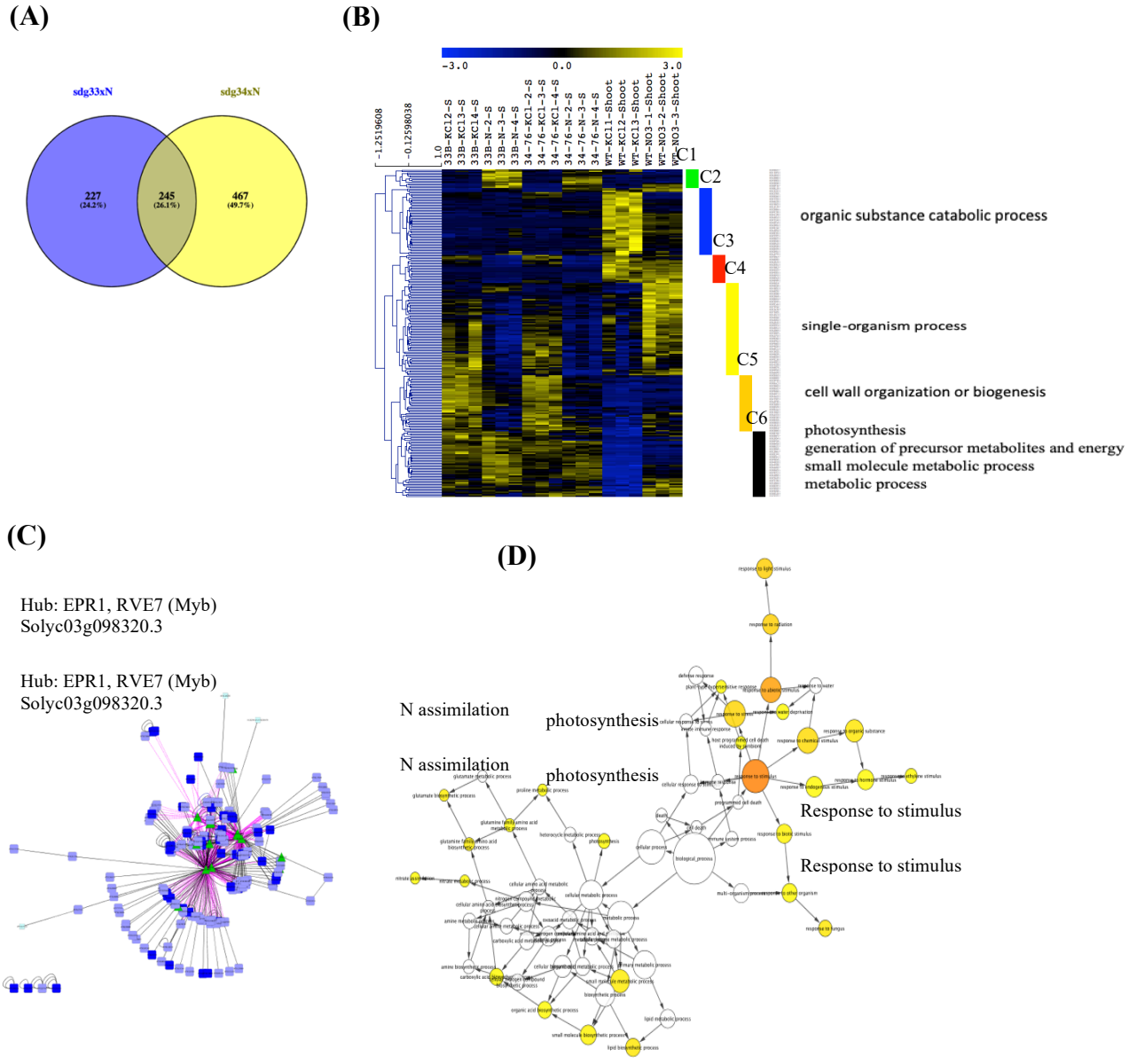

Figure 3.6.SDG33 and SDG34 mediate gene expression in a nitrogen dependent manner in the shoots. **A)** Venn diagram of overlapping and exclusive *sdg33* x nitrogen and *sdg34* x nitrogen (Interaction) DEGs B**)** Hierarchal clustering of relative expression of DEGs regulated by *sdg33* or *sdg34* and nitrogen treatment. GO terms significant for the clusters are shown on the left **C)** Gene network and **D)** Go terms of gene network of DEGs regulated by *sdg33* or *sdg34* and nitrogen treatment.

We visualised the expression pattern of the common genes and clustered them based on similarity of gene expression pattern. We further did a GO term enrichment on the specific clusters. The 245 genes that are commonly regulated by the interaction between nitrogen and SDG33 or SDG34 clustered into six major groups. Cluster 6 is particularly interesting; it contains genes that are induced by nitrogen in the WT but are expressed highly in the mutants despite the N treatment. This cluster is enriched with the GO terms such as 'photosynthesis', 'generation of precursor molecules and energy', small molecule metabolic processes' and' metabolic process' (Figure 3.6B). Cluster 2 had genes that are induced by nitrogen starvation in the WT but not in the mutant. This cluster is enriched with the GO term 'organic substance catabolic process' (Figure 3.6B). Similarly, to the analysis of root gene network, gene network analysis was also performed with the 245 genes commonly regulated by the interaction between nitrogen and SDG33 or SDG34. Interestingly, the same hub gene Solyc03g098320.3 (Arabidopsis homology AT1G18330) was identified as the master regulator of the shoot regulatory gene network, as well as the root regulatory gene network (Figure 3.6C). The gene network was enriched with GO terms such as 'N assimilation', 'Photosynthesis' and 'response to stimulus' (Figure 3.6D). The 'N assimilation' includes genes such as nitrate reductase (NR) and glutamate synthetase while the 'photosynthesis' group includes genes such as chlorophyll a-b binding protein, photosystem1 and photosystem II subunits proteins (Figure 3.7), which are misregulated in the mutant compared to WT. Overall, our data shows that SDG33 and SDG34 mediates genome-wide transcriptome changes in response to nitrogen.

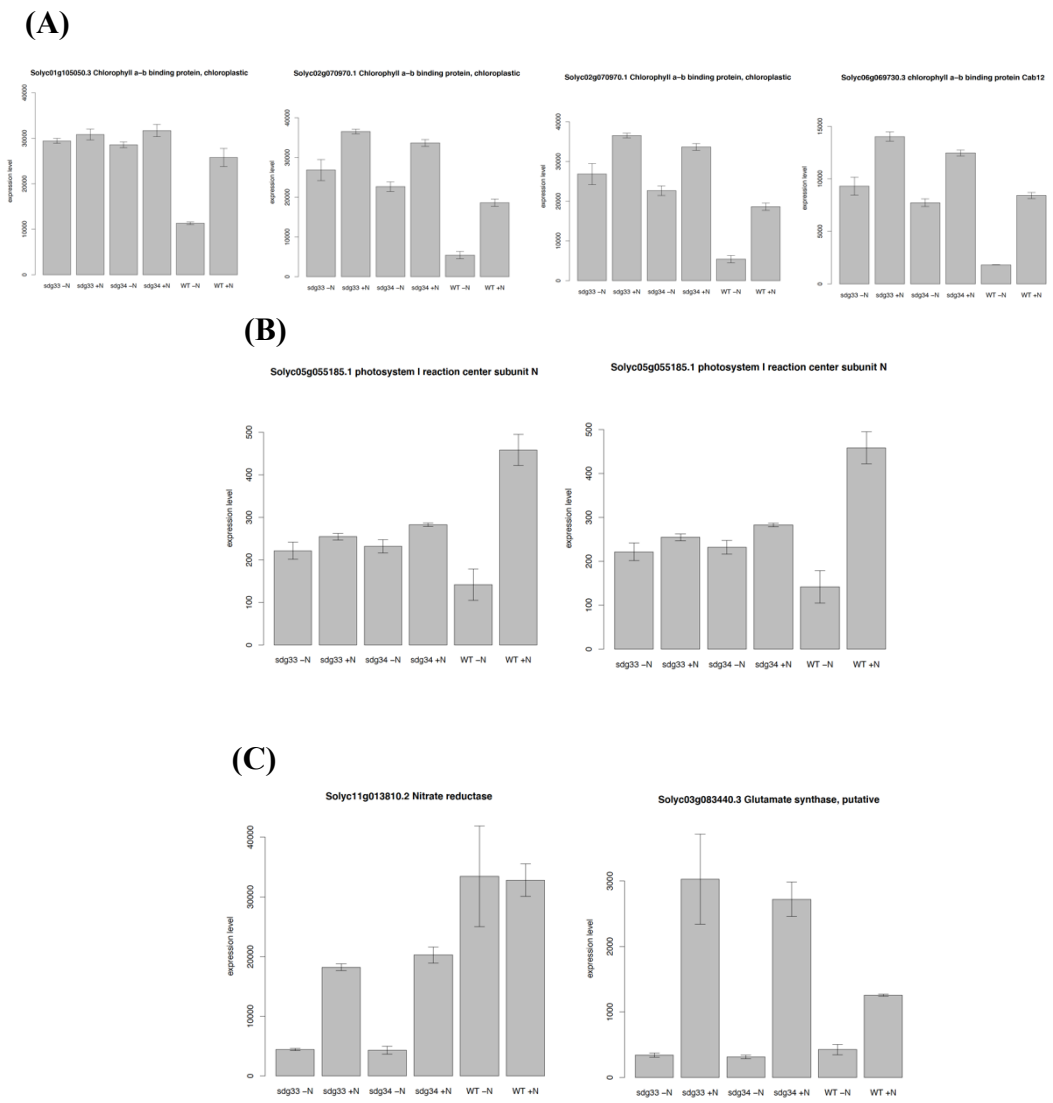

Figure 3.7.SDG33 and SDG34 mediate gene expression in a nitrogen dependent manner in the shoots. Expression of a representative set of genes whose expression is mediated by *sdg33* or *sdg34* and nitrogen treatment. A) Nitrogen assimilation genes, B) Transcription factors and D) Auxin responsive genes.

3.4.5 Mutation in SDG33 and SDG34 alters nitrogen physiological response in tomato roots.

The RNA-Seq data showed that SDG33 and SDG34 regulate the expression of a variety nitrogen responsive genes during nitrogen responses. Thus, we tested weather this altered transcriptional regulation translates to an altered physiological response in tomato. *sdg33* and *sdg34* mutants and wild type plants were grown in nitrate rich media hydroponically for two weeks, starved for nitrogen for forty-eight hours, transferred either into media supplemented with nitrate and ammonium (+N) or into media with control salts (-N). Plants where growth in respective treatments for seven days and phenotyped on the eight day. Twenty-one root phenotypic traits were evaluated at the end of the experiment using GiA roots software. Interestingly, bushiness gave consistent and significant data (Figure 3.8A). Bushiness is the ratio of the maximum to the median number of roots, counted in transverse sections along the longitudinal axis of the root system. In another word, business measures the growth of lateral roots. Bushiness was significantly affected by genotype, nitrogen treatment and the interaction between genotype and nitrogen treatment (Table 3.5). Specifically, bushiness was increased significantly by the nitrogen treatment in the wild type, but not in the *sdg33* and *sdg34* mutants (Figure 3.8A).

Table 3.5. Analysis of variance of Chlorophyll A (chlA), Chlorophyll B (chlB) Chlorophyll a/b ratio (chla.b ratio), total chlorophyll, bushiness and root dry weight in response to nitrogen supply.

Genotype	Relative chlA nmol/mg FW		Relative chlB nmol/mg FW		chl a.b ratio		Total chl nmol/mg FW		Bushiness		Root dry weight	
	+N	-N	+N	-N	+N	-N	+N	-N	+N	-N	+N	-N
WT	0.524583	0.315494	0.150361	0.096478	3.51192	3.46078	0.202483	0.130634	3.15758	1.94896	0.593	0.478
SDG33#64B	0.467383	0.28713	0.183488	0.079657	2.693	3.602284	0.195261	0.110036	2.26638	1.83057	0.488	0.455
SDG33#64S	0.472313	0.336573	0.169068	0.094192	2.94758	3.581213	0.192414	0.12923	2.66281	1.76604	0.52	0.469
SDG34#27	0.503898	0.311653	0.219296	0.093161	2.67304	3.342806	0.216958	0.121864	1.6733	1.96404	0.433	0.431667
SDG34#76	0.499723	0.305358	0.181733	0.088114	2.82691	3.465899	0.204437	0.121444	2.01509	1.82318	0.478	0.45
Significance level												
Genotype	0.0831 ^{ns}		0.1838 ^{ns}		0.0222*		0.2274^{ns}		0.02114 *		0.0417 *	
Nitrogen treatment	<2e-16***		<2e-16***		6.29e-09***		<2e-16 ***		0.00168 **		0.0503 .	
Genotype x Nitrogen Treatment	0.2286^{ns}		0.0171*		0.00374**		0.0895 .		0.01434 *		0.5005 ^{ns}	

Therefore, our data suggest that nitrogen stimulates lateral root growth in the WT but not in the mutant. This is further confirmed by the measurement of root dry biomass at the end of the experiment. Root biomass responded similarly to network bushiness, significantly affected by genotype ($P \leq 0.05$) and genotype by nitrogen treatment interaction ($P > 0.05$) (Table 3.4, Figure 3.8B). For nitrogen response, the wild type had a significant change in root biomass between the +N and -N treatments. By contrast *sdg33* and *sdg34* mutants were compromised in nitrogen response, showing no significant differences in root biomass between the +N and -N conditions (Figure 3.8C). Taken together this data shows that *sdg33* and *sdg34* mutants have a compromised root growth response to the availability of nitrogen.

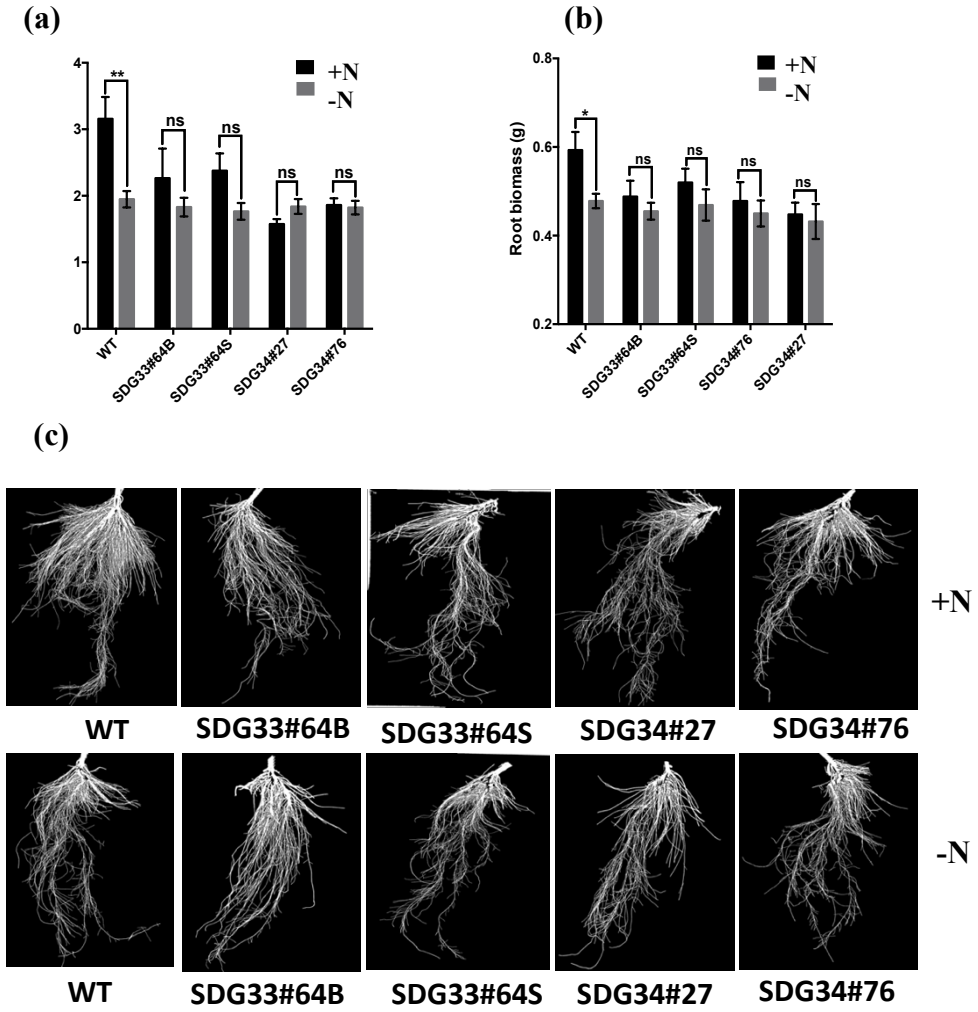

Figure 3.8. SDG33 and SDG34 mediates nitrogen response in tomato roots. Root phenotypic traits of *sdg33* and *sdg34* mutants and the wild type; A) Bushiness, B) Root biomass. C) Pictures of root phenotypes of the data presented in a. Data represent means ± SE (n = 10). Error bars indicate standard error (SE). Asterisk represent level of statistical significance based on student t test; * $P \leq 0.05$, ** $P \leq 0.01$, and *** $P \leq 0.001$. The experiment was repeated two times with similar results and representative data from one of the experiments is shown.

3.4.6 Chlorophyll a/b ratio is altered in *sdg33* and *sdg34 in* response to nitrogen

70% of nitrogen in leaves is contained in chlorophyll molecules (225) hence chlorophyll content reflects the nitrogen status of the plant. We measured extracted chlorophyll using methanol, the measured absorbance was used to calculate the different chlorophyll components at the end of nitrogen and KCl treatments. Total chlorophyll, chlorophyll a and chlorophyll b were significantly affected by nitrogen treatment but not by genotype ($P \geq 0.05$, table 3.4). *sdg33* and *sdg34* mutants had slightly less chlorophyll a and slightly more chlorophyll b than the wild type, but the differences were not statistically different (Figure 3.9A and B). In -N treatment, total chlorophyll, chlorophyll a and chlorophyll b were not different between the mutants and the wild type (Figure 3.9A-C).

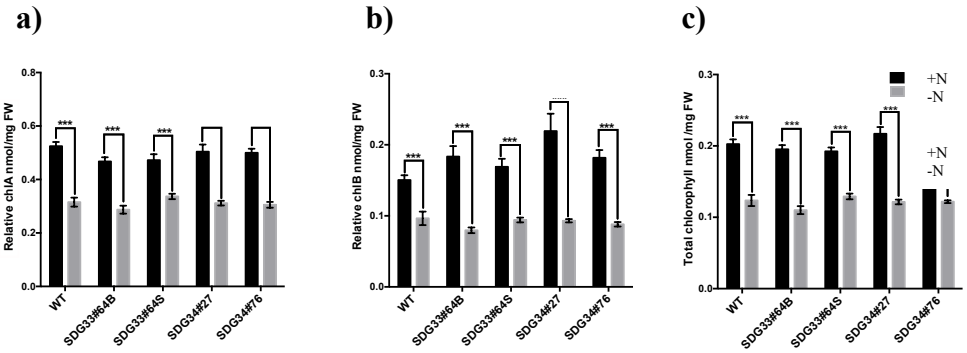

Figure 3.9. SDG33 and SDG34 mutation does not alters chlorophyll content in response to nitrogen. a) Chlorophyll a, b) chlorophyll b and c) total chlorophyll content of sdg*33* and *sdg34* mutants and the wild type in response to nitrogen. Data represent means ± SE (n = 10). Bars labelled with different letters indicate significant difference between the treatments. Asterisk represent level of statistical significance based on student t test; * $P \leq 0.05$, ** $P \leq 0.01$, and *** $P \leq 0.001$. The experiment was repeated two times with similar results and representative data from one of the experiments is shown.

The ratio of chlorophyll a/b was however significantly affected by genotype, nitrogen treatment, and the interaction between nitrogen treatment and genotype ($P \leq 0.05$, table 3.4). Chlorophyll a/b ratio in the wild type is not affected by nitrogen treatment and is high in both in nitrogen and KCl treatment ($P \geq 0.05$, Figure. 3.10). By contrast, in the mutants, chlorophyll a/b is greatly influenced by the nitrogen treatment ($P \leq 0.05$, Figure. 3.10). In the mutants, the ratio of Chl a and b is significantly lower in nitrogen compared to KCl treatments (Figure. 12). This data implies that SDG33 and SDG34 play a role in maintaining the chlorophyll a/b ratio in changing nitrogen conditions.

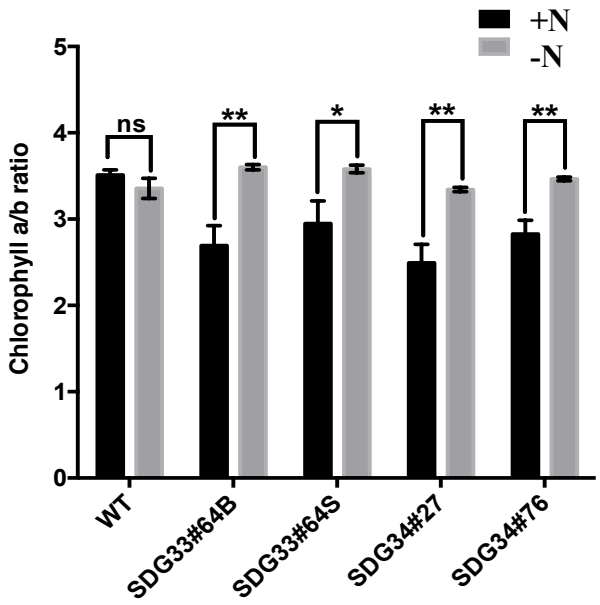

Figure 3.10. Chlorophyll a/b ratio is altered in *sdg33* and *sdg34 in* response to nitrogen. a) Chlorophyll a/b) ratio of sdg*33* and *sdg34* mutants and the wild type in response to nitrogen. Data represent means ± SE (n = 10). Bars labelled with different letters indicate significant difference between the treatments. Asterisk represent level of statistical significance based on student t test; * $P \leq 0.05$, ** $P \leq 0.01$, and *** $P \leq 0.001$. The experiment was repeated two times with similar results and representative data from one of the experiments is shown.

3.5 Discussion

Post translational histone modifications such as histone lysine methylation alter chromatin structure thereby influencing transcription and other DNA dependent processes. In recent years histone lysine methylation through transcriptional regulation of key genes has been shown to mediate plant response to environmental stress. In this study we show that SDG33 and SDG34 associated with H3K4 and H3K36 methylation (ref) are important epigenetic regulators of nitrogen responsive genes in tomato. Mutation in SDG33 and SDG34 results in misregulation of nitrogen responsive genes. This results in altered physiological nitrogen response in tomato roots and shoot. We further show that SDG33 and SDG34 have overlapping and distinct functions in tomato.

The function of tomato putative histone methyltransferases has not been determined and a few histone methyltransferases have been characterised in *Arabidopsis*. SDG33 and SDG34 are tomato homologues of *Arabidopsis* SDG8, sharing 100% similarity in the SET domain responsible for the catalytic activity indicating conserved function (169). In Arabidopsis, the target of SDG8 are commonly down regulated in the *sdg8* mutant, indicating the role of SDG8 as an activator (Li et al., 2015). Interestingly, in our data, not only the down-regulated but also the up-regulated genes

in *slsdg33* and *slsdg34* mutants have significant overlap with the *bona fide* AtSDG8 targets ($p<0.001$; Table 3), supporting that a certain level of conservation of targets and thus function between AtSDG8 and the tomato homologs SDG33 and SDG34. Functional divergence, however, cannot be ruled out as some of the gene activated by AtSDG8 were repressed by the tomato homolog. The basal and induced expression and repression of many genes has been shown to depend on *At*SDG8 (148, 192). Consistently, genome-wide transcriptome analysis revealed that both SDG33 and SDG34 are required for the expression and repression of a significant number of genes in the shoot and roots of tomato. It is interesting to note that although SDG33 and SDG34 are associated with methylation marks associated with gene activation, several genes are upregulated in the mutants. It is plausible that loss of SDG33 and SDG34 leads to other modifications that results in upregulation of downstream genes. Indeed, H3K36me3 show negative crosstalk with H3K36ac mediated by SDG8 and GNC5 in Arabidopsis and both H3K36me3 and H3K36ac histone modification are associated with gene expression (226). Consistent with similarity in protein architecture (169), SDG33 and SDG34 have overlapping functions. Several genes were differentially expressed in *sdg33* and *sdg34* and a significant portion is common between *sdg33* and *sdg34*. However, there remain a portion of genes that are uniquely regulated by SDG33 or SDG34. Furthermore, the GO terms for the unique genes to SDG33 or SDG34 is different, for example in the shoot SDG33 uniquely activate genes involved in DNA binding while the genes activated by SDG34 had no significant GO term in the same tissue. The differential regulation by SDG33 and SDG34 are further supported by the occurrence of different regulatory motifs in the promoters of genes regulated by SDG33 and that of SDG34.

Our genome-wide analysis of nitrate regulated gene expression in *sdg33* and *sdg34* identifies multiple nitrogen responsive genes misregulated in the roots and shoots (Table 3). Loss of SDG33 and SDG34 caused reprogramming of genome wide transcriptional response to nitrate affecting the expression of genes enriched with GO terms such as regulation of gene expression, regulation of nitrogen metabolism and regulation of hormone stimuli in the roots (Figure 3.4). The altered transcriptional response is associated with altered root growth in response to nitrogen. The WT roots increase in bushiness and root biomass in nitrogen treatment relative -N treatment while the mutants are insensitive to this morphological response (Figure 3.8). The adaptive root response to nitrate (NO_3-) depends on the Nitrate transporter 1.1 (NRT1.1). At low NO_3- concentration, NRT1.1 which is also an auxin transporter facilitates basipetal auxin transport of auxin, lowering

auxin accumulation in the lateral root tips. This inhibits lateral root growth and elongation. However, in high (NO_3-) the auxin transport facilitation by NRT1.1 is inhibited, allowing auxin to accumulate in lateral root tips which results in lateral root growth (227, 228). Therefore, NRT1.1 is essential for plants to sense the availability of nitrate and to stimulate lateral root growth to colonize the nitrogen rich soil patch (Remans 2016), In agreement with this notion, our data shows that in WT, the *NRT1.1* transcript level in the presence of NO_3- is high, associated with increased lateral roots while under N-deprived condition, the level of *NRT1.1* transcripts is lower and is associated with less lateral root growth. This regulation of *NRT1.1* is however abrogated in the mutants; In the mutant, the *NRT1.1* transcript level is repressed by high (NO_3-) and is associated with a loss of the growth response of lateral roots. This shows that the regulation of *NRT1.1* by nitrogen requires functional SDG33 and SDG34. Moreover, NRT1.1 mediated regulation of lateral roots involves an interplay of auxin accumulation. Our genome-wide analysis has also identified "response to auxin" as a significant GO term enriched among the genes regulated by SDG33 and SDG34. Indeed, auxin plays a vital role in controlling plant growth and development via the control of cell division, growth (expansion and elongation) and differentiation (229). Recently, Small Auxin-Upregulated RNA (SAUR) genes have been shown to regulate cell expansion. Auxin induces the expression of SAUR which inhibit PP2C.D phosphatase mediated dephosphorylation of plasma membrane H^+-ATPase Thr^{947} resulting in equilibrium shift in the plasma membrane H^+-ATPase towards the phosphorylated active state. This in turn results in increased apoplastic acidification and cell expansion (230). In this work, SAUR genes (Solyco01g091030.3, Solyco01g096340.3, Solyco05g056640.2) (Figure 3.5C) are induced in response to (NO_3-) in the WT but not in the mutants suggesting that the expression of these SAUR genes requires SDG33 and SDG34. Altogether, our data provides evidence for another level of regulation of nitrate induced lateral root growth. From this study it is plausible to hypothesize that high nitrogen inhibits auxin transport by NRT1.1 resulting in auxin accumulation in the lateral root tips. The auxin induced growth of lateral roots, however, requires SAUR expression which is regulated by SDG33 and SDG34. Thus, without SDG33 and SDG34 in the mutants the low expression of SAUR inhibits nitrate dependent, auxin induced lateral root growth. It will be however interesting to study the methylation pattern on SAUR genes in response to nitrate to understand how SDG33 and SDG34 regulate their expression.

In the shoots, the altered transcriptional response highlighted genes related to photosynthesis, nitrogen assimilation and response to stimulus pathways (Figure 3.7). Indeed, chlorophyll a-b binding protein and photosystem reaction centre proteins are misregulated in the mutants in response to nitrate. Photosystem (PS I)1 contains largely chlorophyll a molecule with little or no chlorophyll b molecule. On the other hand, photosystem II (PS II) contain chlorophyll a and well as up to 50% chlorophyll b (231). Hence chlorophyll a/b ratio could reflect the ratio of photosystem I to photosystem II. The WT chlorophyll a/b ratio in (+N) is not responsive to changes in nitrogen while in the mutants it tends to decrease in (+N) condition. In the mutants, lower chlorophyll a/b in response to a supply of nitrogen is associated with lower chlorophyll a and higher amount of chlorophyll b (Figure 3.9A and B) and hence an increase in ratio of PS II to PS1. From the transcriptome data, we observed that the PSI subunit transcripts are lower in (+N) condition in mutants than the WT, while the PSII subunit transcripts are higher in the mutants than the WT, which is in agreement with the low chlorophyll a and high chlorophyll b and hence low chlorophyll a/b ratio in (+N) The physiological consequence of the shift of chlorophyll a/b ratio in the mutants require further investigation. It is possibly an adaptive mechanism, as increasing chlorophyll b increases the range of wavelength to capture light and optimise photosynthesis (232). Indeed, we also observed that the Nitrate transporter 1.5 (NRT1.5) transcripts are low in (+N) treatments in the mutants compared to the WT, (Figure 3.5A) thus the root to shoot transport of nitrate (233) is affected in the mutants in (+N) condition. Hence the shoots of mutants will reflect a low chlorophyll a as a direct correlation of the low nitrate (232) caused by the defective long-distance transport of nitrate and high chlorophyll b as an adaptation to maximise photosynthetic capacity. Overall, SDG33 and SDG34 are required for the expression of (*NRT1.5*) in (+N) conditions to mediate root to shoot transport of nitrate and thus normal chlorophyll a/b ratios.

In conclusion, our study demonstrated that histone methyltransferases SDG33 and SDG34 play overlapping and distinct roles in regulating gene expression in tomato. We show that some of these roles are conserved with the Arabidopsis homologue SDG8 and that SDG33 and SDG34 have evolved other function specific to tomato. Additionally, SDG33 and SDG34 are required for nitrogen response in the roots and shoots of tomato. We posit new insights of regulation in nitrate dependent NRT1.1 induced lateral root growth that requires SAUR gene expression that dependent on SDG33 and SDG34 in the roots. We also show that SDG33 and SDG34 regulate expression of many genes in a nitrogen dependent manner either directly or indirectly. SDG33 and SDG34 are

histone methyltransferase associated with H3K4 and H3K36 methylation, it will be however interesting to analyse what methylation marks are present on SDG33 and SDG34 nitrogen-related targets, and how these mediate nitrogen responses.

CHAPTER 4. TOMATO HISTONE LYSINE METHYL TRANSFERASE SDG20 REGULATES PLANT IMMUNITY AND IS REQUIRED FOR PLANT VIABILITY

4.1 Abstract

Plant defense to pathogens is complex and involve sophisticated recognition and signalling networks leading to resistance to infection. Recently, histone lysine methylation has emerged as one of the mechanisms that modulate plant immunity to pathogens. We have identified Set Domain Group 20 (*Sl*SDG20) an orthologue of Arabidopsis SDG25 in tomato. *SlSDG20* protein is a member of the class III of SDG proteins, contains the SET, Post-SET domain and GYF domain important for proline-rich sequence recognition. *SlSDG20* is highly induced by *B. Cinerea*, Methyl Jasmonate and Ethylene. To further understand the functions of SlSDG20 in tomato development and plant immunity we produced *slsdg20* knockout mutants through CRSIPR/Cas9. We identified one homozygous *slsdg20* mutant with 151bp deletion in an exon immediately before the SET domain. Global methylation assay on the *slsdg20* mutant confirmed that *SlSDG20* is an H3K4 methyltransferase. The *slsdg20* mutant displays shorter plant stature than the wild type, produced more adventitious shoots causing prolific branching, and narrow leaves. Further, the mutant plants produce abnormal fruit and fewer seeds that hardly germinate. We characterised the *slsdg20* mutants' response to the necrotrophic pathogen *B. cinerea* and the bacterial pathogen *Pst* DC3000. *slsdg20* mutant is highly susceptible to *B. cinerea* compared to the wild type indicating that *SlSDG20* may mediate tomato response to *B. cinerea*. By contrast, the in response to *Pst* DC3000 inoculation, *slsdg20* mutants were comparable to the wild type. Interestingly, *slsdg20* response to the non-pathogenic *hrcC* strain of *Pst* DC3000, was severely impaired in the *slsdg20* mutant, suggesting a possible role of *SlSDG20* in PAMP Triggered Immunity. Our data genetic data implicates tomato SDG20 in plant immunity and growth functions.

4.2 Introduction

Plant defence against pathogens involve sophisticated microbial sensing and signalling mechanisms which result in activation of plant immune responses (132-136). Plants respond to pathogens by distinct yet overlapping mechanisms that impede the growth and establishment of

the pathogen. Generally, Plants recognise conserved pathogen molecular structures called pathogen associated molecular patterns (PAMPs) and plant generated molecules that signal damage called damage associated molecular patterns (DAMPs) to induce defense responses called pattern triggered immunity (PTI). PTI is a basal form of defense response and is effective against diverse pathogens independent of the lifestyle of the pathogen. On the other hand, pathogens can deploy a plethora of effectors, breaching the first line of defense. Each effector is specifically recognised by plant resistance proteins resulting in effector triggered immunity (ETI). ETI results in hypersensitive response at the infection site, and usually disease resistance (234). Downstream of ETI and PTI are plant hormones that modulate plant immunity signalling network regulating the expression of well characterised defense genes (235, 236). The hormone salicylic acid (SA), mediates resistance to biotrophic pathogens, while resistance to necrotrophic pathogens is mediated by ethylene (ET) and Jasmonic acid (JA) (132-136). In addition, regardless of the pathway, plant immune pathways merge into common immune responses. Accumulation of ROS, biosynthesis of hormones, MAPK activation widely occur regardless of the pathway. The distinction between ETI and PTI also gets blurred at the early stages at the effector and receptor levels (237). Although great strides have been made in understanding plant defense response, it has become clear in the last decade that it is more complex than the accepted models. There are still knowledge gaps in understanding plant immunity signalling pathways and how they are associated with transcriptional reprogramming in the nucleus.

In the nucleus, genomic DNA in eukaryotes does not appear as a free linear strand but is condensed into nucleoprotein complex called chromatin. The basic structural unit of chromatin is the nucleosome which is made up of approximately 147 base pairs of DNA wound around a histone octameric core with two cores of each histone proteins H2A, H2B, H3, and H4. The histone linker protein H1 locks DNA into place by binding at the entry and exit sites of DNA thus creating a compact hierarchical architecture (238, 239). Condensed chromatin state poses a barrier to all DNA templated processes such as transcription and DNA repair. Histones have N-terminal tails rich in basic amino acids which protrude from the nucleosomes, and these can be modified post translationally by acetylation, methylation, ubiquitylation, sumoylation, ADP-ribosylation, deamination, Proline isomeration, and phosphorylation (6, 10). These modifications influence chromatin structure, affecting accessibility of the transcriptional machinery to the corresponding DNA thus modulating gene expression and/or repression (6).

Several studies have shown that post-translational modification of histones, together with corresponding histone modifiers plays an important role in expression of defense genes (240). Histone lysine methylation (HLM) has emerged as one of the mechanisms that modulate plant immunity to biotrophic and necrotrophic pathogens (137). HLM is the transfer of methyl groups from the cofactor S-adenosylmethionine to the ε-nitrogen of specific lysine residues to the N-terminal tails of H3 and H4 and is catalysed by histone lysine methyltransferases (HKMTs). Reversible HLM alters chromatin, influencing the accessibility of the transcriptional machinery to the corresponding DNA thus modulating transcription, establishing permissive or repressive states of targeted genes. Histone lysine residues can be mono, di or tri-methylated resulting in different regulatory impacts. Plant HKMTs have a conserved SU- (VAR) 3-9, Enhance of zeste E (Z) and Trithorax (TRX) (SET) domain responsible for their enzymatic activity. Many SET Domain Group (SDG) proteins have been identified in plants (6, 10).

In *Arabidopsis thaliana* Set Domain Group 8 (SDG8) is an H3K36 and/ or H3K4 methyl transferase required for H3K36me3 at the chromatin of *LAZARUS 5 (LAZ5),* a TIR-class NB-LRR R-protein, regulating its transcription and to maintain its transcriptionally active state. In the same study, *SDG8* mutation resulted in low H3K36me3 on chromatin of *RPM1* and *RPS5* regulatory regions and thus their low transcripts which correlated with the susceptibility to the bacterial pathogen *Pseudomonas syringae* DC3000 (PstDC3000) expressing *AvrRpm1* and *AvrPphB,* respectively (140). *SDG8* is also required for the expression of *PLANT DEFENSIN1.2 (PDF1.2), VEGETATIVE STORAGE PROTEIN2 (VSP2)* and *Mitogen-Activated Protein Kinase (MAPK) Kinase 5 (MKK5)* genes involved in the JA/ET mediated defense pathway in response to *B. cinerea* and *Alternaria brassicicola* thus playing an important role in plant immunity to necrotrophic pathogens.

SDG25/ATRX7 a H3K4 methyltransferase, was shown to interact *with MODIFIER OF SNC1 9 (MOS9)* and this interaction is required for the full expression of *SUPPRESSOR OF NPR1-1, CONSTITUTIVE 1* (*SNC1*) and *RECOGNITION OF PERONOSPORA PASITICA 4 (RPP4*) which are Toll Interleukin1 Receptor (TIR) like Nucleotide Binding Leucine Rich Repeat (NB-LRR) containing R-proteins (TIR-NLR) involved in plant immunity. Furthermore, loss of *SDG25* results in reduced H3K4me3 marks on the promoter region of *RPP4* and *SNC1* which correlates to their reduced expression and thus increased susceptibility to *Hyaloperenospora arabidopsidis* (141).

Recently, SDG8 and SDG25 were further characterised in detail for their role in plant immune pathways(148). The *sdg8* and *sdg25* mutants are impaired in flagellin22, pep1, effector triggered immunity, systemic acquired resistance to *Pst* DC3000, *B. cinerea* and *A. brassicicola.* The loss of resistance in the mutants is attributed to altered global and CAROTENOID ISOMERASE2 *(*CCR2*)* and ECERIFERUM3 *(*CER3) specific histone lysine methylation (148). CCR2 is involved in carotenoid biosynthesis and CER3 in cuticle biosynthesis. Mutants in *CCR2* and *CER* genes and the *sdg8, sdg25* and double mutants resulted in lower levels of lipids, cuticular wax and increased cuticle permeability. Moreover, *ccr2* and *cer3* mutants are also susceptible to *B. cinerea and A. brassicicola.* Loss of SDG8 and SDG25 significantly affected CCR2 and CER3 H3K4 and H3K36 methylation patterns. Globally SDG25 affects H3K4me1 methylation while SDG8 affects negatively H3K4me1 and H3K36me1 and positively H3K36me2 and H3K36me3 methylations (148).

We identified the tomato *SDG20*, an orthologue to *Arabidopsis SDG25* based on sequence comparisons and studied its functions in plant immunity. Tomato SDG20 is a SET domain protein suggesting histone lysine methyltransferase activity (169). In addition to the SET and Post-SET domain, *SDG20* has a GYF domain important for proline-rich sequence recognition (169). Tomato *SDG20* is highly induced by the fungal pathogen *Botrytis cinerea*, and the plant hormones jasmonate and ethylene, indicative of its role in plant defence. To determine the functions of SDG20, we generated tomato *sdg20* knockout mutants through CRSIPR/Cas9. The *sdg20* mutant is highly susceptible to the fungal pathogen *B. cinerea* and to the non-pathogenic bacterial strain *Pst* DC3000 *hrcC*$^{-}$, impaired in the type three secretions system, but is competent to induce PAMP triggered immunity. The data suggest that SDG20 is required for PTI to fungal and bacterial pathogens. Global HLM assay in the *sdg20* mutant revealed that *SDG20* is required for H3K4 di- and tri-methylation and all levels of H3K36 methylation. In addition, the loss of fertility and grossly altered leaf shape, plant stature in the *sdg20* mutants suggest that SDG20 is also required for plant growth traits.

4.3 Materials and methods

4.3.1 Plant materials and growth conditions

Tomato (*Solanum lycopersicum)* cultivar Casstlemart11 were grown in plastic pots containing compost soil (Sun Grow Metro mix 510) in a growth chamber under extended 12-hour photoperiod at 24 ^{0}C. Castlemart11 is referred to as the wild throughout this paper and all the mutants were generated in the CastlemartII background. For seedling growth response assays, seeds were surface sterilised with 20% Sodium Hypochlorite, washed several times in distilled water and germinated on full Murashige and Skoog (MS) medium with 2% (w/v), sucrose 0.8% (w/v), 1.5% bacto agar, and supplemented with Gamborg's vitamins under 16 hour light, 8 hour dark at 24 ^{0}C.

4.3.2 Generation of *sdg20* mutants

To generate *sdg20* mutants, two specific guide RNA (gRNA) were designed using the CRISPR Plant gRNA design software https://www.genome.arizona.edu/crispr/CRISPRsearch.html. The two gRNA were cloned into the CRISPR/Cas9 vector pKSE401 according to (165). Tomato cultivar Castlemart II cotyledons explants were suspended in *Agrobacterium* carrying the constructs for 30 minutes and the explants blot dried on sterile blot paper to remove excess *Agrobacterium*. *Agrobacterium* infected explants were co-cultivated on media consisting of strength MS salts and vitamins (241), 0.8% gelrite + acetosyringone + and incubated in the dark at 21 °C 48 hours. The explants were then transferred to regeneration medium (MS salts and vitamins (241), + Zeatin + Cefotaxime 75mgL^{-1} +Ticarcillin + 0.8% gelrite + 75mgL^{-1} Kanamycin, pH. 6.0) to induce callus formation. Green callus was transferred to shoot induction medium (MS salts and vitamins (241), + Zeatin + Cefotaxime 75mgL^{-1} +Ticarcillin + 0.8% gelrite + 75mgL^{-1} Kanamycin)0.8% gelrite pH. 6.0) Regenerated plantlets were transferred to rooting medium (MS + Zeatin + Cefotaxime 75mgL^{-1} +Ticarcillin + 0.8% gelrite + 75mgL^{-1} Kanamycin, pH. 6.0). Fully rooted plants were transferred into the soil and genotyped by PCR with primers covering the expected deletion. The deletions were confirmed by sequencing.

4.3.3 Global methylation assay

Core histone proteins were extracted form 4 weeks old *sdg20* and WT plants as described by (166). Proteins were separated on 15% SDS-PAGE gel and transferred to PVDF membranes. The membranes were immunoblotted with primary antibodies anti-H3K4me1 (07-436; EMD Millipore), anti-H3K4me2 (07-030; EMD Millipore), anti-H3K4me3 (07-473; EMD Millipore), anti-H3K36me1 (ab9048; Abcam), anti-H3K36me2 (07-369-I; EMD Millipore), anti-H3K36me3 (ab9050; Abcam), and anti-H3 (ab1791; Abcam) as a loading control. Anti-rabbit was used as the secondary antibody. Visualisation of the bound primary antibody was done with the enhanced chemiluminescence (Thermo Scientific) detection system according to the manufacturer's protocol.

4.3.4 Fungal culture and disease assays

To start plants for disease assays, *sdg20* and WT seeds were surface sterilised germinated on filter paper. When the radicle emerged, they were transferred to soil. 4-week-old plants were used in all our disease assays. Botrytis strain B05-10 was grown on V8 media and conidia prepared as previously described (242). For gene expression, conidia were sprayed on whole plants and for disease assays detached leaves were drop inoculated with 5µL of spore suspension (2.5 x10^5 spores/mL). Leaves were incubated in high humidity and lesion diameter was measured 3 days after inoculation.

4.3.5 Bacterial disease assays

P. syringae strains were cultured in King's B medium (20 g peptone, 10 g glycerol, 1.5 g K_2HPO_4, and 6 mL of 1 M $MgSO_4$/L, pH 7.2) with appropriate antibiotics on a rotary shaker overnight. The bacteria were then suspended in 10 mM $MgCl_2$. Bacterial disease assay were done as previously described (243). Briefly, leaves of 4-week-old tomato plants were syringe infiltrated with bacterial suspension of (OD_{600} = 0.001 in 10 mM $MgCl_2$). Bacterial growth was determined by collecting leaf discs of infected plants at 0 and 3 days after inoculation. The leaf discs were ground in 10 mM $MgCl_2$ and bacterial titre per leaf area was determined.

4.3.6 RNA extraction

Total RNA was extracted from the shoot and root using the Trizol (Invitrogen) according to the manufacturer's instructions. After extraction, RNA was treated with DNASE (New England Biolabs) according to the manufacturer's instruction. RNA was precipitated with 3M Sodium acetate and three-times with 100% ethanol. Integrity of RNA was assessed by the Agilent Bioanalyzer (Agilent technologies).

4.4 Results

4.4.1 Characterization of tomato SDG20, a putative histone methyltransferase.

Tomato SDG20 was previously identified from a genome wide sequence analysis (169) that identify and describe 52 putative histone methyltransferases in tomato. SDG20 has 19 exons which encodes a 1597 amino acid protein with an estimated molecular weight of 174.813kD (Figure 4.1A). SDG20 belongs to class III family of SDGs according to classification by Springer and colleagues (244), annotated as homologous to THITORAX (TRX) originally identified in *Drosophilla melongaster*. SDG20 like any other class III protein, contains SET (PF00856) domain responsible for the catalytic activity and post-SET (SM00508) domain with no known functions. Unlike its Arabidopsis orthologue SDG25, tomato SDG20 (*Sl*SDG20) has an additional GYF domain (SM00444) that is important for proline-rich sequence recognition. Domain architecture and sequence comparisons suggest that SDG20 is a putative histone methyl transferase.

Sequence and phylogenetic analysis were performed to decipher the relationship between SDG20 and other class III histone methyltransferases. SDG20 shares 36-76% amino acid sequence similarity with other class IIII histone methyltransferase form other plant species. SDG20 is similar to Arabidopsis SDG25 showing the highest amino acid sequence identity of 76%. Also, the rice putative histone methyltransferase *Os*SDG717 is very similar to SDG20 sharing 73% amino acid sequence. Furthermore, the phylogenetic analysis clusters tomato SDG20, Arabidopsis SDG25 and rice SDG717 into the same clade (Figure 4.1B) consistent with the amino acid sequence analysis.

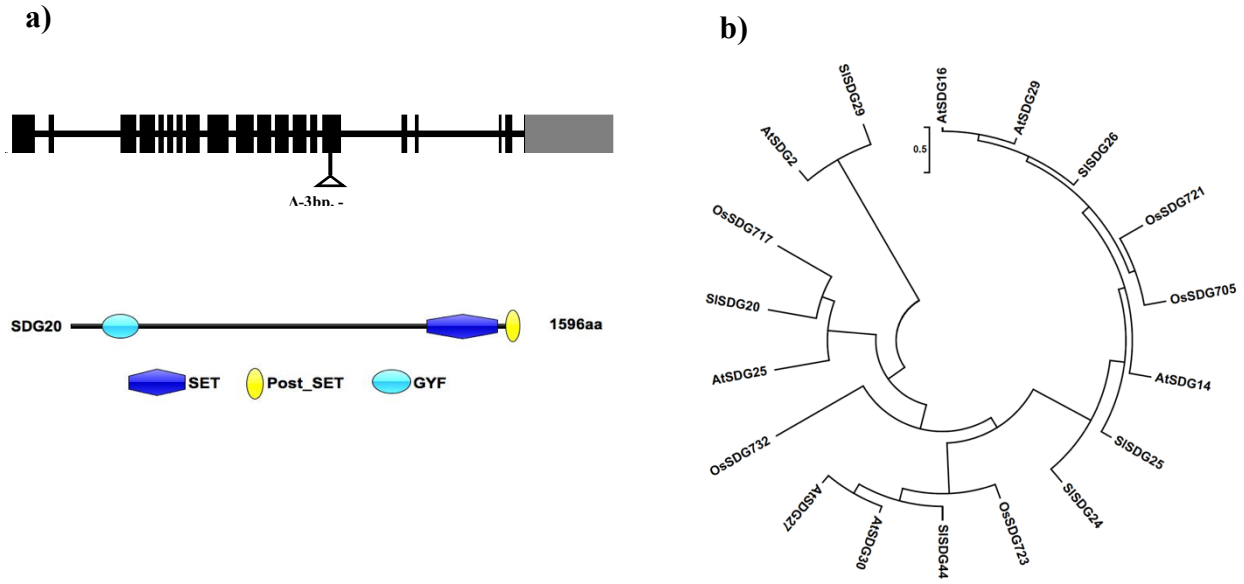

Figure 4.1. Genomic structure and proteins domain in tomato SDG20. A) SDG20 genomic organization, protein structure and domain architecture of SDG20 showing the exons and intron. Exons- dark shaded bars and introns- horizontal lines between the exons. B) Maximum Likelihood phylogenetic analysis of class III SDG proteins from *Arabidopsis thaliana (*At*)*, *Solanum lycopersicum* (Sl), and *Oryza sativa* (Os). Phylogenetic analysis was performed using Mega7 package. The tree is drawn to scale with branch length measured in the number of substitutions per site. Bootstrap values higher than 50% are shown.

To gain insight into the biological functions of SDG20, we examined its expression patterns in leaves, roots, flower structures, green fruits, and red fruits using RT-qPCR (Figure 4.2A). SDG20 transcripts are expressed in all tissues with the highest expression in the stigma, followed by the sepals. Leaves have higher SDG20 transcripts compared to the roots, petals, stamens, green and red fruits whose SDG20 expression in these tissues is not statistically significant from each other. To determine the functions of SDG20, we looked at the expression profile after pathogen infection and treatments with plant hormones. SDG20 is highly induced by *B. cinerea* as early as 24 hours after inoculation and this increases further at 48 hours after inoculation to at least 3 folds difference compared to mock inoculated plants (Figure 4.2B). Methyl jasmonate (MeJA) induced the SDG20 transcripts. Further, SDG20 transcripts are higher than in the mock treated samples at 24 hours after 1-Aminocyclopropane-1-carboxylic acid (ACC) treatment, but lower than the mock at 12 and 36 hours after treatment. In response to *Pst DC 3000*, SDG20 transcripts are lower than mock treatment at 24 and 48 hours after treatment. SDG20 is

transcriptionally regulated by biotic stress, and hormones suggesting the role of SDG20 in plant defense to disease.

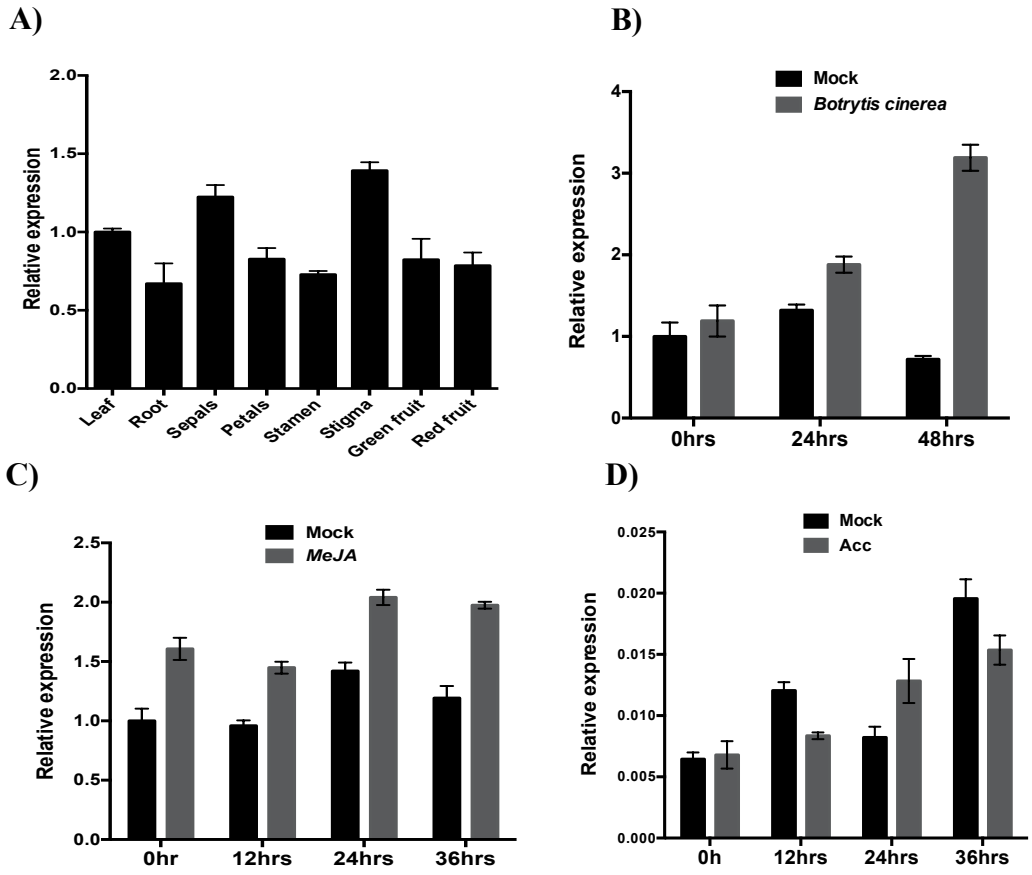

Figure 4.2. The expression profiles of SDG20 in WT and under different elicitors. A) Tissue specific expression of SDG20 in WT tomato plants. B) *B.cinerea* induced expression of SDG20 in 4 weeks old WT plants treated with 2.5 x10^5 spore/mL *B. cinerea* spore. C) Expression of SDG20 in the mock treated and MeJA and D) Expression of SDG20 in the mock treated and Acc treated WT plants. Bars represent the means; the error bars represent the standard deviations of three technical replicates of each treatment. The β-actin gene was used as an internal control in the qRT-PCR. The experiment was repeated at least 2 times with similar results.

4.4.2 Characterization of *sdg20* loss of function mutants.

To study the function of SDG20, we generated gene edited lines through CRISPR/Cas9-induced sgRNAs were specific and to avoid off target mutagenesis we used the gRNA design software www.genome.arizona.edu/crispr. The gRNAs were expressed under the control of Arabidopsis U6 promoter. One homozygous and other heterozygous and chimeric mutations for SDG20 were generated in T0 generation. The *sdg20.1* mutant allele carried a deletion of 3bp in the first target and a148bp deletion in the second target (Figure 4.3A-B). Further analysis indicated

that the that the deletions in *sdg20.1* introduced premature stop codons which suggest that a truncated protein is produced. Furthermore, quantitative Reverse Transcription Polymerase Chain Reaction qRT-PCR showed that SDG20 transcripts were severely reduced in the *sdg20.1* mutant compared to the WT (Figure 4.3E-F).

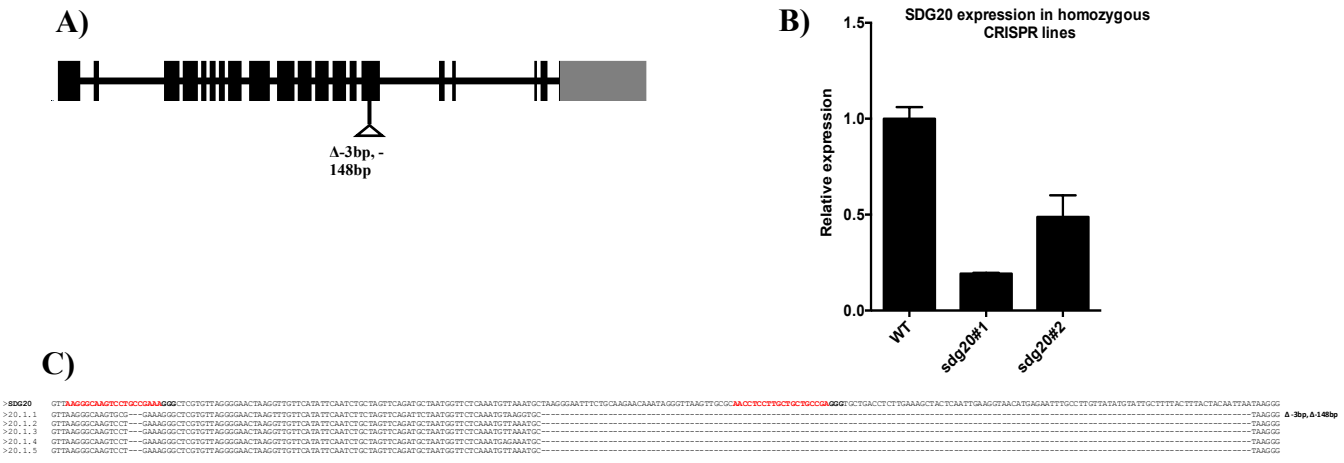

Figure 4.3. Molecular characterisation of *sdg20* loss of function mutants. A) Schematic diagrams showing the position of the deletions in *sdg20* mutant. Black shaded boxes represent exons, the grey shaded boxes represent the UTRs boxes represent exon, and introns are shown as horizontal lines. B). SDG20 expression in the mutants. C) Alignment of mutated alleles sequences identified from cloned PCR genotyping fragments and the WT sequences. The mutated alleles include deletions (shown by dashed lines) and insertions (shown by blue letters). Only aligned sequences and the mutations are shown. The targets are shown by letters in red and the protospacer adjacent motif (PAM) is shown by the bold-faced letters after the targets.

The homozygous line did not produce viable seeds. The fruits produced were small had an average of less than five seeds which did not germinate. We crossed the homozygous line to the WT and this mutation was maintained as a heterozygote which was fertile and produced seeds. To study the effects of the mutations on SDG20, the heterozygous and chimeric seeds were selfed and plants carrying the homozygous mutations were identified by PCR and used in all experiments described here. The data suggest that *sdg20.1* mutant is a loss of function mutation in the SDG20 gene, and only the homozygous plants showed the altered growth phenotypes suggesting that this is a recessive mutation.

4.4.3 Global histone lysine methylation is mediated by SDG20.

The protein domain structure and phylogenetic relationships suggest that SDG20 is a putative histone methyltransferase. We determined whether loss of SDG20 affect any histone methylations globally. Using western blot and antibodies specific to the different histone lysine modifications, we analysed global histone methylation patterns in *sdg20* mutant plants (Figure 4). Loss of tomato SDG20 decreased the accumulation of H3K4me1 and H3K4me2 globally compared to the WT but levels of H3K4me3 were not affected (Figure 4.4A). All modifications mono-, di- and tri-H3K36 methylations were lower in *sdg20* mutant compared to the WT (Figure4B). Taken together, this data indicate SDG20 plays a major role in global H3K36 di- and tri-H3K4 methylation in tomato.

4.4.4 SDG20 is required for vegetative growth and proper leaf development.

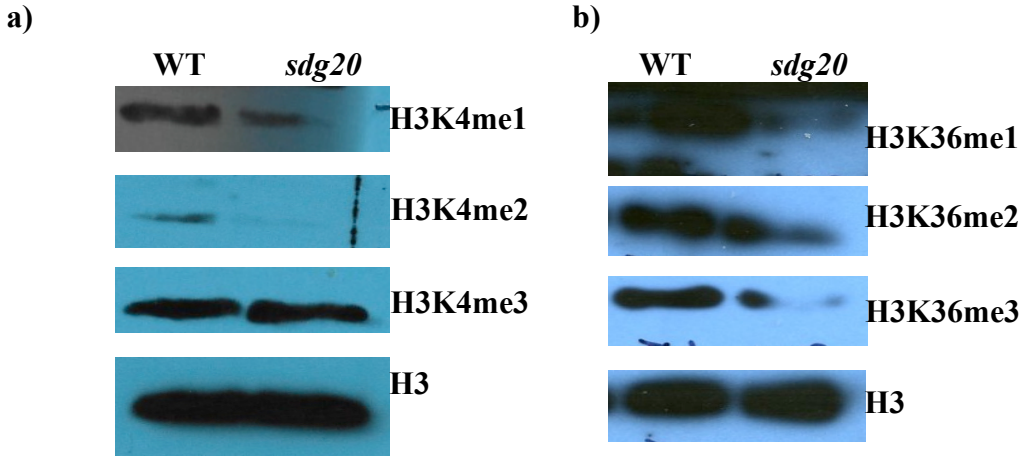

Figure 4.4. Global histone lysine methylation levels in *sdg20*. Western blot analysis of A) H3K4 B) H3K36 in Wt and, *sdg20* mutants. Core histones were extracted from 4-week old plants and the blot probed with specific H3K4 and H3K36 antibodies.

sdg20 mutant plants display a shorter than the WT plants (Figure 4.5A). Reduced plant height can be attributed to fewer internodes and or shorter internode length. We examined internode number and length in *sdg20* and WT. SDG20 mutation results in fewer internode number compared to the WT (Figure 4.5B). However, Internode length is the same between the *sdg20* mutant and the WT (Data not shown). Leaves of *sdg20* are thinner with more serrations at the leaf edge than the WT. Furthermore, the *sdg20* leaves have light green blotches over the normal dark green colour (Figure 4.5C). We also observed that flowers are smaller on the *sdg20*

mutant plants and only a few of the flowers set fruit compared to the WT. Fruits of *sdg20* plants were sometimes parthenocarpic, contain only jelly and flesh and some had less than five seeds. Thus, SDG20 is required for vegetative growth, leaf development, fruit and seed set.

4.4.5 SDG20 is required for disease resistance in tomato.

SDG20 is highly induced by *B. cinerea* and MeJA suggesting an important role of SDG20 in resistance to *B. cinerea.* To investigate the possible the role of SDG20 in defense against *B. cinerea*, we tested the *sdg20* plants for resistance to *B. cinerea.* We used detached leaf assays to compare disease phenotypes between *sdg20* and WT plants. *sdg20* plants showed increased susceptibility to *B. cinerea,* with larger disease lesions and tissue maceration than the WT (Figure 4.6A-B). This data shows that plants carrying loss of function alleles of SDG20 were susceptible to *B. cinerea* and thus SDG20 is required for resistance to *B. cinerea* in tomato. To determine specificity of SDG20 in plant immunity to distinct pathogen groups, we examined the role of SDG20 in defense to bacterial pathogens. We analysed disease resistance phenotypes of *sdg20* to two *Pst* DC3000 strains; non-pathogenic *Pst* DC3000 *hrcC*$^{-}$ which is non-pathogenic, it lacks the type III secretion system but retains all the PAMPs that trigger plant immune response. We infiltrated leaves on whole plants with the bacteria and disease severity was measured by quantification of bacterial growth as the number of colony-forming units after three days of incubation. *sdg20* plants were highly susceptible to the non-pathogenic *Pst* DC3000 *hrcC*$^{-}$ supporting more bacterial growth than the WT plants indicating impaired PTI in *sdg20* plants (Figure 4.6C).

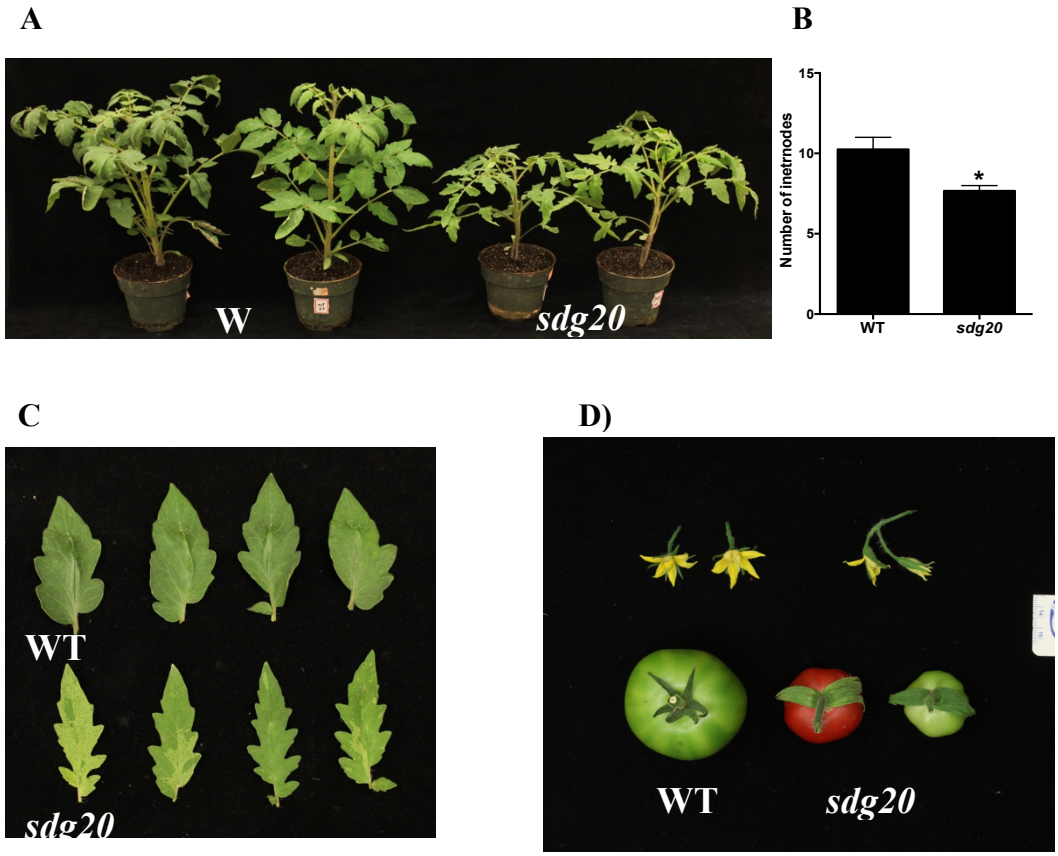

Figure 4.5. Phenotypic Characterisation of in *sdg20* mutant. A) *sdg20* plants are shorter than the WT plants, B) Internode number in the *sdg20* mutant and WT plants. The data shown are the mean ± SE (n ≥ 10). Asterisks indicate significant differences using Student's t-test (*P < 0.05, **P < 0.01, ***P<0.001). C) Leaf and, D) Flowers and fruits phenotypes of *sdg20* mutant and WT plants, D) Flowers and fruits.

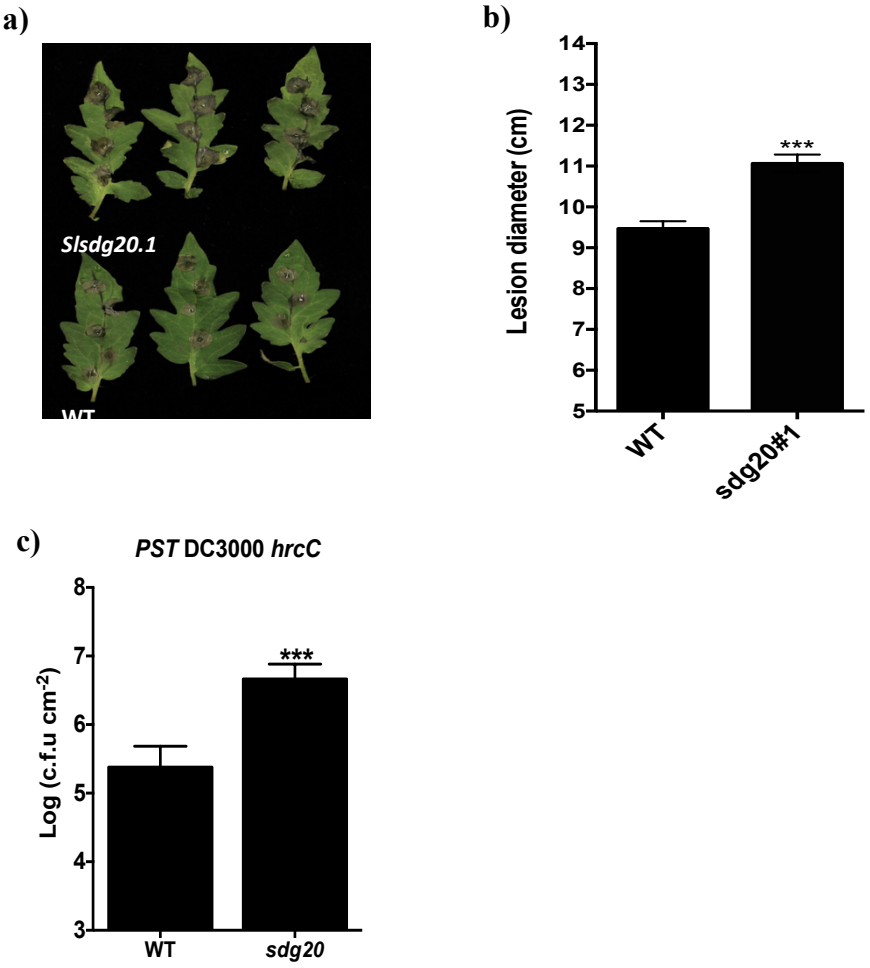

Figure 4.6. SDG20 is required for defense against fungal and bacterial pathogens. A) Disease phenotypes of *sdg20* mutants and WT plants inoculated with *B. cinerea*, B) Lesion diameter of *sdg20* mutants and WT plants inoculated with *B. Cinerea.* Bacterial growth in *sdg20* mutants and WT plants inoculated with C) *Pst* DC3000 *hrcC*$^{-}$. The data shown are the mean ± SE (n ≥ 10) for *B. cinerea*, (n=6) for Pseudomonas assays. Asterisks indicate significant differences using Student's t-test (*P < 0.05, **P < 0.01, ***P<0.001). The experiments were repeated at least 2 times with similar results, representative data is shown.

4.5 Discussion

Histone lysine methylation (HLM) is an epigenetic modification that modulate chromatin state, thereby allowing transcription and other DNA dependent processes. Hence mutations in histone lysine methyltransferases (enzymes that catalyse the HLM process) have a plethora of phenotypes like susceptibility to bacterial and fungal diseases (18, 21, 148), sensitivity to abiotic stress (114), growth pertubations and deviations (19, 182, 183) among others. However, in tomato the functions of histone methyltransferases have not been characterised. In this study we functionally deciphered the role of Set Domain Group 20 (SDG20) a putative histone

methyltransferase (169) in growth, development and tomato immunity to bacterial and fungal pathogens. We show that 1) SDG20 is highly expressed in the stigma, sepal and leaves; 2) SDG20 is induced by *B. cinerea*, and Methyl jasmonate; 3) SDG20 is required for resistance to *B. cinerea* and *Pst* DC3000 *hrcC*$^{-}$, and 4) SDG20 is required for growth, flower and fruit development and seed set.

Arabidopsis SDG25, a homologue of tomato SDG20, has been previously shown to regulate immunity to plant bacterial and fungal pathogens by mediating histone lysine methylation marks at chromatin of defense responsive genes (141, 148). The first line of defence against *B. cinerea* involves barriers provided by the plant cuticle and cell wall (245). Consequently, genes that play a role in the formation and maintenance of these barriers are required for resistance to *B. cinerea.* Reduced expression of CCR2 and CER reduce lipid accumulation and increase permeability of the leaf cell and thus results in susceptibility to *B. cinerea*. Furthermore, the expression of CCR2 and CER requires H3K4me4 and H3K36me3 mediated by Arabidopsis SDG25 and SDG8 (148). Defence against *B. cinerea* is also mediated by the JA/ET pathway. Histone lysine methyltransferase SDG8 has been show to regulates the expression of several genes in this pathway through H3K36 methylations at these genes (18). The *sdg20* mutants is required for H3K4me2 and 3 and H3K36me1, 2 and 3 global methylation (Figure 4.4). and displays susceptibility to the fungal pathogen *B. cinerea* (Figure 4.6A, B) and However, questions on how the reduced methylation patterns in *sdg20* relate to susceptibly to *B. cinerea* remain. Genome wide transcriptome profiling of *sdg20* in response to *B. cinerea* will provide insights to the genes and pathways regulated by SDG20. Further analysis of these targets in terms of methylation state before and after *B. cinerea* infection in *sdg20* will reveal the mechanism of SDG20 in regulating basal and induced defense responses to *B. cinerea*.

Mutation in SDG20 results in susceptibility to the non-pathogenic *Pst* DC3000 *hrcC*$^{-}$ (Figure 4.6C) and thus we hypothesised that SDG20 is required for PTI responses. *Pst* DC3000 *hrcC*$^{-}$ lacks the Type III secretion system and transcriptional programming by such mutants is usually due to a collective action of multiple PAMPs (246). We ask questions like does SDG20 mediate response to a collective number of PAMPs or is it specific to Flagellin, or chitin or EF-Tu. Thus, the mechanism of how SDG20 mediate PTI needs further studies. We propose studying the disease resistance phenotype of *sdg20* after Flagellin 22 (flg22) or chitin, discovering target

genes who expression in regulated by the PAMP treatment and SDG20, and deciphering the gene specific methylation in response to flg22 or chitin treatments.

We have identified interesting phenotypes suggesting the role of *SlSDG20* tomato growth, development and plant immunity. However, the preliminary studies were done only on one mutant allele of *SlSDG20,* but two independent alleles are required to confirm the phenotypes we observed. Furthermore, the molecular mechanism of function of SlSDG20 in growth, development and tomato immunity is not known. Hence, we propose to identify the second allele of *slsdg20* mutant and decipher the molecular mechanism underlying the function of *SlSDG20* histone methyltransferase in tomato growth, development and immunity to pathogen.

CHAPTER 5. IDENTIFICATION OF TOMATO RECEPTOR LIKE CYTOPLASMIC KINASES REQUIRED FOR RESISTANCE TO FUNGAL PATHOGENS.

5.1 Abstract

Plant Receptor like cytoplasmic kinases (RLCKs) are a subclass of the plant Receptor like kinase (RLKs) superfamily of proteins that function at early stages of immune signalling. Plants perceive the presence of pathogens through Pattern Recognition Receptors (PRR) which are predominantly RLKs, and subsequently recruit RLCKs to signal to downstream regulators of defense responses. The RLKs CERK1, FLS2, are two examples that have been well studied in fungal and bacterial response signaling. Similarly, many RLCKs were characterized from model plants such as Arabidopsis for their role in signalling of responses to bacterial infection. An example of RLCKs is Arabidopsis BIK1 and related proteins which are implicated in signal transmission of pathogen recognition event at the cell surface. The tomato genome encodes 647 RLK/RLCKs comprising about 2% of its predicted genes. The functions of most of these predicted tomato RLCKs and RLKs have not been determined. Previously, our lab characterized the Arabidopsis BIK1, tomato TPK1b RLCKs for fungal resistance. Here, we conducted a reverse genetic screen focused on BIK1 and TPK1b related tomato RLCKs to identify a subset with defense functions. Virus induced gene silencing and pathogen assays conducted on 15 RLCKs identified four RLCK genes with potential role in plant immunity to fungal pathogens. Then, tomato knock out mutants were generated for four RLCK genes through CRISPR/cas9 genome editing to validate the VIGS data. Subsequently, fungal disease response assays on the mutant lines demonstrated that TPK07, TPK09, TPK011 and TRK04 are required for resistance to *B. cinerea*. This is supported by the pathogen induced expression of these genes. Furthermore, *trk04* seedlings are impaired in Jasmonic acid responses. Our study establishes that tomato TPK07, TPK09, TPK011 and TRK04 contribute to defense against *B. cinerea* but their mechanism of function needs to be elucidated in future studies.

5.2 Introduction

Plants are sessile in nature hence they are constantly challenged by diverse pathogens. To defend themselves, they rely on innate immune system where each plant cell initiates and maintains response mechanisms to ward off potential pathogens (247, 248). The first layer plant innate immune system involves recognition of Pathogen Associated Molecular Patterns (PAMPs) or host derived Damage Associated Molecular Patterns (DAMPs) by Pattern Recognition Receptors (PRR) resulting in activation of downstream defense responses that culminate in halting of pathogen proliferation. This immune response is referred to as Pattern Triggered Immunity (PTI), it repels pathogens and contribute to basal level of immunity during infection (249-251). To overcome PTI, pathogens have evolved effector proteins which are secreted directly into host cells to supress host immunity and/or to manipulate host metabolism for virulence. In parallel, plants have evolved intracellular immune receptors that specifically recognise pathogen derived effectors and activate immune responses often accompanied by the hypersensitive cell death, a known plant immune response. This is referred to as Effector Triggered Immunity (ETI) and it encompass the second layer of plant immune system (248, 250).

Protein kinases take a central role plant immune signaling. The presence of pathogens is recognized through receptor-like protein kinases (RLKs). Most PRRs encode Receptor Like Kinases (RLKs) and Receptor like Proteins (RLPs). RLKs have a extracellular domain, transmembrane domain, and a intracellular kinase domain while RLPs are structurally similar to RLKs but they lack the intracellular kinase domain (252, 253). The most well characterised RLKs are FLAGELLIN-SENSING 2 (FLS2), PEP1 RECEPTOR 1 (PEPR1), ELONGATION FACTOR-TU (EF-Tu) RECEPTOR (EFR) and CHITIN ELICITOR RECEPTOR KINASE 1 (CERK1). FLS2 recognise conserved 22-amino-acid peptide (flg22) from bacterial flagellin (254), PEPR1 recognise endogenous plant elicitor peptides (Peps) (255), EFR recognise the conserved 18-amino-acid epitope (elf18) from the bacterial EF-Tu (256) and CERK1 recognise recognize the fungal chitin oligomers (257). Plant PRRs form complexes with other regulatory receptor kinases such as BRI1-ASSOCIATED RECEPTOR KINASE 1 (BAK1) and recruit Receptor Like Cytoplasmic Kinases (RLCKs) to activate immune signalling thereby linking extracellular ligand perception and downstream signalling (247, 258). Other protein kinases such as mitogen-activated protein kinase (MAPK), calcium-dependent protein kinases (CDPKs) play a role in ETI and PTI signaling pathways (259, 260).

Downstream of PAMP recognition are RLCKs such as BIK1 and related proteins which are involved in signal transmission of extracellularly-detected events(248, 261, 262). Interestingly, tomato Pto and Fen as well as Arabidopsis PBS1 RLCKs recognize bacterial effectors in the host cell cytoplasm. RLCKs are a subgroup of RLKs that lack the extracellular and transmembrane domain. They interact directly with PRRs to transduce defense signals. Arabidopsis *BOTRYTIS*-INDUCES KINASE 1 (BIK1) and its closely related subfamily members PBS-LIKE 1 (PBL1) act downstream of FLS2 the coreceptor BAK1 complex and are required for FLS2 mediated responses (259). Upon PAMP perception BIK1 is phosphorylated by BAK1 and it dissociates from PRR-BAK1 complex to initiate downstream immune responses. The *bik1* and *pbl1* mutants are impaired flg22-mediated responses like ROS burst, MAP KINASE (MPK) signalling, calcium influx, actin filament bundling, callose deposition and stomata closure(261, 263). In addition to FLS2, BIK1 and PBL1 also mediate PTI responses from other PRRs including EFR, PEPR1, PEPR2, and LYK5. (259, 264, 265). BR-SIGNALINGKINASE1 (BSK1) is another RLCK that interact with FLS2 to mediate specific subset of flg22 responses (266). MAP KINASE (MAPK) cascade represents key convergent module regulating different immune responses. PBS1-LIKE 27 (PBL27) is phosphorylated by CERK1 which in turn phosphorylate MAPKKK5 conveying the chitin induced immune signal (267, 268).

Consistent with the importance of protein kinases in plant immunity, pathogens have targeted these components to subvert plant immunity and promote bacterial infection (ref). Type III effectors AvrPto and AvrPtoB, for example, disrupt FLS2/BAK1 by binding to the kinase domains of these proteins, and HopAI1 irreversibly alters a key phosphorylation site of MAPKs to interfere with PTI signaling (261).

In tomato (*Solanum lycopercicum*) there are 128 RLCKs classified into 18 subfamilies based on sequence similarities (269). The physiological function of most of these have not been characterised. Tomato RCLK Pto, n required for resistance to bacterial speck disease of tomato caused by *P. syringae* pv *tomato* carrying the effector AvrPto/ AvrPtoB. Pto is activated by AvrPtoB, and physically interact with PTO RESISTANCE AND FENTHION SENSITIVITY (Prf) allowing indirect detection of AvrPtoB. This results in a variety of defense responses such as Hypersensitive Response (HR) (270, 271). TOMATO PROTEINKINASE1b (TPK1b), another RLCK mediates disease resistance to necrotrophic pathogens in an ethylene dependent manner

(243). Recently, PTO-INTERACTIN 1 (PTI1) was shown to be required for ROS production in response to flagellin perception thus mediating resistance to *P.syringae* (272).

In the current study, we provide a preliminary description of RLCKs TPK07, TPK09, TPK011 and TRK04 and show that these RLCKs play important roles in regulating resistance to *B. cinerea*. Moreover, TRK04 is required for Jasmonic acid seedling responses. Further studies are required to dissect the molecular and biochemical functions of RLCKs in plant immunity and other plant physiological functions.

5.3 Materials and methods

5.3.1 Plant materials and growth conditions

Tomato (*Solanum lycopersicum)* cultivar Casstlemart11 were grown in plastic pots containing compost soil (Sun Grow Metro mix 510) in a growth chamber under extended 12-hour photoperiod at 24 ^{0}C. Castlemart11 is referred to as the wild throughout this paper and all the mutants were generated in the Castlemart11 background. For seedling assays, seeds were surface sterilised with 20% Sodium Hypochlorite, washed several times in distilled water and germinated on full Murashige and Skoog (MS) medium with 2% (w/v), sucrose 0.8% (w/v), 1.5% bacto agar, and supplemented with Gamborg's vitamins under 16hour light, 8 hour dark at 24 ^{0}C.

5.3.2 Generation of tpk07, tpk09, tpk011 and trk04 mutants

To generate RLCKs mutants, two specific guide RNA (gRNA) for each RLCK were designed using the CRISPR Plant gRNA design software then ensures specifity https://www.genome.arizona.edu/crispr/CRISPRsearch.html . The two gRNA were cloned into the CRISPR/Cas9 vector pKSE401 according to (165). Tomato cultivar Casstlemart11 cotyledons explants were suspended in *Agrobacterium* carrying the constructs for 30 minutes and the explants blot dried on sterile blot paper to remove excess *Agrobacterium*. *Agrobacterium* infected explants were co-cultivated on MS medium with 0.8% gelrite + acetosyringone + and incubated in the dark at 21 °C 48 hours. The explants were then transferred to regeneration MS medium supplemented with 75mgL^{-1} Kanamycin to induce callus formation. Green callus was transferred to shoot induction medium MS medium. Regenerated plantlets were transferred to rooting medium with

MS +. Full rooted plants were transferred into the soil and genotyped by PCR with primers covering the expected deletion. The deletions were confirmed by sequencing.

5.3.3 Fungal culture and disease assays

For disease assays, *trk04* and WT seeds were surface sterilised germinated on filter paper. When the radicle emerged, they were transferred to soil. 4 weeks old plants were used in all our disease assays. *Botrytis* strain B05-10 was grown on V8 media and conidia prepared as previously described (242). For gene expression, conidia were sprayed on whole plants and for disease assays detached leaves were drop inoculated with 5µL of spore suspension at 2.5 x10^5 spores/mL. Leaves were incubated in high humidity and lesion diameter was measured 3days after inoculation.

5.3.4 Bacterial disease assays

Bacterial pathogens were cultured in King's B medium (20 g peptone, 10 g glycerol, 1.5 g K_2HPO_4, and 6 mL of 1 M $MgSO_4$/L, pH 7.2) with appropriate antibiotics on a rotary shaker overnight. The bacterial was then suspended in 10 mM $MgCl_2$. Bacterial disease assay were done as previously described by (243). Briefly, leaves of 4-week-old tomato plants were syringe infiltrated with bacterial suspension of (OD_{600} = 0.001 in 10 mM $MgCl_2$). Bacterial growth was determined by collecting leaf discs of infected plants the trk04 mutants and WT at 0 and 3 days after inoculation. The leaf discs were ground in 10 mM $MgCl_2$ and bacterial titre per leaf area was determined.

5.3.5 RNA extraction

Total RNA was extracted from the shoot and root using the Trizol (Invitrogen) according to the manufacturer's instructions. After extraction, RNA was treated with DNASE (New England Biolabs) according to the manufacturer's instruction. RNA was precipitated with 3M Sodium acetate and three-times volume of 100% ethanol. Integrity of RNA was accessed by the Agilent Bioanalyzer (Agilent technologies).

5.3.6 Virus Induced Gene Silencing

We used the Tobacco Rattle Virus system previous described by (273). To generate pTRV2-RLCK (TPK07/TPK09/TPK011/TRK04)construct, about 300bp of the 5' on the cDNA was cloned into PYL156 (274). After confirming the sequences, the constructs were transformed into *Agrobacterium tumefaciens* strain GV3101. pTRV1 and pTRV2-RLCK constructs were agroinfiltrated into cotyledons of one-week old tomato seedlings. After four weeks, the plants were analysed for RLCK gene expression and plants that showed at least 70% silencing were used in disease assays.

5.3.7 Co-immunoprecipitation and immunoblot assays

Nicotiana Benthamiana transiently co-expressing RLCK-MYC, RLCK-HA were used in the co-immunoprecipitation assays. Tissues were harvested at 24 hours after agroinfiltration and frozen in liquid nitrogen. Tissues were the homogenised in cold protein extraction buffer (20mM Tris-HCl pH 7.5, 150mM NaCl, 1mM EDTA, I mM EGTA, I mM NaF, 10mM β-glycerophosphate, 0.1% tween-20, protease inhibitor cocktail (Sigma-Aldrich), 1mM PMSF, I mM DTT, 1 mM Na_3VO_4 and 0.1% Triton-X100). Tissue lysate was spun down and the supernatant was collected and incubate with conjugated HA agarose beads (Sigma -Aldrich) overnight. The beads were washed several times to remove unbound proteins and the proteins denatured by heating. Proteins were separated on SDS PAGE gel and visualised by Western blotting using corresponding antibodies.

5.4 Results

5.4.1 Characterisation of Tomato Receptor Like Cytoplasmic Kinases (RLCKs)

We screened for RLCKs orthologous to *Arabidopsis* BIK1 (263, 275) and homologous to tomato TPK1b (243) in the tomato genome. Many genes encoding RLCKs were identified (Table 5.1). We identified 15 tomato genes closely related to Arabidopsis BIK1.

Table 5.1. Tomato Receptor Like Cytoplasmic Kinases (RLCKs) similar to *At*BIK1 and *Sl*TRK1

Protein	Ortholog	Gene
413	TPK1b	TPKO1
394		TPKO2
416		TPKO3
409		TPKO4
419		TPKO5
420		TPKO6
478		TPKO7
481		TPKO8
418		TPKO9
440		TPKO10
415		TPKO11
433	TRK1	TRKO1
469		TRKO2
430		TRKO3
409		TRKO4

To test if any of these genes show possible plant defense functions, we tested whether any of the proteins interacted with RPM1 Interacting Protein 4 (RIN4) and Flagellin Sensitive 2 (FLS2) previously characterised proteins that play a role in tomato immunity to bacterial pathogens (254, 276). Interestingly all but one protein (TPK07) interacted with RIN4 and FLS2 (Figure 5.1 and 5.2).

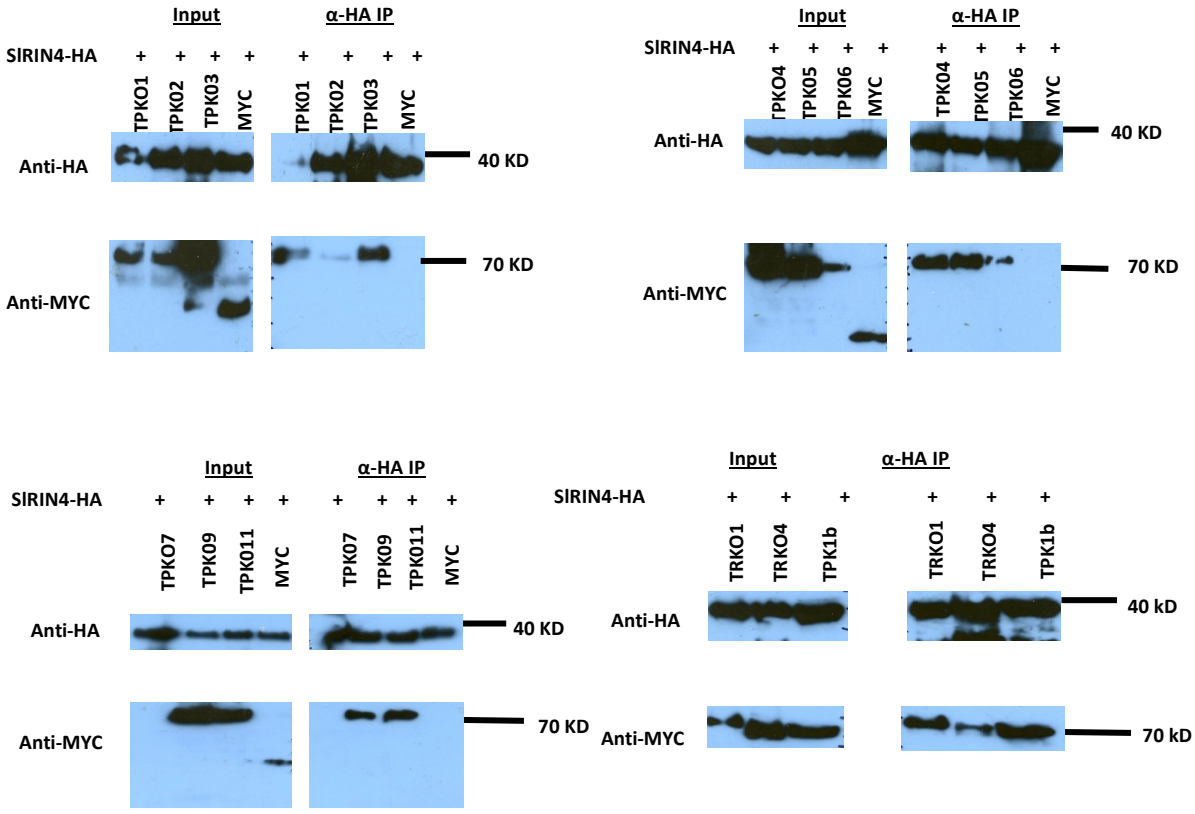

Figure 5.1. Tomato Receptor Like Cytoplasmic Kinases (RLCKs) interacts with tomato RIN4. RIN4- HA was transiently co-expressed with RLCK-MYC by agroinfiltration in *N. benthamiana* leaves. The empty vector expressing MYC was used as a negative control. Anti-HA (α-HA) and anti-MYC (α-MYC) antibodies were used to detect protein accumulation in input or immunoprecipitated (IP) samples.

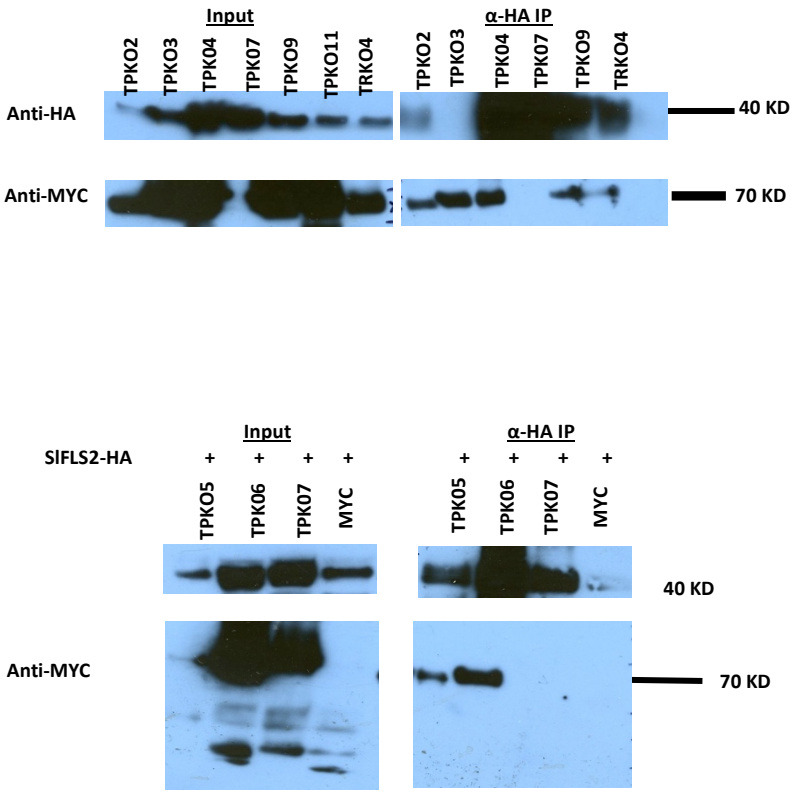

Figure 5.2. Tomato Receptor Like Cytoplasmic Kinases (RLCKs) interacts with FLS2. FLS2-HA was transiently co-expressed with RLCK -MYC by agroinfiltration in *N. benthamiana* leaves. The empty vector expressing MYC was used as a negative control. Anti-HA (α-HA) and anti-MYC (α-MYC) antibodies were used to detect protein accumulation in input or immunoprecipitated (IP) samples.

We used Virus Induced Gene Silencing (VIGs) to screen for RLCKs susceptible to *B. cinerea*. Of the fifteen RLCKs tested, silencing of TPK07, TPK09, TPK011 and TRK04 resulted in susceptibility to *B. cinerea* (Figure 5.3A). We did not find any significant differences when these VIGS plants were tested for resistance to *P. syringae* (Figure 5.3B).

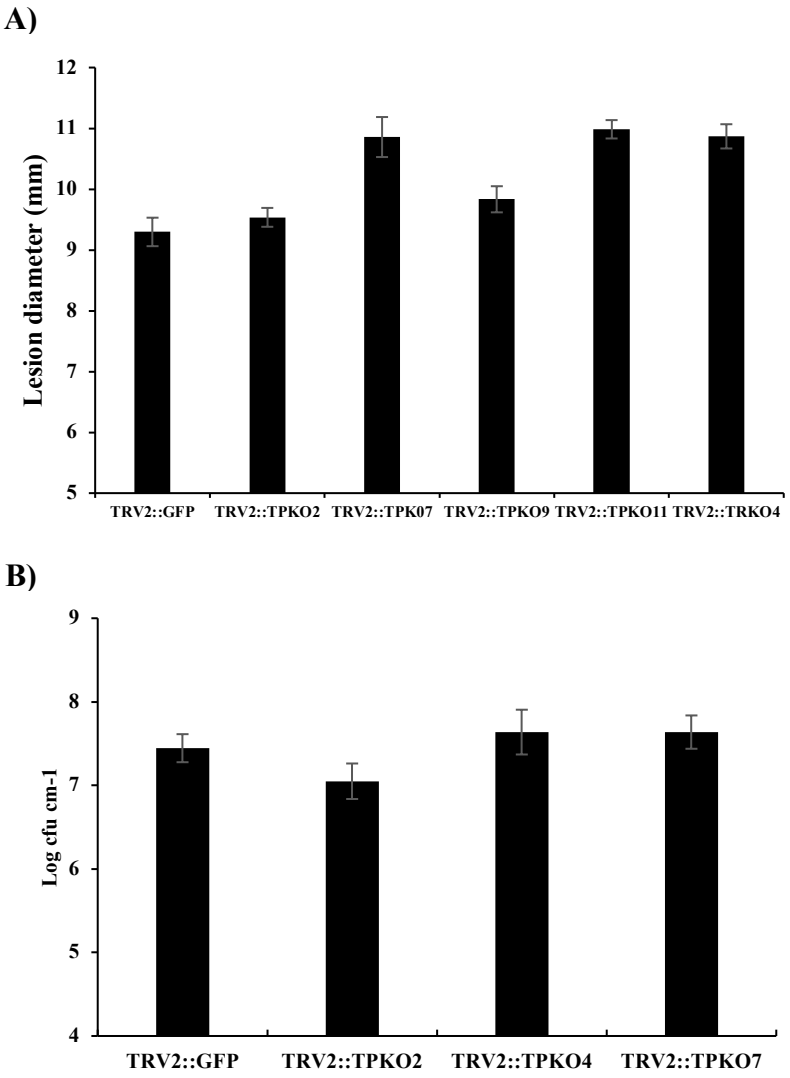

Figure 5.3. TRKO4, TPKO7, TPKO9 and TPKO9 are required for *B. cinerea* disease resistance. A) Lesion diameter 3 days after drop inoculation with *B.cinerea* spores on TPKO2, TPKO7, TPKO9, TPKO11 and TRKO4 Virus Induced Gene Silenced (VIGS) plants. B) Bacterial growth *(P. syringae) in* VIGs silenced plants.

5.4.2 Phylogenetic analysis of TPK07, TPK09, TPK011 and TRK04.

TPK07 encodes a 478 amino acid open reading frame encoding an 53kD estimated protein. TPK09 encodes a 418 amino acid protein with an estimated weight of 45.9kD. TPK011 is a 416 amino acid protein weighing about 45.3kD. TPK07, TPK09, TPK011 are RLCKs with the signature kinase catalytic domain (PS50011). TRK04, is a 4304bp gene with four exons and four introns. TRK04 has 409aa open reading frame encoding an estimated 45.8kD RCLK protein. TRK04 has a protein kinase catalytic domain (PS50011) (residues 78-363), ATP binding site

region signature (PS00107) (residues 83-113) and the Serine/Threonine protein kinase signature (PS00108) (residues 208-220). TPK07, TPK09, TPK011 and TRK04 have been previously classified as a RLCK VIIa class proteins (269). Sequence and phylogenetic analysis were performed to decipher the relationship between TPK07, TPK09, TPK011 and TRK04 and other previously characterised RLCKs from *Arabidopsis* and maize. TPK07 is closer to other tomato RLCKs like TPK08 and TPK010. While TPK09 and TPK011 share a nodes. These do not share nodes with any Arabidopsis or maize protein analysed. TRK04 is closer to *Arabidopsis* PBL19 and PBL20. In tomato it is closely related to TRK03 (Figure 5.4A).

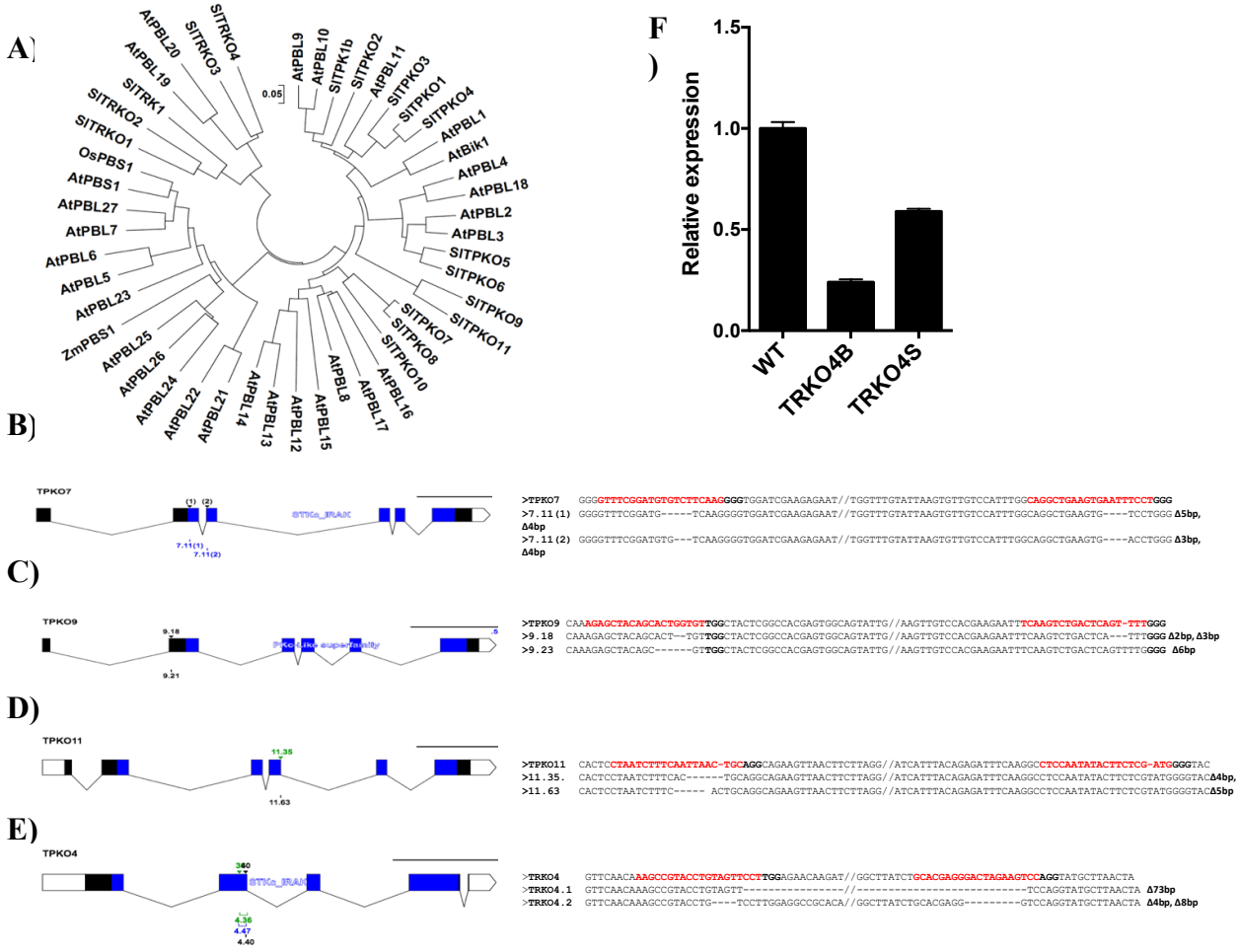

Figure 5.4. Phylogenetic analysis, genomic structures and CRIPR/Cas9 deletions of TRKO4, TPKO7, TPKO9 and TPKO11. A) Maximum Likelihood phylogenetic analysis of RLCKs proteins from *Arabidopsis thaliana (*At*)*, and *Solanum lycopersicum* (Sl). Phylogenetic analysis was performed using Mega7 package. The tree is drawn to scale with branch length measured in the number of substitutions per site. Bootstrap values higher than 50% are shown. Schematic diagram showing gene and CRIPSR/Cas9 deletions of B) TPK07, C) TPK09, D) TPK011 and E) TRK04. Blue shaded boxes represent exons, the black shaded boxes represent the UTRs boxes represent exon, and introns are shown as horizontal lines. F) Relative expression of TRK04 in trk04 mutant alleles.

5.4.3 Characterization of *tpk07, tpk09, tpk011 and trk04* loss of function mutants.

To study the function of TPK07, TPK09, TPK011 and TRK04, we generated gene edited lines through CRISPR/Cas9-induced mutation. Two guide RNAs (gRNAs) were designed to generate mutations in each RLCK TRK04, TPK07, and TPK09. To ensure that the sgRNAs were specific and to avoid off target mutagenesis we used the gRNA design software www.genome.arizona.edu/crispr. The gRNAs were expressed under the control of *Arabidopsis* U6 promoter. Heterozygous mutations in the RLCKs were identified in T0 generation which were segregated in the next generation to produce homozygous lines. The two *tpk07* mutant alleles had 4bp and 5bp deletions on one target and 4bp and 3bp deletions on the other, both resulting in premature stop codons (Figure 5.4B). The two *tpk09* mutant alleles had 2bp and 6bp deletions, both resulting in frame shifts (Figure 5.4C). The two *tpk011*mutant alleles had 4bp and 5bp deletions, both resulting in premature stop codons 2 (Figure 5.4D). The *tpk011*mutant, makes flowers that fell off, did not make any fruits and hence we were not able to recover seed from it. The *tpk07* and *tpk09* mutants produced viable seeds, but due to time constraints no phenotypic characterisation has been conducted. The *trk04.1* mutant allele has a 73bp deletion generating a stop codon in the open reading frame resulting in a truncated protein. The *trk04.2* mutant allele has two deletion of 4bp and 8bp causing a frame shift mutation. All the deletions for both alleles were in exon 2 (Figure 5.4E). Quantitative Reverse Transcription Polymerase Chain Reaction (qRT-PCR) showed that TRK04 transcripts were severely reduced in the *trk04.1* and *trk04.2* mutants compared to the WT (Figure 5.4F). This data suggests that *trk04.1* and *trk04.2* mutants are loss of function mutants.

5.4.4 TRK04 is required for resistance to *Botrytis cinerea* in tomato.

To gain insight into the biological functions of TRK04, we examined its expression patterns in leaves, roots, flower structures, green fruits, and red fruits using RT-qPCR. TRK04 transcript are abundantly expressed in the roots and least expressed in the leaves. In the sepals, anthers and green fruits TRK04 transcripts are moderately expressed however they get lower when the fruit ripens (Figure 5.5A). To determine the functional relevance of TRK04, we looked at the expression profile under disease and treatment with plant hormones. TRK04 is induced by *B. cinerea* only at 24 hours after treatment (Figure 5.6B). In response to treatment with the plant

hormones Methyl jasmonate **(**MeJA), 1-aminocyclopropane-1-carboxylic acid (ACC), and salicylic acid (SA), TRK04 is highly induced as early as 12 hours after treatment and this induction is sustained up to 36 hours after treatment (Figure 5.5B-E).

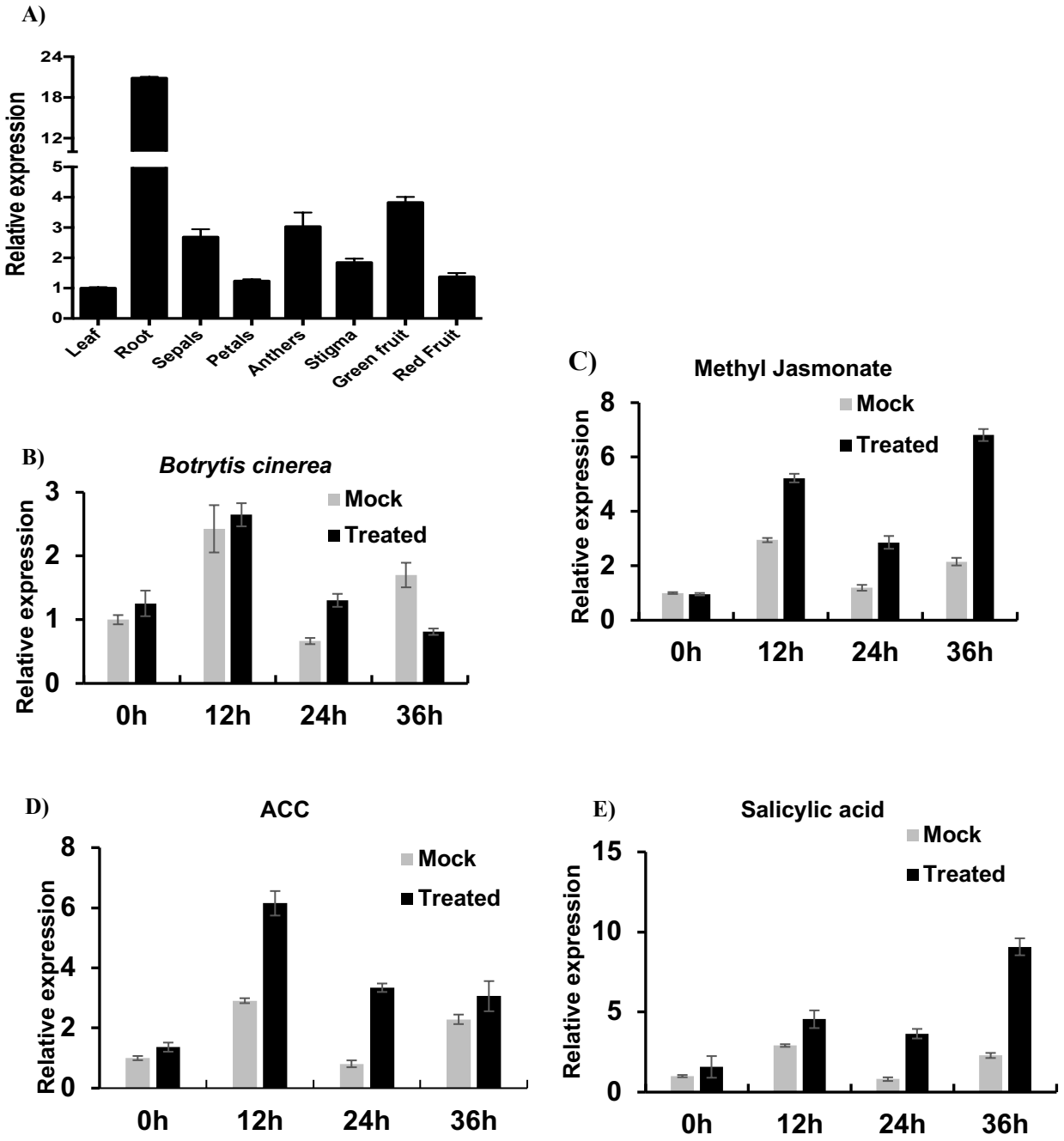

Figure 5.5. Basal and induced expression of TRKO4. A) Tissue specific expression of TRK04 in WT tomato plants. Induced expression of TRK04 in response to B) *B. Cinerea*, C) Methyljasmonate (MeJA), D) 1-aminocyclopropane-1-carboxylic acid ACC, and E) Salicylic acid (SA). Bars represent the means; the error bars represent the standard deviations of three technical replicates of each treatment. The β-actin gene was used as an internal control in the qRT-PCR. The experiment was repeated at least 2 times with similar results

TRK04 is highly induced by hormones that function in plant defence as well as by B. *cinerea* suggesting an important role for TR04 in plant immunity. To investigate the possible role of TRK04 in defense against *B. cinerea*, we tested the *trk04.1* and *trk04.2* mutants for resistance to *B. cinerea.* Detached leaf assays were conducted to compare disease phenotypes between *trk04* mutants and WT plants. *trk04* mutants showed increased susceptibility to *B. cinerea,* with larger disease lesions and tissue maceration than the WT (Figure 5.6A, B). This data shows that loss of TRK04 results in susceptibility to *B. cinerea* and thus TRK04 is required for resistance to *B. cinerea* in tomato.

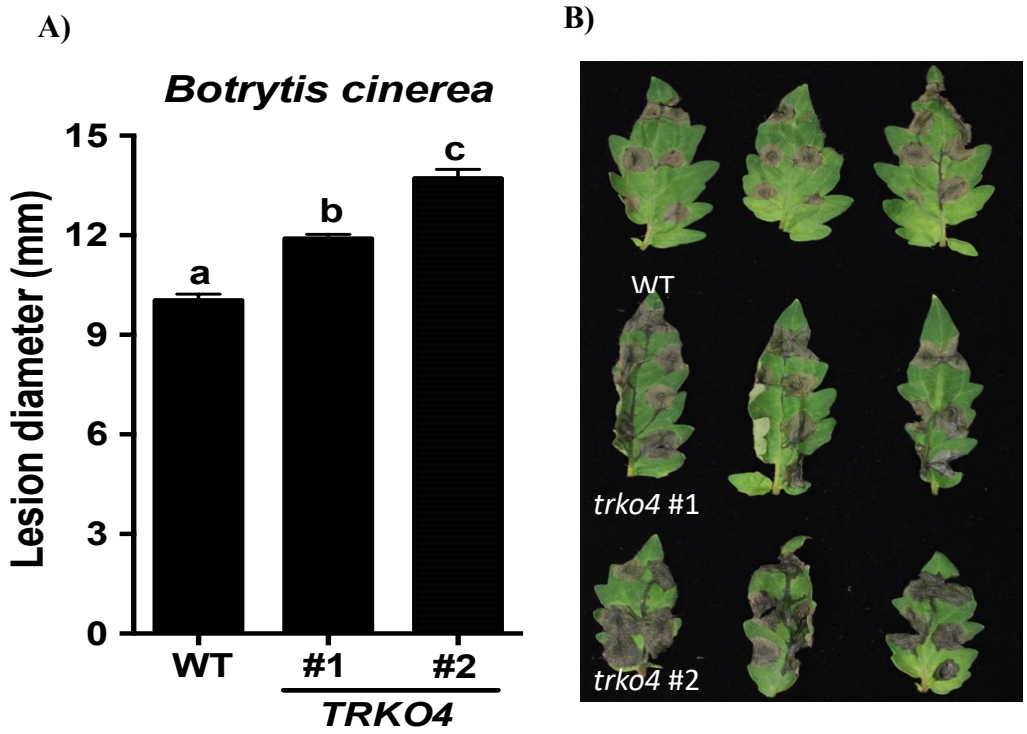

Figure 5.6. TRKO4 mediates resistance to *B. Cinerea*. A) *B. Cinerea* disease lesion size and B) disease symptoms of *trk04* mutants. Bars represent the means; the error bars represent the standard deviations of three technical replicates of each treatment. Samples with different letters are statistically significant different (Student's *t* test, $P < 0.001$)

5.4.5 trk04 mutants are impaired in seedling growth response to Jasmonic acid

TRK04 is highly induced by MeJA. To establish the role of TRK04 in Jasmonic acid response pathway, we studied JA sensitivity of *trk04* mutants and WT through analysis of seed germination and growth in the prescense of MeJA. The WT exhibited MeJA sensitivity depicted by reduced hypocotyl and root length when grown in 0.5 and 1 µM MeJA. However, in the *trk04*

mutant's hypocotyl length was not altered by MeJA treatment. Root length was slightly reduced in *trk04* mutants with MeJA treatment, but this root length was significantly (*P<0.05)* higher than the WT (Figure 5.7A-C). This show that TRK04 is required for JA-mediated seed germination and seedling growth.

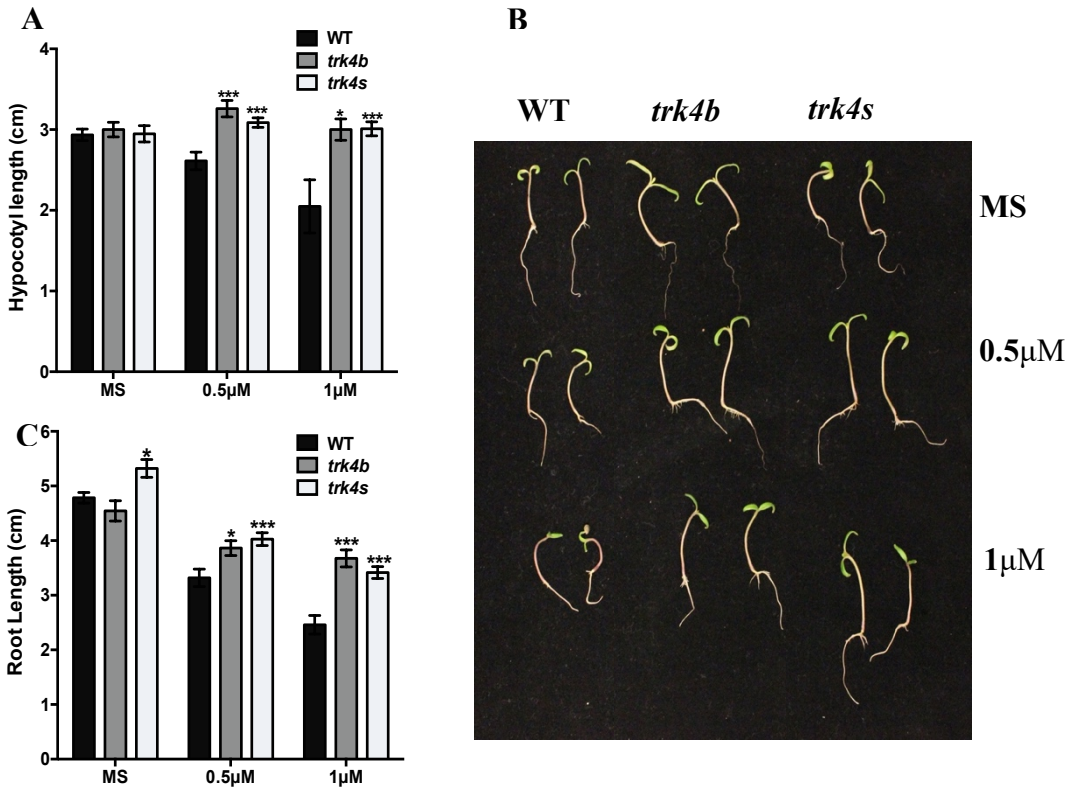

Figure 5.7. TRK04 mediates seedling growth responses to Jasmonic acid in tomato. A) Hypocotyl length, B) Overall seedling stature and C) Root length of trk04 mutants and WT seedlings grown in MS medium supplemented with or without Methyljasmonate (MeJA). Bars represent the means; the error bars represent the standard deviations of three technical replicates of each treatment. Asterisk represents statistically significant differences (Student's *t* test, *p < 0.05, **p < 0.01. *p < 0.05, **p < 0.01).

5.5 Discussion

In this study we studied fifteen Receptor Like Cytoplasmic Kinases (RLCKs) related to Arabidopsis *BIK1*. Reduction in the expression of TPK07, TPK09 TPK011 and TRK04 through Virus Induced Gene Silencing (VIGS) results in susceptibility to *B.cinerea*. Since VIGS is transient, we generated CRISPR/Cas9 knockout mutants to further study the functions of TPK07, TPK09 TPK011 and TRK04. We confirm the role of TRK04 in mediating responses to *B. cinerea*

using knockout mutants. We further show that TRK04 is required for Jasmonic acid mediated seedling responses.

Receptor like kinases (RLKs) recognise PAMPs and activate immune responses. RLCKs associates with RLKs and regulate multiple downstream signalling pathways to orchestrates defense response against pathogens. All but one of the RLCKs we identified interacted with FLS2 and RIN4 (Figure 5.1 and 5.2). TPK07, TPK09 TPK011 and TRK04 belong to RLCK VIIa subfamily suggesting structural relatedness and hence similar functions. Indeed, similar structural patterns of kinase activity sites and structural patterns of intron/exon have been observed among members of the same subfamily indicating a close evolutionary relationship. (277). Though the RLCKs physically interacts with RIN4 and FLS2, the functional relevance of these interactions still needs to be elucidated. Studies showing whether the RLCKs phosphorylates RIN4 and/or FLS2 or vice versa will be important to determine the biochemical function of the RLCKs. Also, whether these interactions translate to a physiological response in ETI or PTI is an important aspect to study. It is however interesting to study why TPK07 show some functional divergence despite have similar catalysis domain and protein structure to other members of RLCK VIIa subfamily. Furthermore, there are 128 RLCKs in the tomato genome, and hence some functional redundancy cannot be overruled. Accordingly, PBS1, PBL1 and PBL2 members of the RLCKVII subfamily and BSK1 a member of the RLCKXII subfamily mediate Flagellin 22(flg22) dependent PTI signalling like BIK1 downstream of FLS2 (266, 278).

Our data shows that TPK07, TPK09 TPK011 and TRK04 mediate tomato physiological reponses to *B. cinerea*. However the mechanism of how TPK07, TPK09 TPK011 and TRK04 regulates tomato responses to *B.cinerea* are not known. Analysis of genome wide regulatory effects of the RLCKs in response to *B.cinerea* will assist in identifying the RLCKs' mechanism of function in mediating *B.cinerea* responses in tomato. Identifying which Pathogen Recognition Receptrors (PRRs) asssociates with the RLCKs, how they dissociate form the PRR upon pathogen perception, the downstream targets and localisation of the RLCKs will be cruical in chracterising the functions of the RLCKs. The impaired jasmonic acid mediated growth in *trk04* mutants suggests that TRK04 is required for the expression of jasmonic acid responsive genes. The jasmonic acid signalling pathway is important for necrotrophic pathogen response (18) and response to insects wounding (242). It Is plausible to think that TRK04 may also regulate reponses to insect wounding. Analyses that will unravel the regulatory link between pathogen and insect

responses mediated by TRK04 are important. No RLCK mutation to date has been identified to impair Jasmonic acid responses. Furthermore, RLCKs are understudied in tomato, hence this study will provide novel insight into RLCKs mediated response to disease, jasmonic acid signalling pathway and possibly insect responses.

REFERENCES

1. N. J. Atkinson, F. o. B. S. Centre for Plant Sciences, University of Leeds, Leeds LS2 9JT, UK, P. E. Urwin, F. o. B. S. Centre for Plant Sciences, University of Leeds, Leeds LS2 9JT, UK, The interaction of plant biotic and abiotic stresses: from genes to the field. *Journal of Experimental Botany* **63**, 3523-3543 (2019).

2. S. Kumar, A. Singh, Epigenetic Regulation of Abiotic Stress Tolerance in Plants. (2016).

3. S. Barak, N. Singh Yadav, A. Khan, DEAD-box RNA helicases and epigenetic control of abiotic stress-responsive gene expression. *Plant Signal Behav* **9**, e977729 (2014).

4. G. Pandey, N. Sharma, P. P. Sahu, M. Prasad, "Chromatin-Based Epigenetic Regulation of Plant Abiotic Stress Response" in Curr Genomics. (2016), vol. 17, pp. 490-498.

5. D. Secco, J. Whelan, H. Rouached, R. Lister, Nutrient stress-induced chromatin changes in plants. *Curr Opin Plant Biol* **39**, 1-7 (2017).

6. T. Kouzarides, Chromatin modifications and their function. *Cell* **128**, 693-705 (2007).

7. V. Chinnusamy, J. K. Zhu, Epigenetic regulation of stress responses in plants. *Curr Opin Plant Biol* **12**, 133-139 (2009).

8. K. D. Kasschau *et al.*, Genome-wide profiling and analysis of Arabidopsis siRNAs. *PLoS Biol* **5**, e57 (2007).

9. I. R. Henderson, S. E. Jacobsen, Epigenetic inheritance in plants. *Nature* **447**, 418-424 (2007).

10. H. Spotswood, B. Turner, An increasingly complex code. *The Journal of clinical investigation* **110**, 577-582 (2002).

11. R. B. a. A. Berr, Abiotic and Biotic Stress in Plants - Recent Advances and Future Perspectives. (2016).

12. Z. Lippman *et al.*, Role of transposable elements in heterochromatin and epigenetic control. *Nature* **430**, 471-476 (2004).

13. Z. Xiaoyu, "Chromatin Modifications in Plants | SpringerLink" in Plant genome diversity, J. G. Jonathan F. Wendel, Jaroslav DolezelIlia J. Leitch, Ed. (SpringerLink, 2012), vol. 1.

14. J. Xiao, U. S. Lee, D. Wagner, Tug of war: adding and removing histone lysine methylation in Arabidopsis. *Curr Opin Plant Biol* **34**, 41-53 (2016).

15. J. Lamke, K. Brzezinka, S. Altmann, I. Baurle, A hit-and-run heat shock factor governs sustained histone methylation and transcriptional stress memory. *Embo j* **35**, 162-175 (2016).

16. Y. Ding *et al.*, ATX1-generated H3K4me3 is required for efficient elongation of transcription, not initiation, at ATX1-regulated genes. *PLoS Genet* **8**, e1003111 (2012).

17. Y. Ding, M. Fromm, Z. Avramova, Multiple exposures to drought 'train' transcriptional responses in Arabidopsis. *Nat Commun* **3**, 740 (2012).

18. A. Berr *et al.*, Arabidopsis histone methyltransferase SET DOMAIN GROUP8 mediates induction of the jasmonate/ethylene pathway genes in plant defense response to necrotrophic fungi. *Plant Physiol* **154**, 1403-1414 (2010).

19. W. Y. Kim, K. A. Hicks, D. E. Somers, "Independent Roles for EARLY FLOWERING 3 and ZEITLUPE in the Control of Circadian Timing, Hypocotyl Length, and Flowering Time1" in Plant Physiol. (2005), vol. 139, pp. 1557-1569.

20. Z. Zhao, Y. Yu, D. Meyer, C. Wu, W. H. Shen, Prevention of early flowering by expression of FLOWERING LOCUS C requires methylation of histone H3 K36. *Nat Cell Biol* **7**, 1256-1260 (2005).

21. K. Palma *et al.*, Autoimmunity in Arabidopsis acd11 is mediated by epigenetic regulation of an immune receptor. *PLoS Pathog* **6**, e1001137 (2010).

22. Y. Tamada, J. Y. Yun, S. C. Woo, R. M. Amasino, ARABIDOPSIS TRITHORAX-RELATED7 is required for methylation of lysine 4 of histone H3 and for transcriptional activation of FLOWERING LOCUS C. *Plant Cell* **21**, 3257-3269 (2009).

23. T. Thorstensen *et al.*, The Arabidopsis SET-domain protein ASHR3 is involved in stamen development and interacts with the bHLH transcription factor ABORTED MICROSPORES (AMS). *Plant Mol Biol* **66**, 47-59 (2008).

24. F. Roudier *et al.*, Integrative epigenomic mapping defines four main chromatin states in Arabidopsis. *Embo j* **30**, 1928-1938 (2011).

25. Y. Jacob *et al.*, Regulation of heterochromatic DNA replication by histone H3 lysine 27 methyltransferases. *Nature* **466**, 987 (2010).

26. C. Kohler *et al.*, The Polycomb-group protein MEDEA regulates seed development by controlling expression of the MADS-box gene PHERES1. *Genes Dev* **17**, 1540-1553 (2003).

27. G. Makarevich *et al.*, Different Polycomb group complexes regulate common target genes in Arabidopsis. *EMBO Rep* **7**, 947-952 (2006).

28. C. C. Sheldon, A. B. Conn, E. S. Dennis, W. J. Peacock, Different regulatory regions are required for the vernalization-induced repression of FLOWERING LOCUS C and for the epigenetic maintenance of repression. *Plant Cell* **14**, 2527-2537 (2002).

29. J. P. Jackson, A. M. Lindroth, X. Cao, S. E. Jacobsen, Control of CpNpG DNA methylation by the KRYPTONITE histone H3 methyltransferase. *Nature* **416**, 556-560 (2002).

30. M. L. Ebbs, L. Bartee, J. Bender, H3 lysine 9 methylation is maintained on a transcribed inverted repeat by combined action of SUVH6 and SUVH4 methyltransferases. *Mol Cell Biol* **25**, 10507-10515 (2005).

31. K. Naumann *et al.*, Pivotal role of AtSUVH2 in heterochromatic histone methylation and gene silencing in Arabidopsis. *Embo j* **24**, 1418-1429 (2005).

32. Y. Ding *et al.*, SDG714, a histone H3K9 methyltransferase, is involved in Tos17 DNA methylation and transposition in rice. *Plant Cell* **19**, 9-22 (2007).

33. J. K. Zhu, Salt and drought stress signal transduction in plants. *Annu Rev Plant Biol* **53**, 247-273 (2002).

34. S. Basu, V. Ramegowda, A. Kumar, A. Pereira, Plant adaptation to drought stress. *F1000Res* **5** (2016).

35. Y. Osakabe, K. Osakabe, K. Shinozaki, L. S. P. Tran, Response of plants to water stress. *Front Plant Sci* **5** (2014).

36. Y. Fang, L. Xiong, General mechanisms of drought response and their application in drought resistance improvement in plants. *Cell Mol Life Sci* **72**, 673-689 (2015).

37. A. Blum, ablum@plantstress.com, Drought resistance, water-use efficiency, and yield potential—are they compatible, dissonant, or mutually exclusive? *Australian Journal of Agricultural Research* **56**, 1159-1168 (2019).

38. B. Simane, J. M. Peacock, P. C. Struik, Differences in developmental plasticity and growth rate among drought-resistant and susceptible cultivars of durum wheat (Triticum turgidum L. var. durum). *Plant and Soil* **157**, 155-166 (1993).

39. Y. Shavrukov *et al.*, Early Flowering as a Drought Escape Mechanism in Plants: How Can It Aid Wheat Production? *Front Plant Sci* **8** (2017).

40. e. a. Farooq M Broader leaves result in better performance of indica rice under drought stress. - PubMed - NCBI. (2019).

41. R. K. Pandey, W. A. T. Herrera, A. N. Villegas, J. W. Pendleton, Drought Response of Grain Legumes Under Irrigation Gradient: III. Plant Growth 1. (--).

42. W. J. Cox, G. D. Jolliff, Crop-Water Relations of Sunflower and Soybean under Irrigated and Dryland Conditions 1. (--).

43. M. A. M. M. Hussain, M. Farooq, M. B. Khan, M. Akram, M. F. Saleem, Exogenous Glycinebetaine and Salicylic Acid Application Improves Water Relations, Allometry and Quality of Hybrid Sunflower under Water Deficit Conditions - Hussain - 2009 - Journal of Agronomy and Crop Science - Wiley Online Library. *Journal of Agronomy and Crop Science* **95**, 95-109 (2019).

44. Z. Xu, G. Zhou, Responses of leaf stomatal density to water status and its relationship with photosynthesis in a grass. *J Exp Bot* **59**, 3317-3325 (2008).

45. P. J. Seo *et al.*, The MYB96 transcription factor mediates abscisic acid signaling during drought stress response in Arabidopsis. *Plant Physiol* **151**, 275-289 (2009).

46. R. Ijaz *et al.*, Overexpression of annexin gene AnnSp2, enhances drought and salt tolerance through modulation of ABA synthesis and scavenging ROS in tomato. *Scientific Reports* **7**, 12087 (2017).

47. R. M. Seyed Y. S. Lisar, Mosharraf M. Hossain and Ismail M. M. Rahman, Water Stress. (2012).

48. S. N.H., "Understanding How Plants Respond to Drought Stress at the Molecular and Whole Plant Levels | SpringerLink" in Drought Stress Tolerance in Plants, W. S. Hossain M., Bhattacharjee S., Burritt D., Tran LS, Ed. (SpringerLink, Switzerland, 2016), vol. 2.

49. M. S. A. A. Ghotbi-Ravandi, M. Shariati, P. Mulo, Effects of Mild and Severe Drought Stress on Photosynthetic Efficiency in Tolerant and Susceptible Barley (Hordeum vulgare L.) Genotypes - Ghotbi-Ravandi - 2014 - Journal of Agronomy and Crop Science - Wiley Online Library. *Journal of Agronomy and Crop Science* **200**, 403-415 (2014).

50. R. N. Mutava *et al.*, Understanding abiotic stress tolerance mechanisms in soybean: a comparative evaluation of soybean response to drought and flooding stress. *Plant Physiol Biochem* **86**, 109-120 (2015).

51. Z. S. Li Wenrao, Shan Lun, Responsibility of non-stomatal limitations for the reduction of photosynthesis—response of photosynthesis and antioxidant enzyme characteristics in alfalfa (Medicago sativa L.) seedlings to water stress and rehydration | SpringerLink. *Frontiers of Agriculture in China* **1** (2007).

52. M. F. Grassi G, Stomatal, mesophyll conductance and biochemical limitations to photosynthesis as affected by drought and leaf ontogeny in ash and oak trees - GRASSI - 2005 - Plant, Cell & Environment - Wiley Online Library. *Plant Cell Environment* (2005).

53. W. Ouyang *et al.*, Stomatal conductance, mesophyll conductance, and transpiration efficiency in relation to leaf anatomy in rice and wheat genotypes under drought. *Journal of Experimental Botany* **68**, 5191-5205 (2019).

54. H. M. Josefina Bota, Jaume Flexas, Is photosynthesis limited by decreased Rubisco activity and RuBP content under progressive water stress? - Bota - 2004 - New Phytologist - Wiley Online Library. *New Phytologist* **162**, 671-681 (2004).

55. C. Gimenez, V. J. Mitchell, D. W. Lawlor, Regulation of Photosynthetic Rate of Two Sunflower Hybrids under Water Stress. *Plant Physiol* **98**, 516-524 (1992).

56. H. Medrano, J. M. Escalona, J. Bota, J. GulÍAs, J. Flexas, Regulation of Photosynthesis of C3 Plants in Response to Progressive Drought: Stomatal Conductance as a Reference Parameter. *Ann Bot* **89**, 895-905 (2002).

57. W. Tezara, V. J. Mitchell, S. D. Driscoll, D. W. Lawlor, Water stress inhibits plant photosynthesis by decreasing coupling factor and ATP. *Nature* **401**, 914 (1999).

58. A. C. Tang, Y. Kawamitsu, M. Kanechi, J. S. Boyer, Photosynthetic oxygen evolution at low water potential in leaf discs lacking an epidermis. *Ann Bot* **89 Spec No**, 861-870 (2002).

59. e. a. Younis HM Conformation and activity of chloroplast coupling factor exposed to low chemical potential of water in cells. - PubMed - NCBI. (2019).

60. H. Chen, Z. Li, L. Xiong, A plant microRNA regulates the adaptation of roots to drought stress. *FEBS Lett* **586**, 1742-1747 (2012).

61. K. I. Deak, J. Malamy, Osmotic regulation of root system architecture. *Plant J* **43**, 17-28 (2005).

62. D. Sengupta, A. R. Reddy, "Water deficit as a regulatory switch for legume root responses" in Plant Signal Behav. (2011), vol. 6, pp. 914-917.

63. H. Yu *et al.*, "Activated Expression of an Arabidopsis HD-START Protein Confers Drought Tolerance with Improved Root System and Reduced Stomatal Density[W][OA]" in Plant Cell. (2008), vol. 20, pp. 1134-1151.

64. A. Henry, A. J. Cal, T. C. Batoto, R. O. Torres, R. Serraj, Root attributes affecting water uptake of rice (Oryza sativa) under drought. *J Exp Bot* **63**, 4751-4763 (2012).

65. R. Serraj, T. R. Sinclair, Osmolyte accumulation: can it really help increase crop yield under drought conditions? *Plant Cell Environ* **25**, 333-341 (2002).

66. I. S. V. Alexieva, S. Mapelli, E. Karanov, The effect of drought and ultraviolet radiation on growth and stress markers in pea and wheat - Alexieva - 2001 - Plant, Cell & Environment - Wiley Online Library. *Plant Cell Environ.* **24**, 1337–1344 (2001).

67. M. Yamada *et al.*, Effects of free proline accumulation in petunias under drought stress. *J Exp Bot* **56**, 1975-1981 (2005).

68. L. H. Yu *et al.*, Arabidopsis EDT1/HDG11 improves drought and salt tolerance in cotton and poplar and increases cotton yield in the field. *Plant Biotechnol J* **14**, 72-84 (2016).

69. M. A. M. M. Hussain, M. Farooq, M. B. Khan, M. Akram, M. F. Saleem, Exogenous Glycinebetaine and Salicylic Acid Application Improves Water Relations, Allometry and Quality of Hybrid Sunflower under Water Deficit Conditions - Hussain - 2009 - Journal of Agronomy and Crop Science - Wiley Online Library. *Journal of Agronomy and Crop Science* **95**, 95-109 (2009).

70. N. Samarah, R. Mullen, S. Cianzio, Size Distribution and Mineral Nutrients of Soybean Seeds in Response to Drought Stress. *http://dx.doi.org/10.1081/PLN-120030673* (2007).

71. M. M. Chaves, J. Flexas, C. Pinheiro, "Photosynthesis under drought and salt stress: regulation mechanisms from whole plant to cell" in Ann Bot. (2009), vol. 103, pp. 551-560.

72. A. W. M. Farooq, N.Kobayashi, D. Fujita, S. M. A. Basra, Plant drought stress: effects, mechanisms and management | SpringerLink. **29**, 185-212 (2009).

73. M. M. Chaves, J. Marôco, J. H. S. Pereira, Understanding plant responses to drought — from genes to whole plant . Func Plant Biol. *Functional Plant Biology* (2003).

74. S. S. Gill, N. Tuteja, Reactive oxygen species and antioxidant machinery in abiotic stress tolerance in crop plants. *Plant Physiol Biochem* **48**, 909-930 (2010).

75. Z. M. E.-B. Nemat M.Hassan, Ahamed K.El-Sayed, Heba T.Ebeed, Mamdouh M.Nemat Alla, Roles of dehydrin genes in wheat tolerance to drought stress. *Journal of Advanced Research* **6**, 179-188 (2015).

76. A. Sauter, W. J. Davies, W. Hartung, The long-distance abscisic acid signal in the droughted plant: the fate of the hormone on its way from root to shoot. *J Exp Bot* **52**, 1991-1997 (2001).

77. Y.-S. K. Osakabe Y, Shinozaki K, Tran LS, ABA control of plant macroelement membrane transport systems in response to water deficit and high salinity - Osakabe - 2014 - New Phytologist - Wiley Online Library. *New Phytology* **202:**, 35–49 (2014).

78. R. R. Finkelstein, S. S. L. Gampala, C. D. Rock, "Abscisic Acid Signaling in Seeds and Seedlings" in Plant Cell. (2002), vol. 14, pp. s15-45.

79. A. Frey *et al.*, Epoxycarotenoid cleavage by NCED5 fine-tunes ABA accumulation and affects seed dormancy and drought tolerance with other NCED family members. *Plant J* **70**, 501-512 (2012).

80. J. Y. Kang, H. I. Choi, M. Y. Im, S. Y. Kim, Arabidopsis basic leucine zipper proteins that mediate stress-responsive abscisic acid signaling. *Plant Cell* **14**, 343-357 (2002).

81. R. M. Rivero *et al.*, Delayed leaf senescence induces extreme drought tolerance in a flowering plant. *Proc Natl Acad Sci U S A* **104**, 19631-19636 (2007).

82. T. Werner *et al.*, Root-specific reduction of cytokinin causes enhanced root growth, drought tolerance, and leaf mineral enrichment in Arabidopsis and tobacco. *Plant Cell* **22**, 3905-3920 (2010).

83. R. Nishiyama *et al.*, Analysis of cytokinin mutants and regulation of cytokinin metabolic genes reveals important regulatory roles of cytokinins in drought, salt and abscisic acid responses, and abscisic acid biosynthesis. *Plant Cell* **23**, 2169-2183 (2011).

84. Y. Yu *et al.*, The ethylene response factor OsERF109 negatively affects ethylene biosynthesis and drought tolerance in rice. *Protoplasma* **254**, 401-408 (2017).

85. H. Zhang *et al.*, EAR motif mutation of rice OsERF3 alters the regulation of ethylene biosynthesis and drought tolerance. *Planta* **237**, 1443-1451 (2013).

86. Y. Wang *et al.*, An ethylene response factor OsWR1 responsive to drought stress transcriptionally activates wax synthesis related genes and increases wax production in rice. *Plant Mol Biol* **78**, 275-288 (2012).

87. J. I. Kim *et al.*, Overexpression of Arabidopsis YUCCA6 in potato results in high-auxin developmental phenotypes and enhanced resistance to water deficit. *Mol Plant* **6**, 337-349 (2013).

88. M. Lee *et al.*, Activation of a flavin monooxygenase gene YUCCA7 enhances drought resistance in Arabidopsis. *Planta* **235**, 923-938 (2012).

89. J. E. Park *et al.*, GH3-mediated auxin homeostasis links growth regulation with stress adaptation response in Arabidopsis. *J Biol Chem* **282**, 10036-10046 (2007).

90. P. E. V. Elizabeth S. Haswell, The ongoing search for molecular basis of plant osmosensing. *Journal of General physiology* **145**, 389 (2015).

91. S. Ramanjulu, D. Bartels, Drought- and desiccation-induced modulation of gene expression in plants. *Plant Cell Environ* **25**, 141-151 (2002).

92. Y. Ma *et al.*, Regulators of PP2C phosphatase activity function as abscisic acid sensors. *Science* **324**, 1064-1068 (2009).

93. S. Pandey, D. C. Nelson, S. M. Assmann, Two novel GPCR-type G proteins are abscisic acid receptors in Arabidopsis. *Cell* **136**, 136-148 (2009).

94. S. Y. Park *et al.*, Abscisic acid inhibits type 2C protein phosphatases via the PYR/PYL family of START proteins. *Science* **324**, 1068-1071 (2009).

95. A. S. Raghavendra, V. K. Gonugunta, A. Christmann, E. Grill, ABA perception and signalling. *Trends Plant Sci* **15**, 395-401 (2010).

96. Y. Uno *et al.*, Arabidopsis basic leucine zipper transcription factors involved in an abscisic acid-dependent signal transduction pathway under drought and high-salinity conditions. *Proc Natl Acad Sci U S A* **97**, 11632-11637 (2000).

97. B.-C. T. Yan-Zhuo Yang, A Distal ABA Responsive Element in AtNCED3 Promoter Is Required for Positive Feedback Regulation of ABA Biosynthesis in Arabidopsis. *Plos one* **9** (2014).

98. D. Singh, A. Laxmi, Transcriptional regulation of drought response: a tortuous network of transcriptional factors. *Front Plant Sci* **6** (2015).

99. B. A. G. Kaur, Molecular responses to drought stress in plants | SpringerLink. *Biollogia Plantarum* **61**, 201-209 (2017).

100. L. S. Tran *et al.*, Isolation and functional analysis of Arabidopsis stress-inducible NAC transcription factors that bind to a drought-responsive cis-element in the early responsive to dehydration stress 1 promoter. *Plant Cell* **16**, 2481-2498 (2004).

101. K. Shinozaki, K. Yamaguchi-Shinozaki, Molecular responses to dehydration and low temperature: differences and cross-talk between two stress signaling pathways. *Curr Opin Plant Biol* **3**, 217-223 (2000).

102. J. S. Kim *et al.*, An ABRE promoter sequence is involved in osmotic stress-responsive expression of the DREB2A gene, which encodes a transcription factor regulating drought-inducible genes in Arabidopsis. *Plant Cell Physiol* **52**, 2136-2146 (2011).

103. S. J. Lee *et al.*, DREB2C interacts with ABF2, a bZIP protein regulating abscisic acid-responsive gene expression, and its overexpression affects abscisic acid sensitivity. *Plant Physiol* **153**, 716-727 (2010).

104. Z. Y. Xu *et al.*, The Arabidopsis NAC transcription factor ANAC096 cooperates with bZIP-type transcription factors in dehydration and osmotic stress responses. *Plant Cell* **25**, 4708-4724 (2013).

105. S. E. Castel, R. A. Martienssen, RNA interference in the nucleus: roles for small RNAs in transcription, epigenetics and beyond. *Nat Rev Genet* **14**, 100-112 (2013).

106. J. A. Law, S. E. Jacobsen, Establishing, maintaining and modifying DNA methylation patterns in plants and animals. *Nat Rev Genet* **11**, 204-220 (2010).

107. C. S. Pikaard, O. Mittelsten Scheid, Epigenetic regulation in plants. *Cold Spring Harb Perspect Biol* **6**, a019315 (2014).

108. B. K. A. Kovarˇik, M. Bezdeˇk, Z. Opatrn, Hypermethylation of tobacco heterochromatic loci in response to osmotic stress | SpringerLink. **95**, 301-306 (1997).

109. R. M. González, M. M. Ricardi, N. D. Iusem, "Epigenetic marks in an adaptive water stress-responsive gene in tomato roots under normal and drought conditions" in Epigenetics. (2013), vol. 8, pp. 864-872.

110. W. S. Wang *et al.*, Drought-induced site-specific DNA methylation and its association with drought tolerance in rice (Oryza sativa L.). *J Exp Bot* **62**, 1951-1960 (2011).

111. L. Wu *et al.*, DNA methylation mediated by a microRNA pathway. *Mol Cell* **38**, 465-475 (2010).

112. F. R. Kulcheski *et al.*, Identification of novel soybean microRNAs involved in abiotic and biotic stresses. *BMC Genomics* **12**, 307 (2011).

113. R. D. Mutum *et al.*, Evolution of variety-specific regulatory schema for expression of osa-miR408 in indica rice varieties under drought stress. *Febs j* **280**, 1717-1730 (2013).

114. J. M. Kim *et al.*, Alterations of lysine modifications on the histone H3 N-tail under drought stress conditions in Arabidopsis thaliana. *Plant Cell Physiol* **49**, 1580-1588 (2008).

115. J. M. Kim *et al.*, Transition of chromatin status during the process of recovery from drought stress in Arabidopsis thaliana. *Plant Cell Physiol* **53**, 847-856 (2012).

116. H. Fang, X. Liu, G. Thorn, J. Duan, L. Tian, Expression analysis of histone acetyltransferases in rice under drought stress. *Biochem Biophys Res Commun* **443**, 400-405 (2014).

117. S. Li *et al.*, Histone Acetylation Cooperating with AREB1 Transcription Factor Regulates Drought Response and Tolerance in Populus trichocarpa. *Plant Cell* (2018).

118. X. Chen *et al.*, POWERDRESS interacts with HISTONE DEACETYLASE 9 to promote aging in Arabidopsis. *Elife* **5** (2016).

119. Y. J. Kim *et al.*, POWERDRESS and HDA9 interact and promote histone H3 deacetylation at specific genomic sites in Arabidopsis. *Proc Natl Acad Sci U S A* **113**, 14858-14863 (2016).

120. Y. Zheng *et al.*, Histone deacetylase HDA9 negatively regulates salt and drought stress responsiveness in Arabidopsis. *J Exp Bot* **67**, 1703-1713 (2016).

121. Z. Han *et al.*, AtHD2D Gene Plays a Role in Plant Growth, Development, and Response to Abiotic Stresses in Arabidopsis thaliana. *Front Plant Sci* **7** (2016).

122. S. Sridha, K. Wu, Identification of AtHD2C as a novel regulator of abscisic acid responses in Arabidopsis. *Plant J* **46**, 124-133 (2006).

123. M. Luo *et al.*, HD2C interacts with HDA6 and is involved in ABA and salt stress response in Arabidopsis. *J Exp Bot* **63**, 3297-3306 (2012).

124. J. Zhao *et al.*, Expression and functional analysis of the plant-specific histone deacetylase HDT701 in rice. *Front Plant Sci* **5**, 764 (2014).

125. J. M. Kim *et al.*, Acetate-mediated novel survival strategy against drought in plants. *Nat Plants* **3**, 17097 (2017).

126. K. van Dijk *et al.*, Dynamic changes in genome-wide histone H3 lysine 4 methylation patterns in response to dehydration stress in Arabidopsis thaliana. *BMC Plant Biol* **10**, 238 (2010).

127. T. Widiez *et al.*, The chromatin landscape of the moss Physcomitrella patens and its dynamics during development and drought stress. *Plant J* **79**, 67-81 (2014).

128. W. Zong, X. Zhong, J. You, L. Xiong, Genome-wide profiling of histone H3K4-tri-methylation and gene expression in rice under drought stress. *Plant Mol Biol* **81**, 175-188 (2013).

129. Y. Ding, Z. Avramova, M. Fromm, The Arabidopsis trithorax-like factor ATX1 functions in dehydration stress responses via ABA-dependent and ABA-independent pathways. *Plant J* **66**, 735-744 (2011).

130. T. Mengiste, Plant Immunity to Necrotrophs. *Annual Review of Phytopathology, Vol 50* **50**, 267-294 (2012).

131. A. Dobon *et al.*, Novel Disease Susceptibility Factors for Fungal Necrotrophic Pathogens in Arabidopsis. *Plos Pathogens* **11** (2015).

132. C. Hernandez-Blanco *et al.*, Impairment of cellulose synthases required for Arabidopsis secondary cell wall formation enhances disease resistance. *Plant Cell* **19**, 890-903 (2007).

133. D. Cantu *et al.*, The intersection between cell wall disassembly, ripening, and fruit susceptibility to Botrytis cinerea. *Proceedings of the National Academy of Sciences of the United States of America* **105**, 859-864 (2008).

134. A. Sanchez-Vallet *et al.*, Tryptophan-derived secondary metabolites in Arabidopsis thaliana confer non-host resistance to necrotrophic Plectosphaerella cucumerina fungi. *Plant Journal* **63**, 115-127 (2010).

135. J. Garcia-Andrade, V. Ramirez, V. Flors, P. Vera, Arabidopsis ocp3 mutant reveals a mechanism linking ABA and JA to pathogen-induced callose deposition. *Plant Journal* **67**, 783-794 (2011).

136. M. Berrocal-Lobo, A. Molina, R. Solano, Constitutive expression of ETHYLENE-RESPONSE-FACTOR1 in Arabidopsis confers resistance to several necrotrophic fungi. *Plant Journal* **29**, 23-32 (2002).

137. M. E. Alvarez, F. Nota, D. A. Cambiagno, Epigenetic control of plant immunity. *Molecular Plant Pathology* **11**, 563-576 (2010).

138. F. Pontvianne, T. Blevins, C. S. Pikaard, Arabidopsis Histone Lysine Methyltransferases. *Advances in Botanical Research, Vol 53* **53**, 1-22 (2010).

139. T. Thorstensen, P. Grini, R. Aalen, SET domain proteins in plant development. *Biochimica et Biophysica Acta (BBA)- ...* (2011).

140. K. Palma *et al.*, Autoimmunity in Arabidopsis acd11 Is Mediated by Epigenetic Regulation of an Immune Receptor. *Plos Pathogens* **6** (2010).

141. S. T. Xia *et al.*, Regulation of Transcription of Nucleotide-Binding Leucine-Rich Repeat-Encoding Genes SNC1 and RPP4 via H3K4 Trimethylation. *Plant Physiology* **162**, 1694-1705 (2013).

142. M. Bevan, S. Walsh, The Arabidopsis genome: A foundation for plant research. *Genome Research* **15**, 1632-1642 (2005).

143. D. Shibata, Genome sequencing and functional genomics approaches in tomato. *Journal of General Plant Pathology* **71**, 1-7 (2005).

144. J. Giovannoni, S. El-Rakshy, Genetic regulation of tomato fruit ripening and development and implementation of associated genomics tools. *Proceedings of the 5th International Postharvest Symposium, Vols 1-3*, 63-72 (2005).

145. L. A. Mueller *et al.*, The SOL Genomics Network. A comparative resource for Solanaceae biology and beyond. *Plant Physiology* **138**, 1310-1317 (2005).

146. B. D. Strahl, C. D. Allis, The language of covalent histone modifications. *Nature* **403**, 41-45 (2000).

147. A. K. Upadhyay, X. Cheng, Dynamics of Histone Lysine Methylation: Structures of Methyl Writers and Eraser. *Prog Drug Res* **67**, 107-124 (2011).

148. S. Lee *et al.*, "Global Regulation of Plant Immunity by Histone Lysine Methyl Transferases" in Plant Cell. (2016), vol. 28, pp. 1640-1661.

149. C. De-La-Pena, A. Rangel-Cano, R. Alvarez-Venegas, Regulation of disease-responsive genes mediated by epigenetic factors: interaction of Arabidopsis-Pseudomonas. *Mol Plant Pathol* **13**, 388-398 (2012).

150. S. K. Bowman *et al.*, "H3K27 modifications define segmental regulatory domains in the Drosophila bithorax complex" in eLife. (2014), vol. 3.

151. Y. Hu *et al.*, Cold stress selectively unsilences tandem repeats in heterochromatin associated with accumulation of H3K9ac. *Plant Cell Environ* **35**, 2130-2142 (2012).

152. J. J. Folsom, K. Begcy, X. Hao, D. Wang, H. Walia, Rice fertilization-Independent Endosperm1 regulates seed size under heat stress by controlling early endosperm development. *Plant Physiol* **165**, 238-248 (2014).

153. A. Pecinka *et al.*, Epigenetic regulation of repetitive elements is attenuated by prolonged heat stress in Arabidopsis. *Plant Cell* **22**, 3118-3129 (2010).

154. Y. Song *et al.*, The dynamic changes of DNA methylation and histone modifications of salt responsive transcription factor genes in soybean. *PLoS One* **7**, e41274 (2012).

155. E. Luna, T. J. Bruce, M. R. Roberts, V. Flors, J. Ton, Next-generation systemic acquired resistance. *Plant Physiol* **158**, 844-853 (2012).

156. A. Slaughter *et al.*, Descendants of primed Arabidopsis plants exhibit resistance to biotic stress. *Plant Physiol* **158**, 835-843 (2012).

157. S. B. Joshi R., Bohra A., Chinnusamy V., "Salt stress signalling pathways: specificity and crosstalk" in Managing Salt Tolerance in Plants: Molecular and Genomic Perspectives, H. M. A. Wani S. H., Ed. (CRC Press, Boca Raton, FL, 2016), pp. 51–78.

158. M. Hanin *et al.*, Plant dehydrins and stress tolerance: versatile proteins for complex mechanisms. *Plant Signal Behav* **6**, 1503-1509 (2011).

159. W. Wang, B. Vinocur, O. Shoseyov, A. Altman, Role of plant heat-shock proteins and molecular chaperones in the abiotic stress response. *Trends Plant Sci* **9**, 244-252 (2004).

160. S. N. B. Wani S. H., Devi T. R., Haribhushan A., Jeberson S. M., Malik C. P, "Engineering abiotic stress tolerance in plants: extricating regulatory gene complex" in Conventional and Non-Conventional Interventions in Crop Improvement, S. G. S. Malik C. P., Wani S. H, Ed. (CABI, New Delhi, 2013), pp. 1-19.

161. W. X. Li *et al.*, The Arabidopsis NFYA5 transcription factor is regulated transcriptionally and posttranscriptionally to promote drought resistance. *Plant Cell* **20**, 2238-2251 (2008).

162. Q. Liu *et al.*, Two transcription factors, DREB1 and DREB2, with an EREBP/AP2 DNA binding domain separate two cellular signal transduction pathways in drought- and low-temperature-responsive gene expression, respectively, in Arabidopsis. *Plant Cell* **10**, 1391-1406 (1998).

163. S. K. Han, D. Wagner, Role of chromatin in water stress responses in plants. *J Exp Bot* **65**, 2785-2799 (2014).

164. M. R. Foolad, "Current Status Of Breeding Tomatoes For Salt And Drought Tolerance | SpringerLink" in Advances in Molecular Breeding Toward Drought and Salt Tolerant Crops. (SpringerLink, 2019).

165. H. L. Xing *et al.*, A CRISPR/Cas9 toolkit for multiplex genome editing in plants. *BMC Plant Biol* **14**, 327 (2014).

166. X. Li *et al.*, Antisilencing role of the RNA-directed DNA methylation pathway and a histone acetyltransferase in Arabidopsis. (2012).

167. R. L. Heath, L. Packer, Photoperoxidation in isolated chloroplasts. I. Kinetics and stoichiometry of fatty acid peroxidation. *Arch Biochem Biophys* **125**, 189-198 (1968).

168. H. Wang *et al.*, The tomato Aux/IAA transcription factor IAA9 is involved in fruit development and leaf morphogenesis. *Plant Cell* **17**, 2676-2692 (2005).

169. R. Aiese Cigliano *et al.*, "Genome-wide analysis of histone modifiers in tomato: gaining an insight into their developmental roles" in BMC Genomics. (2013), vol. 14, pp. 57.

170. H. Sun *et al.*, Strigolactones are involved in phosphate- and nitrate-deficiency-induced root development and auxin transport in rice. *J Exp Bot* **65**, 6735-6746 (2014).

171. X. Zhang, T. C. Bruice, Enzymatic mechanism and product specificity of SET-domain protein lysine methyltransferases. (2008).

172. J. Perry, Y. Zhao, The CW domain, a structural module shared amongst vertebrates, vertebrate-infecting parasites and higher plants. *Trends Biochem Sci* **28**, 576-580 (2003).

173. F. He *et al.*, Structural insight into the zinc finger CW domain as a histone modification reader. *Structure* **18**, 1127-1139 (2010).

174. C. A. Schneider, W. S. Rasband, K. W. Eliceiri, NIH Image to ImageJ: 25 years of image analysis. *Nat Methods* **9**, 671-675 (2012).

175. I. Egea *et al.*, The drought-tolerant Solanum pennellii regulates leaf water loss and induces genes involved in amino acid and ethylene/jasmonate metabolism under dehydration. *Scientific Reports* **8**, 2791 (2018).

176. S. Fahad *et al.*, Crop Production under Drought and Heat Stress: Plant Responses and Management Options. *Front Plant Sci* **8** (2017).

177. G. Gillaspy, H. Ben-David, W. Gruissem, Fruits: A Developmental Perspective. *The Plant cell* **5**, 1439-1451 (1993).

178. P. McAtee, S. Karim, R. Schaffer, K. David, A dynamic interplay between phytohormones is required for fruit development, maturation, and ripening. *Front Plant Sci* **4** (2013).

179. G. Subramaniam *et al.*, Type B Heterotrimeric G Protein gamma-Subunit Regulates Auxin and ABA Signaling in Tomato. *Plant Physiol* **170**, 1117-1134 (2016).

180. M. de Jong, M. Wolters-Arts, R. Feron, C. Mariani, W. H. Vriezen, The Solanum lycopersicum auxin response factor 7 (SlARF7) regulates auxin signaling during tomato fruit set and development. *Plant J* **57**, 160-170 (2009).

181. J. L. Celenza, Jr., P. L. Grisafi, G. R. Fink, A pathway for lateral root formation in Arabidopsis thaliana. *Genes Dev* **9**, 2131-2142 (1995).

182. L. Xu *et al.*, Di- and tri- but not monomethylation on histone H3 lysine 36 marks active transcription of genes involved in flowering time regulation and other processes in Arabidopsis thaliana. *Mol Cell Biol* **28**, 1348-1360 (2008).

183. B. Liu *et al.*, SET DOMAIN GROUP 708, a histone H3 lysine 36-specific methyltransferase, controls flowering time in rice (Oryza sativa). *New Phytol* **210**, 577-588 (2016).

184. C. Lugojan, S. Ciulca, Evaluation of relative water content in winter wheat. (2011).

185. M. Zhu *et al.*, SlDEAD31, a Putative DEAD-Box RNA Helicase Gene, Regulates Salt and Drought Tolerance and Stress-Related Genes in Tomato. *PLoS One* **10**, e0133849 (2015).

186. U. Batlang, N. Baisakh, M. M. Ambavaram, A. Pereira, Phenotypic and physiological evaluation for drought and salinity stress responses in rice. *Methods Mol Biol* **956**, 209-225 (2013).

187. J. G. Dubouzet *et al.*, OsDREB genes in rice, Oryza sativa L., encode transcription activators that function in drought-, high-salt- and cold-responsive gene expression. *Plant J* **33**, 751-763 (2003).

188. F. Qin *et al.*, Cloning and functional analysis of a novel DREB1/CBF transcription factor involved in cold-responsive gene expression in Zea mays L. *Plant Cell Physiol* **45**, 1042-1052 (2004).

189. S. Munir *et al.*, "Overexpression of calmodulin-like (ShCML44) stress-responsive gene from Solanum habrochaites enhances tolerance to multiple abiotic stresses" in Sci Rep. (2016), vol. 6.

190. C. I. Cazzonelli, T. Millar, E. J. Finnegan, B. J. Pogson, "Promoting gene expression in plants by permissive histone lysine methylation" in Plant Signal Behav. (2009), vol. 4, pp. 484-488.

191. R. A. Gaxiola *et al.*, Drought- and salt-tolerant plants result from overexpression of the AVP1 H+-pump. (2001).

192. Y. Li *et al.*, The histone methyltransferase SDG8 mediates the epigenetic modification of light and carbon responsive genes in plants. *Genome Biol* **16**, 79 (2015).

193. M. Jaskiewicz, U. Conrath, C. Peterhansel, Chromatin modification acts as a memory for systemic acquired resistance in the plant stress response. *EMBO Rep* **12**, 50-55 (2011).

194. Y. Ueda, M. Konishi, S. Yanagisawa, Molecular basis of the nitrogen response in plants. *http://dx.doi.org/10.1080/00380768.2017.1360128* (2017).

195. R. Muñoz-Huerta *et al.*, A Review of Methods for Sensing the Nitrogen Status in Plants: Advantages, Disadvantages and Recent Advances. *Sensors* **13**, 10823-10843 (2013).

196. T. Remans *et al.*, The Arabidopsis NRT1.1 transporter participates in the signaling pathway triggering root colonization of nitrate-rich patches. *Proc Natl Acad Sci U S A* **103**, 19206-19211 (2006).

197. H. Zhang, H. Rong, D. Pilbeam, Signalling mechanisms underlying the morphological responses of the root system to nitrogen in Arabidopsis thaliana. *J Exp Bot* **58**, 2329-2338 (2007).

198. K. Xie, J. Zhang, Y. Yang, "Genome-wide prediction of highly specific guide RNA spacers for CRISPR-Cas9-mediated genome editing in model plants and major crops" in Mol Plant. (England, 2014), vol. 7, pp. 923-926.

199. J. E. Lima, S. Kojima, H. Takahashi, N. von Wiren, Ammonium triggers lateral root branching in Arabidopsis in an AMMONIUM TRANSPORTER1;3-dependent manner. *Plant Cell* **22**, 3621-3633 (2010).

200. K. Yoneyama *et al.*, How do nitrogen and phosphorus deficiencies affect strigolactone production and exudation? *Planta* **235**, 1197-1207 (2012).

201. J. Zhang, L. Xu, F. Wang, M. Deng, K. Yi, "Modulating the root elongation by phosphate/nitrogen starvation in an OsGLU3 dependant way in rice" in Plant Signal Behav. (2012), vol. 7, pp. 1144-1145.

202. Y. Sonoda, A. Ikeda, S. Saiki, T. Yamaya, J. Yamaguchi, Feedback regulation of the ammonium transporter gene family AMT1 by glutamine in rice. *Plant Cell Physiol* **44**, 1396-1402 (2003).

203. R. Gu *et al.*, Characterization of AMT-mediated high-affinity ammonium uptake in roots of maize (Zea mays L.). *Plant Cell Physiol* **54**, 1515-1524 (2013).

204. G. Xu, X. Fan, A. J. Miller, Plant nitrogen assimilation and use efficiency. *Annu Rev Plant Biol* **63**, 153-182 (2012).

205. C. A. Griffiths, M. J. Paul, C. H. Foyer, Metabolite transport and associated sugar signalling systems underpinning source/sink interactions. *Biochim Biophys Acta* **1857**, 1715-1725 (2016).

206. E. A. Vidal, T. C. Moyano, J. Canales, R. A. Gutierrez, Nitrogen control of developmental phase transitions in Arabidopsis thaliana. *J Exp Bot* **65**, 5611-5618 (2014).

207. L. Zhao, F. Liu, N. M. Crawford, Y. Wang, "Molecular Regulation of Nitrate Responses in Plants" in Int J Mol Sci. (2018), vol. 19.

208. M. E. Alvarez, F. Nota, D. A. Cambiagno, Epigenetic control of plant immunity. *Mol Plant Pathol* **11**, 563-576 (2010).

209. N. N. P. Chandrika, K. Sundaravelpandian, W. Schmidt, A PHD in histone language. *http://dx.doi.org/10.4161/psb.24381* (2013).

210. T. Widiez *et al.*, High nitrogen insensitive 9 (HNI9)-mediated systemic repression of root NO3- uptake is associated with changes in histone methylation. *Proc Natl Acad Sci U S A* **108**, 13329-13334 (2011).

211. Y. H. Wang, D. F. Garvin, L. V. Kochian, Nitrate-Induced Genes in Tomato Roots. Array Analysis Reveals Novel Genes That May Play a Role in Nitrogen Nutrition1[w]. *Plant Physiol* **127**, 345-359 (2001).

212. J. R. Brian Bushnell, Esther Singer, BBMerge – Accurate paired shotgun read merging via overlap. (2017).

213. A. Kozomara, S. Griffiths-Jones, miRBase: integrating microRNA annotation and deep-sequencing data. *Nucleic Acids Res* **39**, D152-157 (2011).

214. Y. Liao, G. K. Smyth, W. Shi, featureCounts: an efficient general purpose program for assigning sequence reads to genomic features. *Bioinformatics* **30**, 923-930 (2014).

215. M. I. Love, W. Huber, S. Anders, Moderated estimation of fold change and dispersion for RNA-seq data with DESeq2. *Genome Biol* **15** (2014).

216. T. Madden, The BLAST Sequence Analysis Tool. (2013).

217. T. L. Bailey, J. Johnson, C. E. Grant, W. S. Noble, The MEME Suite. *Nucleic Acids Res* **43**, W39-49 (2015).

218. S. Gupta, J. A. Stamatoyannopoulos, T. L. Bailey, W. S. Noble, Quantifying similarity between motifs. *Genome Biol* **8**, R24 (2007).

219. Q. Ling, W. Huang, P. Jarvis, Use of a SPAD-502 meter to measure leaf chlorophyll concentration in Arabidopsis thaliana. *Photosynth Res* **107**, 209-214 (2011).

220. R. J.Porra, The assay of chlorophylls a and b converted to their respective magnesium-rhodochlorin derivatives by extraction from recalcitrant algal cells with aqueous alkaline methanol: prevention of allomerization with reductants. *Biochim Biophys Acta* **1015**, 493–502 (1990).

221. T. Galkovskyi *et al.*, GiA Roots: software for the high throughput analysis of plant root system architecture. *BMC Plant Biol* **12**, 116 (2012).

222. T. L. Bailey, C. Elkan, Fitting a mixture model by expectation maximization to discover motifs in biopolymers. *Proc Int Conf Intell Syst Mol Biol* **2**, 28-36 (1994).

223. M. S. Katari *et al.*, VirtualPlant: a software platform to support systems biology research. *Plant Physiol* **152**, 500-515 (2010).

224. S. Maere, K. Heymans, M. Kuiper, BiNGO: a Cytoscape plugin to assess overrepresentation of gene ontology categories in biological networks. *Bioinformatics* **21**, 3448-3449 (2005).

225. D. Bassi, M. Menossi, L. Mattiello, Nitrogen supply influences photosynthesis establishment along the sugarcane leaf. *Scientific Reports* **8**, 2327 (2018).

226. W. Mahrez *et al.*, "H3K36ac Is an Evolutionary Conserved Plant Histone Modification That Marks Active Genes1[OPEN]" in Plant Physiol. (2016), vol. 170, pp. 1566-1577.

227. G. Krouk *et al.*, Nitrate-regulated auxin transport by NRT1.1 defines a mechanism for nutrient sensing in plants. *Dev Cell* **18**, 927-937 (2010).

228. E. Bouguyon *et al.*, Multiple mechanisms of nitrate sensing by Arabidopsis nitrate transceptor NRT1.1. *Nat Plants* **1**, 15015 (2015).

229. D. L. Rayle, R. E. Cleland, Evidence that Auxin-induced Growth of Soybean Hypocotyls Involves Proton Excretion. *Plant Physiol* **66**, 433-437 (1980).

230. A. K. Spartz *et al.*, SAUR Inhibition of PP2C-D Phosphatases Activates Plasma Membrane H+-ATPases to Promote Cell Expansion in Arabidopsis. *Plant Cell* **26**, 2129-2142 (2014).

231. F. X. Cunningham, R. J. Dennenberg, L. Mustardy, P. A. Jursinic, E. Gantt, Stoichiometry of Photosystem I, Photosystem II, and Phycobilisomes in the Red Alga Porphyridium cruentum as a Function of Growth Irradiance. *Plant Physiol* **91**, 1179-1187 (1989).

232. K. Kitajima, K. P. Hogan, Increases of chlorophyll a/b ratios during acclimation of tropical woody seedlings to nitrogen limitation and high light. *Plant Cell Environ* **26**, 857-865 (2003).

233. S. H. Lin *et al.*, Mutation of the Arabidopsis NRT1.5 nitrate transporter causes defective root-to-shoot nitrate transport. *Plant Cell* **20**, 2514-2528 (2008).

234. J. D. G. Jones, J. L. Dangl, The plant immune system. *Nature* **444**, 323 (2019).

235. C. M. J. Pieterse, D. V. d. Does, C. Zamioudis, A. Leon-Reyes, S. C. M. V. Wees, Hormonal Modulation of Plant Immunity. *http://dx.doi.org/10.1146/annurev-cellbio-092910-154055* (2012).

236. J. S. Ramirez-Prado *et al.*, Modify the Histone to Win the Battle: Chromatin Dynamics in Plant–Pathogen Interactions. *Front Plant Sci* **9** (2018).

237. B. P. Thomma, T. Nürnberger, M. H. Joosten, "Of PAMPs and Effectors: The Blurred PTI-ETI Dichotomy[OA]" in Plant Cell. (2011), vol. 23, pp. 4-15.

238. D. E. Olins, A. L. Olins, Chromatin history: our view from the bridge. *Nat Rev Mol Cell Biol* **4**, 809-814 (2003).

239. K. Luger, J. C. Hansen, Nucleosome and chromatin fiber dynamics. *Curr Opin Struct Biol* **15**, 188-196 (2005).

240. B. Ding, G. L. Wang, Chromatin versus pathogens: the function of epigenetics in plant immunity. *Front Plant Sci* **6**, 675 (2015).

241. F. S. Toshio Murashige, A Revised Medium for Rapid Growth and Bio Assays with Tobacco Tissue Cultures - Murashige - 1962 - Physiologia Plantarum - Wiley Online Library. *Physiologia Plantarum* **15**, 473-497 (21962).

242. S. Xu *et al.*, Tomato PEPR1 ORTHOLOG RECEPTOR-LIKE KINASE1 Regulates Responses to Systemin, Necrotrophic Fungi, and Insect Herbivory. *The Plant cell* **30**, 2214-2229 (2018).

243. S. AbuQamar, M. F. Chai, H. Luo, F. Song, T. Mengiste, Tomato Protein Kinase 1b Mediates Signaling of Plant Responses to Necrotrophic Fungi and Insect Herbivory[W]. *Plant Cell* **20**, 1964-1983 (2008).

244. N. M. Springer *et al.*, Comparative analysis of SET domain proteins in maize and Arabidopsis reveals multiple duplications preceding the divergence of monocots and dicots. *Plant Physiol* **132**, 907-925 (2003).

245. S. AbuQamar, K. Moustafa, L. S. Tran, Mechanisms and strategies of plant defense against Botrytis cinerea. *https://doi.org/10.1080/07388551.2016.1271767* (2017).

246. B. Li, X. Meng, L. Shan, P. He, Transcriptional regulation of pattern-triggered immunity in plants. *Cell Host Microbe* **19**, 641-650 (2016).

247. D. Couto, C. Zipfel, Regulation of pattern recognition receptor signalling in plants. *Nat Rev Immunol* **16**, 537-552 (2016).

248. F. Cui, W. Sun, X. Kong, RLCKs Bridge Plant Immune Receptors and MAPK Cascades. *Trends Plant Sci* **23**, 1039-1041 (2018).

249. A. Miya *et al.*, CERK1, a LysM receptor kinase, is essential for chitin elicitor signaling in Arabidopsis. *Proc Natl Acad Sci U S A* **104**, 19613-19618 (2007).

250. J. D. G. Jones, J. L. Dangl, The plant immune system. *Nature* **444**, 323 (2006).

251. C. Segonzac, C. Zipfel, Activation of plant pattern-recognition receptors by bacteria. *Curr Opin Microbiol* **14**, 54-61 (2011).

252. G. Wang *et al.*, A genome-wide functional investigation into the roles of receptor-like proteins in Arabidopsis. *Plant Physiol* **147**, 503-517 (2008).

253. L. K. Fritz-Laylin, N. Krishnamurthy, M. Tor, K. V. Sjolander, J. D. Jones, Phylogenomic analysis of the receptor-like proteins of rice and Arabidopsis. *Plant Physiol* **138**, 611-623 (2005).

254. L. Gomez-Gomez, T. Boller, FLS2: an LRR receptor-like kinase involved in the perception of the bacterial elicitor flagellin in Arabidopsis. *Mol Cell* **5**, 1003-1011 (2000).

255. Y. Yamaguchi, G. Pearce, C. A. Ryan, The cell surface leucine-rich repeat receptor for AtPep1, an endogenous peptide elicitor in Arabidopsis, is functional in transgenic tobacco cells. *Proc Natl Acad Sci U S A* **103**, 10104-10109 (2006).

256. C. Zipfel *et al.*, Perception of the bacterial PAMP EF-Tu by the receptor EFR restricts Agrobacterium-mediated transformation. *Cell* **125**, 749-760 (2006).

257. Y. Cao *et al.*, The kinase LYK5 is a major chitin receptor in Arabidopsis and forms a chitin-induced complex with related kinase CERK1. *Elife* **3** (2014).

258. H. Bohm, I. Albert, L. Fan, A. Reinhard, T. Nurnberger, Immune receptor complexes at the plant cell surface. *Curr Opin Plant Biol* **20**, 47-54 (2014).

259. D. Lu *et al.*, A receptor-like cytoplasmic kinase, BIK1, associates with a flagellin receptor complex to initiate plant innate immunity. *Proc Natl Acad Sci U S A* **107**, 496-501 (2010).

260. X. Gao, K. L. Cox, P. He, "Functions of Calcium-Dependent Protein Kinases in Plant Innate Immunity" in Plants (Basel). (2014), vol. 3, pp. 160-176.

261. L. Li *et al.*, The FLS2-associated kinase BIK1 directly phosphorylates the NADPH oxidase RbohD to control plant immunity. *Cell Host Microbe* **15**, 329-338 (2014).

262. X. Liang, J. M. Zhou, Receptor-Like Cytoplasmic Kinases: Central Players in Plant Receptor Kinase-Mediated Signaling. *Annu Rev Plant Biol* **69**, 267-299 (2018).

263. K. Laluk *et al.*, Biochemical and genetic requirements for function of the immune response regulator BOTRYTIS-INDUCED KINASE1 in plant growth, ethylene signaling, and PAMP-triggered immunity in Arabidopsis. *The Plant cell* **23**, 2831-2849 (2011).

264. T. Chen *et al.*, Arabidopsis Mutant bik1 Exhibits Strong Resistance to Plasmodiophora brassicae. *Front Physiol* **7**, 402 (2016).

265. E. H. Chung, F. El-Kasmi, Y. He, A. Loehr, J. L. Dangl, A plant phosphoswitch platform repeatedly targeted by type III effector proteins regulates the output of both tiers of plant immune receptors. *Cell Host Microbe* **16**, 484-494 (2014).

266. H. Shi *et al.*, BR-SIGNALING KINASE1 physically associates with FLAGELLIN SENSING2 and regulates plant innate immunity in Arabidopsis. *Plant Cell* **25**, 1143-1157 (2013).

267. T. Shinya *et al.*, Selective regulation of the chitin-induced defense response by the Arabidopsis receptor-like cytoplasmic kinase PBL27. *Plant J* **79**, 56-66 (2014).

268. K. Yamada *et al.*, The Arabidopsis CERK1-associated kinase PBL27 connects chitin perception to MAPK activation. *Embo j* **35**, 2468-2483 (2016).

269. T. Sakamoto *et al.*, The tomato RLK superfamily: phylogeny and functional predictions about the role of the LRRII-RLK subfamily in antiviral defense. *BMC Plant Biology* **12**, 1-18 (2012).

270. T. Aoyama, N. H. Chua, A glucocorticoid-mediated transcriptional induction system in transgenic plants. *Plant J* **11**, 605-612 (1997).

271. J. S. de Vries, V. M. Andriotis, A. J. Wu, J. P. Rathjen, Tomato Pto encodes a functional N-myristoylation motif that is required for signal transduction in Nicotiana benthamiana. *Plant J* **45**, 31-45 (2006).

272. S. Schwizer *et al.*, The Tomato Kinase Pti1 Contributes to Production of Reactive Oxygen Species in Response to Two Flagellin-Derived Peptides and Promotes Resistance to Pseudomonas syringae Infection. *Mol Plant Microbe Interact* **30**, 725-738 (2017).

273. Y. Liu, M. Schiff, S. P. Dinesh-Kumar, Virus-induced gene silencing in tomato. *Plant J* **31**, 777-786 (2002).

274. C. Wu, L. Jia, F. Goggin, The reliability of virus-induced gene silencing experiments using tobacco rattle virus in tomato is influenced by the size of the vector control. *Mol Plant Pathol* **12**, 299-305 (2011).

275. P. Veronese *et al.*, The membrane-anchored BOTRYTIS-INDUCED KINASE1 plays distinct roles in Arabidopsis resistance to necrotrophic and biotrophic pathogens. *The Plant cell* **18**, 257-273 (2006).

276. D. Mackey, B. F. Holt, 3rd, A. Wiig, J. L. Dangl, RIN4 interacts with Pseudomonas syringae type III effector molecules and is required for RPM1-mediated resistance in Arabidopsis. *Cell* **108**, 743-754 (2002).

277. M. Fan *et al.*, Evolution and Expression Characteristics of Receptor-Like Cytoplasmic Protein Kinases in Maize, Rice and Arabidopsis. *Int J Mol Sci* **19** (2018).

278. J. Zhang *et al.*, Receptor-like cytoplasmic kinases integrate signaling from multiple plant immune receptors and are targeted by a Pseudomonas syringae effector. *Cell Host Microbe* **7**, 290-301 (2010).